universidad de león

UNIVERSITY OF LEÓN

DEPARTMENT OF MECHANICAL, COMPUTER AND AEROSPACE ENGINEERING

Genetic Algorithm optimization and characterization of noise, clock and Non-Line-of-Sight uncertainties in time-based positioning systems

A dissertation supervised by

DR. HILDE PÉREZ GARCÍA

and submitted by

RUBÉN ÁLVAREZ FERNÁNDEZ

in fulfillment of the requirements for the Degree of

PHILOSOPHIÆDOCTOR (PH.D.)

In León, August 2020

universidad de león

UNIVERSIDAD DE LEÓN

DEPARTAMENTO DE INGENIERÍA MECÁNICA, INFORMÁTICA Y AEROESPACIAL

Optimización mediante Algoritmos Genéticos y caracterización de incertidumbres de ruido, relojes y Non-Line-of-Sight en sistemas de posicionamiento basados en mediciones temporales

Tesis doctoral dirigida por

DR. HILDE PÉREZ GARCÍA

Desarrollada por

RUBÉN ÁLVAREZ FERNÁNDEZ

Para el cumplimiento de los requerimientos para

DOCTOR POR LA UNIVERSIDAD DE LEÓN EN EL PROGRAMA DE DOCTORADO DE INGENIERÍA DE PRODUCCIÓN Y COMPUTACIÓN

En León, agosto 2020

Agradecimientos

Una tesis doctoral es el broche final a un largo camino de esfuerzo, dedicación y trabajo, el cual es impensable acometer sin el apoyo de muchas personas, importantes desde el punto de vista personal y profesional. Ojalá pudiera en estas líneas expresar toda mi gratitud hacia ellas, y por supuesto, perdonad todos aquellos a los que no he podido referirme en estas líneas,

En primer lugar, soy quien soy gracias a mis padres. Son para mí un referente en todos los aspectos y estoy muy muy orgulloso de ellos, aunque se lo digo menos de lo que debería. Ha habido momentos duros, en ciertas ocasiones seguramente no sea alguien fácil de aguantar, pero ellos siempre han estado y estarán a mí lado. Esto sólo es el comienzo, y estoy seguro de que lo mejor está siempre por venir.

A Hilde, mi directora de tesis, que confió en mí ciegas y me abrió las puertas de la investigación universitaria. Es de esas pocas personas que te encuentras en tu vida que siempre quieres mantener en ella. Gracias por tu conocimiento, por lo que nos has enseñado, por cómo nos has tratado, por lo que hemos compartido, y, sobre todo, por todo lo que nos queda por compartir.

Muy especialmente a Javi, amigo y compañero de tesis, de investigación, de clase… Te estoy tremendamente agradecido por todo lo que has hecho por mí, y como te he dicho más de una vez, no estaría donde estoy de no ser por ti. Ha sido un honor y un placer investigar todos estos años juntos, aprender de ti, y poder entendernos tan bien. Muchas gracias por tu apoyo continuo, y sabes muy bien que sólo estábamos calentando, el partido lo empezamos a jugar ahora.

A Paula y Rubén Ferrero por ayudar durante el proceso final de este trabajo. Tenéis una tenacidad y una capacidad que muy pocas personas poseen, y eso os asegura un futuro brillante en lo que os propongáis. Ahora os toca a vosotros emprender este camino, y estar seguros de que tendréis todo mi apoyo.

A Drotium, lugar en el que desarrollé gran parte de la investigación y que me enseñó muchas de las aptitudes necesarias para poder entrar al mundo laboral. La libertad y la confianza recibida fueron uno de los pilares sobre los que comenzó este largo camino, y solo tengo palabras de agradecimiento. Muchas gracias a Efrén Alonso, Daniel Broco, José Carlos Santiago, Álvaro Sánchez, Álvaro Álvarez, Hugo Villar y Álvaro Rey Antón por toda la

colaboración, buenos ratos y amistad.

A todos mis amigos y conocidos, los que saben cómo soy de verdad, en mis ratos buenos y no tan buenos. Todos aquellos que me hayan sacado una sonrisa, pueden sentir su granito de arena en este trabajo. De todos ellos muchas gracias a mi amigo-hermano Diego, por todos los ratos que hemos pasado juntos y los que nos queda por pasar (te queda mucho que aguantarme).

También agradecer a todos los profesores y docentes que he tenido a lo largo de mi vida. De todos ellos he aprendido algo, y esas aportaciones las llevo conmigo para el resto de mis días.

Finalmente, gracias a la Universidad de León. Hace casi 8 años que comencé mi andadura, primero en mi etapa de formación universitaria y ahora como investigador, y sigo estando tan orgulloso del primer día por pertenecer a ella.

Table of contents

List of figures

List of tables

Abstract

The development and implementation of future applications built upon autonomous navigation technologies are tightly connected to high-performing positioning systems that locate targets with great accuracy, stability, and robustness in harsh environmental conditions.

Local Positioning Systems (LPS) stand out as promising technologies to accomplish these requirements, through the adaptable deployment of multiple sensors of the selected positioning architecture in the proximities of the objects to provide the location service, diminishing the adverse effects on signals and maximizing the global throughput of the system. However, LPS performance is directly dependent on the location of the sensors of the positioning architecture, being this optimization problem characterized into the NP-Hard category problems, for which reaching the exact solution in polynomial time is not possible.

The positioning technology implemented in the LPS also massively impacts the global throughput of the system. Time-based location techniques are universally extended due to their trade-off among accuracy, effectiveness, enforceability, flexibility, robustness, and the ratio between cost and desired performance. Predominantly, Time-of-Arrival (TOA), Time-Difference-of-Arrival (TDOA), and asynchronous Time-Difference-of-Arrival procedures are employed. Nevertheless, there are no models for benchmarking the performance of each architecture in LPS high-demanded applications.

The objective and motivation of this dissertation is the development of a novel procedure to optimize the location of the sensors of time-based positioning architectures in high-demanding LPS applications in complex tridimensional environments. In association, in this doctoral thesis, the generation of new models to characterize the principal sources of errors of time-based positioning systems is addressed. Based on the proposed methodology, a comparative among positioning systems can be carried out, maximizing the performance of each on the desired environment, and even designing on-demand LPS and estimate their capabilities before their real implementation.

To accomplish this aim, the first step was the development of a heuristic tool based on Genetic Algorithms (GA) for optimizing sensor distributions of time-based positioning systems according to a set of pre-defined requirements. In this dissertation a GA with a new "scaling" codification is submitted with the objective of applying GA optimizations in tridimensional complex environments, regardless of the definition of the possible locations

of architecture sensors -i.e. Node Location Environment (NLE)- and objects to locate –i.e. Target Location Environment-.

The second step is the creation of accuracy models based on the Cramér-Rao Lower Bound (CRLB) for estimating the maximum capabilities of time-based positioning systems, regardless of the positioning algorithm implemented. The main advantage of this method is its foundation on the flexibility to characterize heteroscedastic behaviors in the associated variances of the factors that compound the estimation problem. This factor is especially important for LPS, where each architecture sensor is subjected to different operating conditions. Initially, a new CRLB characterization for noise uncertainties in the temporal measurements of asynchronous TDOA architectures is presented. Conventionally, noise models have been only applied to TOA and TDOA systems, where the paths of positioning signals are direct between targets and sensors. For asynchronous TDOA systems, retransmission techniques should feed into the model, together with a characterization of path-loss. Among asynchronous systems, simulations have shown that the Asynchronous Time-Difference-of-Arrival (A-TDOA) architectures outperform the rest in terms of accuracy.

Next, clock errors present in temporal measurement devices and noise uncertainties in the environment were modeled together based on a new CRLB characterization. With this model and the GA optimization with "scaling" a benchmark for estimating accuracy, stability, and robustness was established for comparing the TOA, TDOA, and A-TDOA architectures in tridimensional environments. After the optimizations, the A-TDOA system considerably outperforms the rest of architectures due to the elimination of synchronism related errors –initial time offset and time from the last synchronization– while minimizing the noise uncertainties induced by longer paths signals than other systems, becoming the only candidate to be implemented for high-demanding applications in LPS.

Lastly, Non-Line-of-Sight (NLOS) conditions were modeled into the Cramér-Rao Bound (CRB) for accuracy estimation. The new proposal employs a new ray-tracing algorithm for quantifying NLOS conditions in each communication link of the different positioning architectures in tridimensional complex environments. Also, a novel approach to detect and quantify multipath adverse effects due to the presence of objects in the Fresnel Zone and Minimum Line-of-Sight path Zone for each positioning link was developed. The combination of the proposed techniques allows the completion of multi-objective optimizations for accuracy, multipath, and cost in these positioning systems.

Resumen

El desarrollo e implementación de futuras aplicaciones construidas sobre tecnologías de navegación autónoma está fuertemente conectado a sistemas de posicionamiento de altas prestaciones que puedan localizar objetivos con gran exactitud, estabilidad y robustez en entornos con condiciones de operación severas.

Los Sistemas de Posicionamiento Locales (LPS) se erigen como tecnologías prometedoras para acometer estos requerimientos, gracias a la implementación adaptable de múltiples sensores de la arquitectura de posicionamiento seleccionada en las proximidades de los objetos a los que proporcionar el servicio de localización, disminuyendo con ello los efectos adversos sobre las señales de posicionamiento y maximizando el rendimiento global del sistema. Sin embargo, el comportamiento de los LPS es directamente dependiente de la ubicación de los sensores de las arquitecturas de posicionamiento, estando este problema de optimización caracterizado dentro de la categoría NP-Hard, siendo imposible alcanzar soluciones exactas en tiempo polinómico.

La tecnología de posicionamiento implementada en los LPS también afecta masivamente al rendimiento global del sistema. Los sistemas basados en mediciones temporales se han extendido universalmente gracias a su solución de compromiso entre exactitud, efectividad, estabilidad, flexibilidad, robustez y ratio entre coste y comportamiento del sistema deseado. Se han utilizado predominantemente las arquitecturas TOA, TDOA y TDOA asíncronas. No obstante, no existen modelos para establecer comparativas entre el rendimiento de cada arquitectura para aplicaciones de altos requerimientos en LPS.

El objetivo y motivación de esta tesis doctoral es el desarrollo de un procedimiento novedoso para optimizar la colocación de sensores de sistemas de posicionamiento basados en mediciones temporales para aplicaciones de LPS de altas prestaciones en entornos tridimensionales complejos. Unido a ello, en esta disertación se aborda la generación de nuevos modelos para caracterizar las principales fuentes de error en los sistemas basados en mediciones temporales. A partir de la metodología propuesta, se establecen comparativas entre las arquitecturas de posicionamiento, maximizando el rendimiento de cada una de ellas en el entorno en cuestión, y permitiendo el diseño bajo demanda de LPS y la estimación de sus capacidades con anterioridad a su implementación real.

Para completar este objetivo, el primer paso fue el desarrollo de una herramienta heurística basada en Algoritmos Genéticos (GA) para optimizar distribuciones de sensores

de sistema de posicionamiento de acuerdo a un conjunto de requerimientos predefinidos. En esta tesis se presenta un nuevo GA con una codificación de tipo "scaling" capaz de realizar optimizaciones tridimensionales en entornos complejos, con independencia de la definición de las posibles localizaciones de los sensores de la arquitectura de posicionamiento (NLE) y de los objetivos a ubicar (TLE).

El segundo paso es la creación de modelos de exactitud basados en la CRLB para estimar las máximas capacidades de sistemas de posicionamiento basados en mediciones temporales, independientemente del algoritmo de posicionamiento utilizado. La principal ventaja de este método es su cimentación sobre la flexibilidad a la hora de caracterizar comportamientos heterocedásticos en las varianzas asociadas a los factores que componen el problema de estimación. Este factor es especialmente importante en LPS, donde cada sensor de la arquitectura está sometido a condiciones de operación diferentes. Inicialmente, se presenta una nueva adaptación de la CRLB para incertidumbres introducidas por ruido en las mediciones temporales para arquitecturas TDOA asíncronas. Convencionalmente, los modelos de ruido han sido aplicados a sistemas TOA y TDOA, donde los trayectos de las señales de posicionamiento son directos entre objetivos y sensores. Para sistemas TDOA asíncronos, las técnicas de retransmisión deben ser embebidas dentro del modelo, junto con la caracterización de las pérdidas de propagación introducidas. Entre los sistemas asíncronos, las simulaciones demuestran que las arquitecturas A-TDOA superan en rendimiento al resto en términos de exactitud.

A continuación, los errores de los relojes presentes en los instrumentos de medición y las incertidumbres generadas por el ruido fueron modelizados conjuntamente en base a una nueva caracterización de la CRLB. Con este modelo y la optimización mediante GA con codificación de tipo "scaling" se estableció un banco de pruebas para comparar las arquitecturas TOA, TDOA y A-TDOA en entornos tridimensionales. Después de las optimizaciones, la arquitectura A-TDOA superó considerablemente al resto de sistemas debido a la eliminación de los errores relacionados con el sincronismo –desviación inicial de sincronización y lapso temporal desde la última sincronización– y la reducción de las incertidumbres inducidas por trayectos de las señales más extensos que en el resto de sistema, convirtiéndose en la única arquitectura candidata para ser implementada en LPS de altas prestaciones.

Finalmente, las condiciones de operación NLOS fueron modelizadas en la CRB para estimación de exactitud. La nueva propuesta utiliza un nuevo algoritmo de rastreo para

cuantificar las condiciones NLOS en cada uno de los enlaces de comunicación para las diferentes arquitecturas de posicionamiento en entornos complejos tridimensionales. Adicionalmente, se desarrolló un novedoso enfoque para detectar y cuantificar los efectos adversos del multipath debido a la presencia de objetos en la zona de Fresnel y la zona de Minimum Line-of-Sight path para cada enlace de comunicaciones. La combinación de las todas técnicas propuestas permite la realización de optimizaciones multiobjetivo para exactitud, multipath, y coste en estos sistemas de posicionamiento.

List of symbols and abbreviations

AI	Artificial Intelligence
AGV	Autonomous Ground Navigation
AOA	Angel-of-Arrival
A-TDOA	Asynchronous Time-Difference-of-Arrival
CRB	Cramér-Rao Bound
CRE	Clock Relative Error
CRLB	Cramér-Rao Lower Bound
CS	Coordinate Sensor
D-TDOA	Difference Time-Difference-of-Arrival
FIM	Fisher Information Matrix
FSPM	Free-Space Propagation Model
GA	Genetic Algorithms
GDOP	Geometric Dilution of Precision
GNSS	Global Navigation Satellite Systems
LOS	Line-of-Sight
LPS	Local Positioning Systems
MOP	Multiobjective Optimization
MSE	Mean Squared Error
NLE	Node Location Environment
NLP	Node Location Problem
NLOS	Non-Line-of-Sight
NOMA	Non-Orthogonal Multiple Access
PDOA	Phase Difference of Arrival
PDOP	Position Dilution of Precision
PF	Pareto Front
RMSE	Root Mean Squared Error
RSSI	Received Signal Strength Indicator
RTT	Round Trip Time
SNR	Signal Noise Ratio
TDOA	Time-Difference-of-Arrival
TDOP	Time Dilution of Precision
TLE	Target Location Environment
TOA	Time-of-Arrival
TS	Target Sensor
UAV	Unmanned Autonomous Vehicles
UWB	Ultra-Wide Band
WGN	White Gaussian Node
WS	Worker Sensor

Chapter 1

Objectives and thesis organization

1.1. Objectives

The aim of this dissertation is the generation of a new methodology that optimizes sensor distributions of Local Positioning Systems (LPS) in complex 3D scenarios for high-demanding applications, as autonomous navigation. To attain this major aim, a series of specific objectives are defined:

- Research on Genetic Algorithms (GA) as promising metaheuristic techniques for solving the Node Location Problem (NLP) that is categorized into the NP-Hard mathematical classification.
- Develop a method to combine codifications of different heuristic techniques, enabling the application of these processes to 3D complex environments.
- Quantify the uncertainties induced by the existence of noise in the environment, and derived estimation models for the primary time-based positioning technologies.
- Generate a new model to characterize the location uncertainties triggered by clock instabilities and synchronism errors in time measurement devices for the most commonly deployed time-based positioning systems.
- Address the accuracy effects of NLOS disturbances in the positioning signals in complex operating conditions.
- Design techniques to detect and minimize the multipath phenomena that induced signals degradations and incapacity to distinguish the Line of Sight (LOS) emissions from the different reflected signals from the environment.

1.2. Main contributions

A synopsis of the major contributions of this dissertation is presented hereafter:

I. An adaptation of the Cramér-Rao Lower Bound (CRLB) for noise uncertainties characterized through the Log-normal path propagation model for Asynchronous Time-Difference of Arrival (A-TDOA) and Difference Time-Difference of Arrival (D-TDOA) positioning architectures.

II. A new technique for implementing GA to the NLP on 3D complex scenarios based on a scaling stage during the transformation to binary codifications and genetic operators.

III. A novel CRLB model for accuracy estimation of time-based positioning systems based on the characterization of uncertainties in the temporal measurements induced by noise and clock instabilities.

IV. A new LOS/NLOS ray-tracing algorithm for measuring signal travel distances for positioning communication links in 3D complex environments.

V. A novel multipath detection algorithm for the identification and quantification of destructive interference and incapacity to measure LOS path in communications of time-based positioning systems for 3D complex environments.

VI. A new Cramér-Rao Bound (CRB) for accuracy estimation of time-based positioning systems operating in 3D harsh environments with LOS and NLOS combined conditions.

VII. The complete set of techniques and algorithms presented in this dissertation supplied a procedure for determining the maximum capabilities of accuracy and multipath effects avoidance for time-based positioning systems before real implementation. This enables trade-offs strategies between the accuracy and the cost of their deployment and supports the on-demand design of these systems.

1.3. Thesis organization

This dissertation is structured in the following chapters. In Chapter 2 an introduction to the general topics of the dissertation is provided. Concretely, the state of the art of positioning systems is provided together with the main location techniques based on time measurements. Also, a review of the most significant optimization techniques is supplied, highlighting heuristic methodologies and especially GA due to their suitability to solve the NLP.

Chapter 3 introduces a new characterization of the CRLB accuracy model for estimate uncertainties due to the presence of noise in the environment for Asynchronous Time-Difference of Arrival (A-TDOA) positioning architectures. Besides, a comparison in terms of performance is provided in a 3D scenario with LOS operating conditions.

In Chapter 4, a novel GA for optimizing sensor distributions of positioning systems in 3D complex sensors is explained. This new methodology is based on a new scaling stage that allows to transform Cartesian Coordinates –expressed in real numbers– to binary codification based on the local properties of the environment. Besides, genetic operators are investigated and compared to optimize an A-TDOA architecture in a 3D LOS environment.

Chapter 5 introduces a new CRLB model to jointly estimate the uncertainties induced by noise and clock errors in the environment for the most widely time-based positioning architectures –TOA, TDOA, A-TDOA–. The combination of this modeling with the GA optimization described in Chapter 4 enables the comparative among time-based positioning systems in high-demanding LPS applications.

In Chapter 6 disruptive phenomena caused by obstructions in the positioning signals environment are studied. For NLOS conditions, a new CRB model for time-based positioning architectures is presented in combination with a new LOS/NLOS ray-tracing algorithm to characterize positioning signals links. For multipath phenomena, a new technique is provided to quantify these adverse phenomena induced by the presence of objects in the Fresnel Zone and the Minimum NLOS path zone. The CRB modeling and the multipath quantification are applied in a Multi-Objective optimization (MOP) process with the GA described in Chapter 4 to optimize sensor distributions of A-TDOA architectures in 3D environments with LOS and NLOS operating conditions.

Lastly, Chapter 7 summarizes the conclusions of the dissertation and provides an overview of the future investigations linked to this thesis.

1.4. Research framework

The investigations of this dissertation have been developed under the supervision of Dr. Hilde Perez in the SINFAB group of investigation. The research was funded by the Spanish Ministry of Economy, Industry, and Competitiveness grants number DPI2016-79960-C3-2-P and number PID2019-108277GB-C21.

Chapter 2

General Introduction

2.1. Positioning systems

Real-time positioning has emerged as one of the fundamental aspects of the past and recent advancements of the technology industry. Their influence even increases for future technology breakthroughs, especially all related to autonomous navigation and the applications derived from it, as industrial collaborative robots [1], high-precision farming [2], indoor navigation [3], and precision landings [4].

The advent of autonomous navigation technologies has tightened the requirements of the location service provided by positioning systems. Concretely, these applications demand great throughput in terms of accuracy, stability, and robustness during operation in harsh environments, such as urban scenarios or indoor conditions.

Traditionally, Global Navigation Satellite Systems (GNSS) have been universally widespread for positioning applications offering accurate global coverage services [5]. Also, the deployment of satellite constellations allows to perform positioning in areas of difficult access, representing a great advance for the navigation process. However, GNSS techniques are subjected to adverse ionospheric effects [6] that degrade the positioning signals, rendering them vulnerable to hostile ground phenomena, such as massive signal-path loss [7] due to obstructions and multipath occurrence [8]. These factors induce large uncertainties during the positioning of targets, causing low accuracies and severely limiting the stability and robustness of GNSS. Augmentation techniques [9] can be locally implemented for boosting GNSS performance in pre-defined environments, however, stability and robustness throughputs discourage their deployment to autonomous navigation applications.

Local Positioning Systems (LPS) can address the high-demanding requirements typical of autonomous navigation technologies. These systems are intended over the reduction of the distance among location targets and sensors of the positioning architecture [10]. The diminution of the positioning signal paths, together with the flexibility and adaptability of the location of positioning sensors, allows the reduction of the adverse effects in positioning signals during rough operating conditions and therefore increasing the system throughput in

terms of the accuracy and especially in stability and robustness of LPS.

GNSS and LPS perform positioning based on the collection of certain measurements of physical properties, such as time [11], frequency [12], angle [13], power [14], or combination of the previous techniques [15].

Time-based positioning systems have become predominant due to their trade-off among hardware complexity, accuracy, scalability, effectiveness, robustness, and flexibility to distinct operation requirements. Angle-based architecture stands out as their accuracy and robustness in location service, however, their deployment depends on restricted operating conditions, leading to highly-local applications. Frequency techniques are especially suitable to obtain target velocities, but accuracy is generally poor and their scalability is also limited. Lastly, power-based positioning is widespread for low-demanding accuracy applications due to their implementation cost, effectiveness, and scalability.

Based on the previous description, time-based positioning architectures are the most promising methodologies to achieve high-demanding performances. These systems are distinguished by the time-lapse characteristics for determining the target location.

Time-of-Arrival (TOA) [16] techniques compute the positioning based on the absolute travel times of positioning signals between transmitter/s and receiver/s. In this sense, synchronization among all the components of the system (i.e. targets and architecture sensors) is required for obtaining temporal measurements. Geometrically, targets are situated in circumferences or spheres (2D or 3D positioning) around each TOA architecture sensor. For 3D positioning, at least four TOA sensors are needed to univocally determine the target location, due to the non-linear properties of the positioning problem.

Time-Difference-of-Arrival (TDOA)) [17] architectures perform positioning through the measurement of the difference between the travel time-lapses of the target and a pair of architecture sensor/s. For that purpose, synchronization is only demanded among system components, leaving targets without synchronization requirements for providing the location service. From the geometric point of view, targets are located in the hyperbolas or hyperboloids (2D or 3D positioning respectively) where each of the TDOA pair sensors is located at the related focuses. Contrary to TOA systems, a minimum of five TDOA sensors is requested for mathematically solved the positioning calculation.

Asynchronous TDOA methodologies are founded on the measurement of travel time-lapses from pairs of the sensor to the corresponding target, as TDOA architectures, but

avoiding the synchronism among system sensors (and also with target/s). This can be accomplished through the concentration of all the time measurements on a single sensor per zone, and assigning to the rest functions of retransmission. Depending on the positioning signals paths, different technologies have been developed in the last years [18].

The combination of LPS with time-based positioning architectures encourages the boosting in these systems throughput needed for future high-demanding applications. However, serious difficulties arise when designing their deployment: optimizing LPS sensors distributions based on realistic estimations of the performance of these architectures in complex environments.

2.2. Heuristic techniques: Genetic Algorithms

Apart from the time-based technology implemented and the selected positioning algorithm, location uncertainties are directly influenced by the distribution of architecture sensors, which is commonly referred to as the Node Location Problem (NLP). The NLP has been classified as NP-Hard mathematical problem [19] [20] due to the absence of exact algorithms for solving it in polynomial time.

Heuristic methodologies can provide an approximate solution to the NLP problem, based on an effective exploration of the space of solutions. However, heuristic techniques cannot ensure mathematically the achievement of the global solution of the problem [21]. Besides, the optimization of positioning sensor distributions is usually subjected to non-derivate objective functions, severe discontinuities during the optimization process, and immense search spaces related to the degree of desired spatial resolution, the number of deployed sensors, and the magnitude of the optimization area.

These factors play an important role during the selection of the heuristic optimization procedure for solving each NLP. Plenty of heuristic methodologies based on nature-stochastic behaviors have been presented over the past decades: simulated-annealing [22], evolutionary techniques [23], genetic algorithms [24], ant colony algorithms [25], firefly algorithms [26], and dolphin swarm algorithms [27], are some examples of them. Also, diversified local search strategies [28] and Tabu searches [29] have become popular to solve NP problems. In essence, all heuristic methods present two distinct stages during the exploration of the solutions space. Firstly, a diversification phase is performed where algorithms try to examine multiple zones of the spaces of solutions, applying all the resources to the discovery of a possible global maximum/minimum area. Then, an intensification stage

allows us to deeply explore the most promising areas for finding the global solution. Here relies the complexity of the heuristic methods, during exploration of the solutions space algorithms should escape from local optimizations, without any external source of information for helping the process.

Based on this, the selection of the heuristic procedure is dependent on the adaptation of the diversification and exploration stages for the corresponding problem. For NLP resolution, Genetic Algorithms (GA) present great flexibility to model complex problems, optimizations with non-derivable objective functions, robustness and possibility of parallelization during the optimization process, and control over the diversification and intensification stages, leveraging all the benefits of heuristic approaches.

GA [30] are founded on the paradigms of Darwin's theory of evolution, where the adaptability of the individuals to the environment is the factor that determines their survival and the possibility to engender descendants with better aptitudes than their antecessors, exposed to stochastic behaviors in form of mutations. Based on this, GA are built upon the initial definition of a random population of individuals (i.e. possible solutions to the optimization problem). Their adaptation to the environment is evaluated through the fitness function, which characterizes the optimization problem. Afterward, a set of genetic operators for selection, reproduction and mutation are applied for generating a new population of individuals. Final solutions are obtained via the repetition of this process (i.e. generations), with the progressive enhancement of the fitness function value of the individuals of the new populations, until the conditions of convergence (pre-defined for each optimization) or a pre-fixed number of generations is reached.

GA must implement a codification technique that transforms the variables of the optimization problem to a specified form for applying the generic operators (especially crossover and mutation). In the original GA manuscript, binary codification where introduced ensuring maximum flexibility to design generic operators to each problem and control over the optimization process. Nevertheless, this approach cannot be applied for every optimization problem, and alternative approaches appeared [31].

2.3. Accuracy models in time-based positioning systems

The estimation of accuracy in positioning systems, and particularly time-based architectures, have received massive research attention over the past decades. Historically, accuracy models were dominated by the Geometric Dilution of Position (GDOP) [32]

estimator. This metric assumes homoscedasticity in the variances associated with each temporal measurement, leading to models where probability distributions among architecture sensors were invariants (i.e. independent of the operating conditions and distances between targets-and sensors) [33]. This hypothesis is only assumable for GNSS, where the distance among satellites and the corresponding target and global operating conditions were similar across the architecture. Notwithstanding, LPS present heterogeneous characteristics among distinct sensors for a particular target positioning, leading to high-inaccurate estimations when GDOP models were implemented.

Heteroscedasticity in accuracy models can be introduced through the Cramér-Rao Lower Bound (CRLB) [34] . The CRLB is based on the inverse of the Fisher Information Matrix and allows the obtainment of unbiased and efficient estimations for deterministic parameters. Applied to the positioning field, based on the probabilistic distributions of uncertainties in each temporal measurement input of the positioning systems, the CRLB provides the maximum achievable accuracy regardless of the positioning algorithm implemented. The CRLB is implemented via the characterization of time-based positioning systems in terms of the path of their positioning signals to perform the correspondent time measurements, and the modeling of the uncertainties induced by the environment into these temporal measurements.

2.4. References

1. P. Barattini, C. Morand and N. M. Robertson, "A proposed gesture set for the control of industrial collaborative robots", de 2012 IEEE RO-MAN: The 21st IEEE International Symposium on Robot and Human Interactive Communication, Paris, France, 2012.
2. P. Abouzar, D. G. Michelson and M. Hamdi, "RSSI-Based Distributed Self-Localization for Wireless Sensor Networks Used in Precision Agriculture", IEEE Transactions on Wireless Communications, vol. 15, nº 10, pp. 6638 - 6650, 2016.
3. J. Tiemann, F. Schweikowski and C. Wietfeld, "Design of an UWB indoor-positioning system for UAV navigation in GNSS-denied environments", in Proc. of the 2015 International Conference on Indoor Positioning and Indoor Navigation (IPIN), Banff, AB, Canada, 2015.

4. T. Pavlenko, M. Schütz, M. Vossiek, T. Walter and S. Montenegro, "Wireless Local Positioning System for Controlled UAV Landing in GNSS-Denied Environment", in Proc. of the 2019 IEEE 5th International Workshop on Metrology for AeroSpace (MetroAeroSpace), Torino, Italy, 2019.
5. E. Realini, S. Caldera, P. L. and D. Sampietro, "Precise GNSS Positioning Using Smart Devices", Sensors, vol. 17, nº 10, p. 2434, 2017.
6. M. Mainul Hoque and N. Jakowski, "Higher order ionospheric effects in precise GNSS positioning", Journal of Geodesy, vol. 81, pp. 259-268, 2007.
7. P. D. Groves and M. Adjrad, "Likelihood-based GNSS positioning using LOS/NLOS predictions from 3D mapping and pseudoranges", GPS Solutions, vol. 21, pp. 1805-1816, 2017.
8. F. D. Nunes, F. M. Sousa and J. M. Leitao, "Gating Functions for Multipath Mitigation in GNSS BOC Signals", IEEE Transactions on Aeroespace and Electronic Systems, vol. 43, nº 3, pp. 951-964, 2007.
9. R. Sabatini, T. Moore and S. Ramasamy, "Global navigation satellite systems performance analysis and augmentation strategies in aviation", Progress in Aerospace Sciences, vol. 95, pp. 45-98, 2017.
10. P. Gulden, S. Roehr and M. Christmann, "An overview of wireless local positioning system configurations", in Proc. of the 2009 IEEE MTT-S International Microwave Workshop on Wireless Sensing, Local Positioning, and RFID, Cavtat, Croatia, 2009.
11. C. Mensing and S. Plass, "Positioning Algorithms for Cellular Networks Using TDOA", in Proc. of the 2006 IEEE International Conference on Acoustics, Speech, and Signal Processing, Toulouse, France, IEEE.
12. I. Shames, A. N. Bishop, M. Smith and B. D. Anderson, "Doppler Shift Target Localization", IEEE Transactions on Aerospace and Electronic Systems, vol. 49, nº 1, pp. 266 - 276, 2013.
13. S. Wielandt and L. De Strycker, "Indoor Multipath Assisted Angle of Arrival Localization", Sensors, vol. 17, nº 11, p. 2522, 2017.
14. G. Wang and K. Yang, "A New Approach to Sensor Node Localization Using RSS Measurements in Wireless Sensor Networks", IEEE Transactions on Wireless

Communications, vol. 10, nº 5, pp. 1389-1395, 2011.

15. S. Tomic, M. Beko and R. Dinis, "Distributed RSS-AoA Based Localization With Unknown Transmit Powers", IEEE Wireless Communications Letters, vol. 5, nº 4, pp. 392-395, 2016.
16. A. A. D'Amico, U. Mengali and L. Taponecco, "TOA Estimation with the IEEE 802.15.4a Standard", IEEE Transactions of Wireless Communications, vol. 9, nº 7, pp. 2238-2247, 2010.
17. J. Xu, M. Ma and C. L. Law, "Position Estimation Using UWB TDOA Measurements", in Proc. of the 2006 IEEE International Conference on Ultra-Wideband, Waltham, 2006.
18. S. He and X. Dong, "High-Accuracy Localization Platform Using Asynchronous Time Difference of Arrival Technology", IEEE Transactions on Instrumentation and Measurement, vol. 66, nº 7, pp. 1728 - 1742, 2017.
19. O. Tekdas and V. Isler, "Sensor placement for triangulation-based localization", IEEE transactions on Automation Science and Engineering, vol. 7, nº 3, pp. 681-685, 2010.
20. Y. Yoon and Y.-H. Kim, "An efficient genetic algorithm for maximum coverage deployment in wireless sensor networks", IEEE Transactions on Cybernetics, vol. 43, nº 5, pp. 1473-1483, 2013.
21. D. A. Grossman and O. Frieder, Information Retrieval: Algorithms and heuristics, Springer, 2004.
22. X. Wang, M. Jun-Jie, S. Wang and D.-W. Bi, "Distributed Particle Swarm Optimization and Simulated Annealing for Energy-efficient Coverage in Wireless Sensor Networks", Sensors, vol. 7, nº 5, pp. 628-648, 2007.
23. A. Trivedi, D. Srinivasan, K. Sanyal and A. Ghosh, "A Survey of Multiobjective Evolutionary Algorithms Based on Decomposition", IEEE Transactions on Evolutionary Computation, vol. 21, nº 3, pp. 440-462, 2016.
24. T. Li, G. Shao and W. Zuo, "Genetic Algorithm for Building Optimization: State-of-the-Art Survey", ICMLC 2017: Proc. of the 9th International Conference on Machine Learning and Computing, Singapore, 2017.

25. J. Liu, J. Yang, H. Liu, X. Tian and M. Gao, "An improved ant colony algorithm for robot path planning", Soft Computing, vol. 21, p. 5829–5839, 2017.

26. E. Tuba, M. Tuba and M. Beko, "Two Stage Wireless Sensor Node Localization Using Firefly Algorithm", in Proc. of the Smart trends in systems, security and sustainability, Singapore, 2018.

27. K. Kannadasan, D. R. Edla, M. C. Kongara and V. Kuppili, "M-Curves path planning model for mobile anchor node", Wireless Networks, vol. 26, pp. 2769-2783, 2019.

28. M. Laguna, A. R. Jiménez and F. Seco, "Diversified Local Search for the Optimal Layout of Beacons in an Indoor Positioning System", IIE Transactions, vol. 41, nº 3, pp. 247-259, 2009.

29. Q. Meng, F. Zhuo, R. Eglese and Q. Tang, "A Tabu Search algorithm for the vehicle routing problem with discrete split deliveries and pickups", Computers & Operations Research, vol. 100, pp. 102-116, 2016.

30. J. H. Holland, Adaptation in natural and artificial systems, Ann Arbor, MI: University of Michigan Press, 1992.

31. R. Varela, D. Serrano y M. Sierra, "New Codification Schemas for Scheduling with Genetic Algorithms", de IWINAC 2005: Artificial Intelligence and Knowledge Engineering Applications: A Bioinspired Approach, Las Palmas, Canary Islands, Spain, 2005.

32. W. Huihui, Z. Xingqun y Z. Yanhua, "Geometric dilution of precision for GPS single-point positioning based on four satellites", Journal of Systems Engineering and Electronics, vol. 19, nº 5, pp. 1058-1063, 2008.

33. N. Rajagopal, S. Chayapathy, B. Sinopoli and A. Rowe, "Beacon placement for range-based indoor localization", in Proc. of the 2016 International Conference on Indoor Positioning and Indoor Navigation, Alcalá de Henares, Spain, 2016.

34. Y. Li, G. Qi and A. Sheng, "Performance Metric on the Best Achievable Accuracy for Hybrid TOA/AOA Target Localization", IEEE Communications Letters, vol. 22, nº 7, pp. 1474-1477, 2018.

Chapter 3

Accuracy analysis in sensor networks for asynchronous positioning methods

This chapter has been published as:

Rubén Álvarez, Javier Díez-González, Efrén Alonso, Laura Fernández-Robles, Manuel Castejón-Lima, Hilde Pérez

Sensors (2019)

DOI: 10.3390/s19133024

Abstract

The accuracy requirements for sensor network positioning have grown over the last few years due to the high precision demanded in activities related with vehicles and robots. Such systems involve a wide range of specifications which must be met through positioning devices based on time measurement. These systems have been traditionally designed with the synchronization of their sensors in order to compute the position estimation. However, this synchronization introduces an error in the time determination which can be avoided through the centralization of the measurements in a single clock in a coordinate sensor. This can be found in typical architectures such as Asynchronous Time Difference of Arrival (A-TDOA) and Difference-Time Difference of Arrival (D-TDOA) systems. In this paper, a study of the suitability of these new systems based on a Cramér-Rao Lower Bound (CRLB) evaluation was performed for the first time under different 3D real environments for multiple sensor locations. The analysis was carried out through a new heteroscedastic noise variance modelling with a distance-dependent Log-normal path loss propagation model. Results showed that A-TDOA provided less uncertainty in the Root Mean Square Error (RMSE) in the positioning, while D-TDOA reduced the standard deviation and increased stability all over the domain.

3.1. Introduction

Over the past few years, positioning systems have experienced a growing importance due to the wide range of applications they present in numerous civil and military fields. Positioning methods based on satellite systems, e.g., global navigation satellite systems (GNSS), offer accurate precision with global coverage but still present accuracy issues for specific crucial tasks such as high-precision trajectories or indoor navigation. These issues have recently attracted much attention with the advent of unmanned transportation.

Positioning systems have traditionally been classified into four main groups: Time of Arrival systems (TOA) [1,2], Time Difference of Arrival systems (TDOA) [3,4], Angle of Arrival systems (AOA) [5,6], Received Signal Strength Indication systems (RSSI) [7,8], or a combination of them [9,10]. Methods based on time measurement (i.e., TOA and TDOA) have been the main exponents of recent developments, on account of their robustness, universality, and reliability, in addition to their great accuracy and relative simplicity.

Time measurements have usually been obtained in two different ways. The most common one measures time intervals by synchronizing emitter and receiver clocks, which is mandatory in the case of TOA systems. The other option comes from the synchronization of receivers, and is optional in TDOA systems. This fact significantly affects the accuracy of the positioning determination process due to the appearance of clock instabilities and the introduction of small time-offsets during the process of synchronization among elements.

Owing to the challenging accuracy requirements to be met in sensor networks, the minimization of key factors that increase the uncertainty associated with the calculation of the position is an imperative task. Location systems based on TOA processes present disadvantages in this matter. Their accuracy may be in the order of 10 cm [11–13], but time errors which can occur during the synchronization process significantly increase the uncertainties associated with the position calculation [14–16].

Conventional TDOA methods have been traditionally dependent on global synchronization amongst the receivers, reaching higher accuracy levels requiring less energy than TOA systems. Nevertheless, synchronization instabilities are still present and the system complexity is higher than TOA architectures.

Notwithstanding these previous tendencies, a new pattern has been developed over the last few years, which advocates for the implementation of asynchronous architectures wherein a single clock is used to measure the time differences of arrival characteristic of TDOA

systems. These new systems could overcome synchronization disadvantages in TDOA systems with less architecture complexity and higher sensor ubication flexibility, and they are key to this work. The main advantages of these new methods would include the elimination of the synchronization among receivers and the resulting error introduced in the measurement process [17,18].

In recent years, two different asynchronous systems have been proposed. Asynchronous TDOA [17] and difference-time TDOA [18]. These systems display an architecture based on a coordinator sensor and a collection of worker sensors. The coordinator sensor is in charge of processing the time measurements. The worker sensors collaborate in the determination of time differences. These new architectures avoid the necessity of a clock built into every sensor of the system. This fact reduces the overall costs and the complexity of the system and boosts accuracy by eliminating the interaction among sensor clocks. All these factors enhance indoor and low-level flight sensor positioning accuracy, a key factor that is driving the increasing popularity of these methods.

The aim of this article was to develop for the first time, to the extent of our knowledge, a methodology to select the suitability of these two asynchronous TDOA systems under different sensor placements in a 3D, real environment. This methodology must consider that vehicle navigation in local positioning systems (LPS) is highly affected by noisy environments, thus system evaluations must be performed at a high accuracy level even where time measurements are corrupted by noise.

Cramér–Rao Lower Bound (CRLB) is a commonly used estimator to determine the lowest possible uncertainty associated with a positioning process in line-of-sight (LOS) [19,20] and non-line-of-sight (NLOS) [21] conditions. This method models measurement uncertainties through the variance associated to every sensor range estimation.

Conventional models consider the presence of a constant variance associated to each time measurement [22]. However, to attain a higher level of accuracy in the results, it is imperative to introduce the distance between emitter and receiver in the model allowing for heteroscedasticity in time measurements [23,24]. This phenomenon is especially important in cases with medium and high signal-to-noise ratios (SNRs) in the receivers. If the SNR is reduced, the positioning pulse detection becomes significantly hampered, leading to drastic time measurement errors which reduce the accuracy of the positioning system [25].

Therefore, the hypothesis of heteroscedastic variances needs to be implemented on the

basis of a propagation LOSs model over the signal path between the emitter and the receivers [26,27], depending on the positioning methodology and the characteristics of communication amongst every single sensor of the system.

The remainder of this paper is organized as follows. In Section 3.2, a comparison of the main characteristics of asynchronous TDOA architectures studied is developed. Section 3.3 covers the main path-LOSs models used to calculate the SNR. Section 3.4 includes a study of the Cramér–Rao Lower Bound, based on a matrix model implemented for each system architecture. Section 3.5 gathers the conclusions obtained from all the studies, along with the election of the best system. Lastly, Section 3.6 presents the conclusions and completes the article.

3.2. Asynchronous TDOA Methods

In this section, the asynchronous TDOA methods will be introduced. Neither of these methods need to synchronize any element of the system, using only one clock to measure the differences in times of the TDOA system. The notation used throughout the study is the one described hereafter: TS defines the location of the Target Sensor, Coordinate Sensor (CS) represents the position of the receiver in charge of the time measurements, Worker Sensors (WS) are the rest of emitters/receivers, N is the total number of WS, and additionally, a CS must be considered, t_{START} and t_{END} represent the start and the end of the time measurement process in the CS.

3.2.1. A-TDOA

In Figure 3.1, an A-TDOA architecture is presented [17]. It proposes a passive positioning system based on one single clock in the CS node, using the positioned sensor as signal repeater.

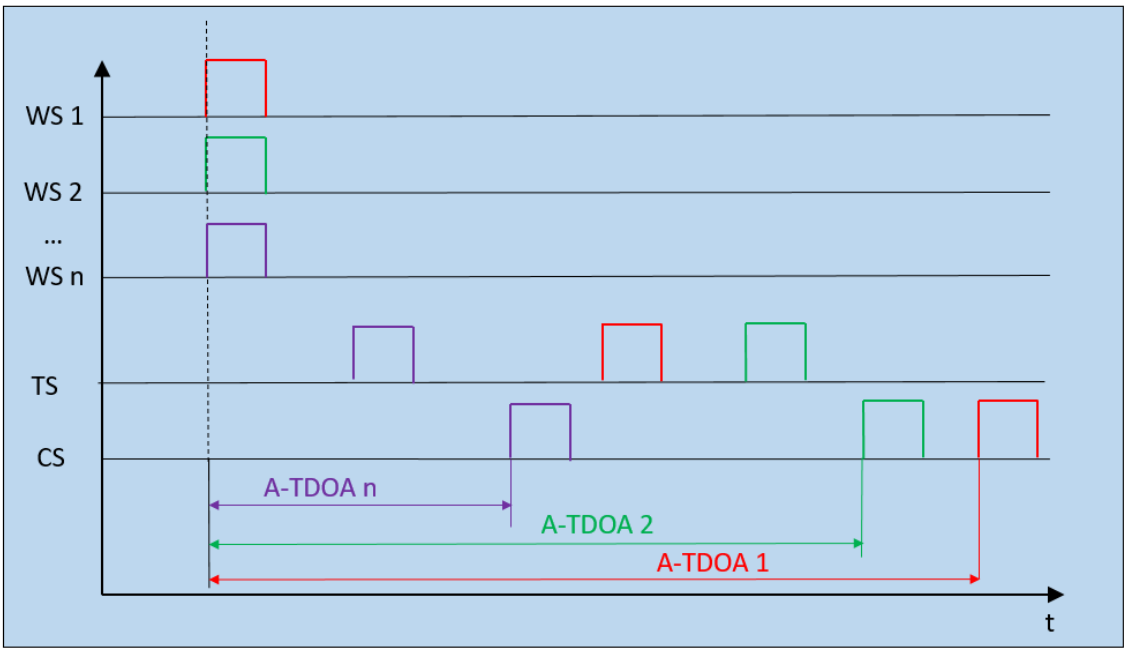

Figure 3.1. Asynchronous Time Difference of Arrival (A-TDOA) system timing diagram. Example of architecture operation with n Worker sensors (WS) nodes (n must be at least equal to 4). Rectangular positioning pulses are emitted from the WS nodes, and when the arrival of the signal to the Target Sensor (TS) node is produced, signals are instantaneously retransmitted to the Coordinate Sensor (CS) node. When the process is completed, A-TDOA time measurements are accomplished.

Positioning pulses are emitted by WS nodes, reaching the CS node with successive time differences which lead to the beginning of the time measurement associated with each WS–CS (t_{START_i}). Conversely, the signal emitted by each WS node is received by the TS node in charge of sending again these signals to the Cs node (t_{END_i}). When the signal is received, the time measurement process comes to an end, completing the time measurement process of each WS–CS pair. The TDOA measurement in terms of distance is represented by the following relation.

$$A - TDOA_i = c\left(t_{END_i} - t_{START_i}\right) - \|WS_i - CS\| \quad i \in [1, N] \tag{3.1}$$

3.2.2. D-TDOA

The D-TDOA method is based on the combination of a traditional TDOA system and a Round Trip Time (RTT) method, accomplishing the goal of obtaining the time difference measurements with only one clock [18], as shown in Figure 3.2.

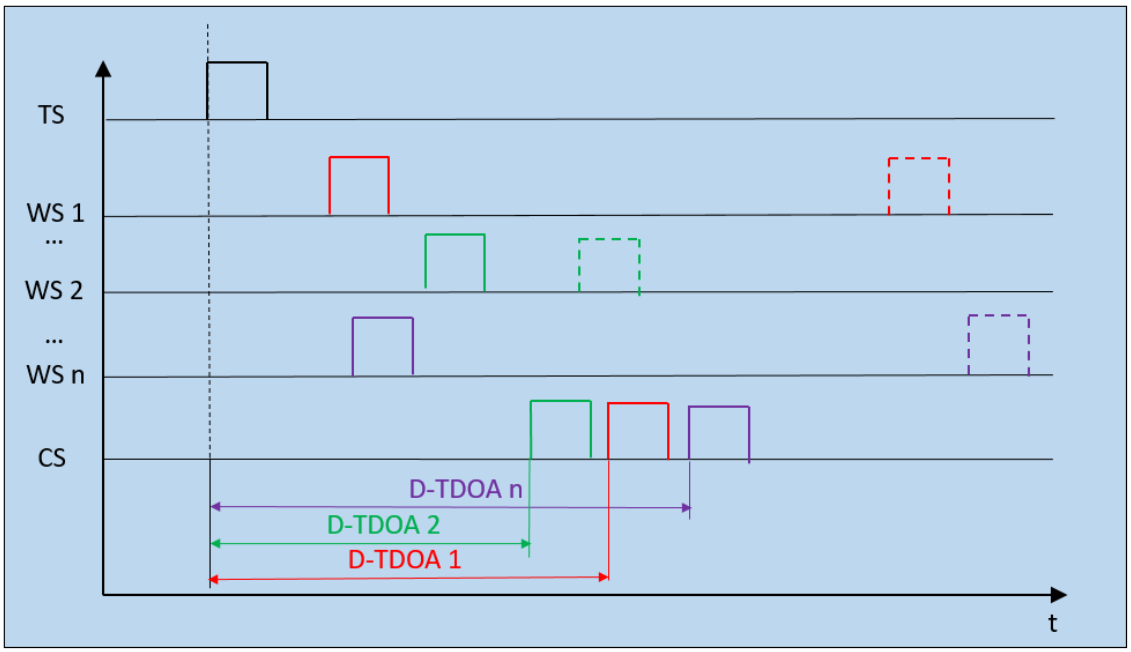

Figure 3.2. Difference-Time Difference of Arrival (D-TDOA) timing diagram. Example of architecture operation with n WS nodes (with a minimum number of 4). The positioning target pulse is received at every WS node of the system that retransmits it towards the CS node. D-TDOA time measurements are completed by a RTT process between each pair of WS–CS nodes.

Positioning pulses are broadcast by the TS node, reaching the CS node at t_{START}. This temporal reference is common to all the time measurements realized by the method. Meanwhile, the TS node emission is received at the WS nodes, which resend it to the CS node (t_{END_i}), completing the time difference measurement of each WS–CS pair of nodes. Lastly, the pulse is emitted from the CS node to WS nodes with the aim of calculating the processing time on each WS node. The TDOA measurement in terms of distance is represented by the following relation:

$$D - TDOA_i = c\left(t_{END_i} - t_{START}\right) - \|WS_i - CS\| \qquad i \in [1, N] \tag{3.2}$$

While $A - TDOA_i$ and $D - TDOA_i$ hold similar equations, the time measurement recordings and positioning pulse travels differ significantly from one method to the other. These characteristics are analyzed in the following sections.

3.3. Heteroscedastic noise model

In this section, a noise variance distance-dependent model is implemented associated to

the process of location in asynchronous TDOAs system, allowing for a better reproducibility of real conditions.

The process starts with the TOA variance range estimate due to the noisy environments. Next, the TDOA variance range estimate is defined based on time measurement correlation assumptions. The heteroscedastic noise variance model is completed with the path-LOSs propagation model implementation that best fit with the multiple sensor network's characteristics.

Amongst the main sources of ranging errors of positioning systems based on time measurements, the most important for TDOA asynchronous techniques is the uncertainty induced by white Gaussian noise (WGN) in the propagation channel. This problem has been deeply studied for TOA architectures, quantifying it with the CRLB [25].

$$\sigma_i{}^2 \geq \frac{c^2}{(2\pi B)^2\, t_s B\, SNR_i}, \quad i = 1, \dots, M \tag{3.3}$$

where M is the total number of sensors, σ_i^2 is the receptor range estimate variance, c is the pulse propagation velocity, B is the bandwidth, t_S is the length of time during which the bandwidth is occupied, and SNR_i is the signal-to-noise ratio for each receiver.

The majority of range estimation architectures consider the product t_sB approximately unitary. This, together with the hypothesis of high levels of SNR at the receivers and efficient estimator, enables the derivation of the following relation for a TOA variance estimation [23,24].

$$\sigma_i{}^2 = \frac{c^2}{(2\pi B)^2\ SNR_i}, \quad i = 1, \dots, M \tag{3.4}$$

Based on the TOA variance estimation, the implementation for TDOA systems is made under some assumptions. He and Dong [17] proposed that the time measurements in asynchronous TDOA architectures are considered independent. Consequently, the off-diagonal elements of the covariance matrix associated with the Gaussian noise modelling are null. According to Kaune et al. [19], the variance associated with a difference distance between two nodes is the sum of the variances for each node, under the assumption of uncorrelated time measurements.

Hence:

$$\begin{gathered}\sigma_{ij}{}^2 = \sigma_i{}^2 + \sigma_j{}^2 \\ i = 1, \dots, M \\ j = 1, \dots, M\end{gathered} \tag{3.5}$$

Consequently,

$$\begin{gathered}\sigma_{ij}{}^2 = \frac{c^2}{B^2}\left(\frac{1}{SNR_i} + \frac{1}{SNR_j}\right) \\ i = 1, \dots, M \\ j = 1, \dots, M\end{gathered} \tag{3.6}$$

In Equation (6), the *SNR* associated with each receiver mainly depends on the power emission, the transmission frequency, and environment. This last aspect is characterized by means of path-LOSs propagation models for indoor and outdoor environments. Large-scale models predict the mean signal strength in LOS environments based on the distance between emitter/receiver and the characteristics of the signal. Small-scale or fading models characterize the rapid fluctuations of the signal when the distance of the emitter/receiver is short, in both conditions (LOS and NLOS) [27].

Multiple sensor networks with high location accuracy are used in many applications. However, in the majority of systems, path loss during operation presents a higher level of dependency on large distances of the emitter/receiver and LOS propagation.

Consequently, large-scale models seem more appropriate for this analysis. Assuming invariant power transmission and homogeneity in the operation of receivers, the following relations are established:

$$SNR_i = \frac{P_{R_i}}{P_n} = \frac{P_T/PL_i}{P_n} = \frac{P_T}{P_n}\frac{1}{PL_i}, \quad i = 1, \dots, M \tag{3.7}$$

where P_T is transmission power, P_{R_i} is the received power in each receiver, PL is the path LOSs, and P_n is the mean noise power, obtained from the Johnson–Nyquist equation:

$$P_n = k_B T_0 B \tag{3.8}$$

where k_B is the Boltzmann's constant, T_0 is the absolute temperature of the receiver input, and B is the receiver bandwidth.

Large-scale path loss models have been deeply studied in the last decades for modelling

mobile communications. The vast majority of these methods were built under some of these restrictions: emitter and receiver heights, transmission frequency, and emitter–receiver distance, among others. Under these limitations, the modelling of asynchronous TDOA architecture is not possible due to the emitter/receiver's characteristics in multiple sensor networks.

Based on the preceding assumptions, the path loss propagation model selected for the simulation is the Log-normal, which eliminates the restrictions on emitter–receiver geometry.

$$LOG-NORMAL: \quad PL_i = PL(d_0)\left(\frac{d_i}{d_0}\right)^n \tag{3.9}$$

The noise model final implementation in the CRLB variance definition is presented below:

$$\sigma_{ij}{}^2 = \frac{c^2}{B^2\left({}^{P_T}/_{P_n}\right)} PL(d_0)\left[\left(\frac{d_i}{d_0}\right)^n + \left(\frac{d_j}{d_0}\right)^n\right] \quad \begin{matrix} i = 1,\dots,M \\ j = 1,\dots,M \end{matrix} \tag{3.10}$$

where d_0 is the reference distance to the emitter, the basis from which the Log-normal model hypothesis is valid, $PL(d_0)$ is the path loss for this distance, and n is the path loss exponent.

3.4. CRLB derivation for A-TDOA and D-TDOA systems

The prediction of the uncertainty associated with the position calculation process is one of the most significant accomplishments in the design and development of positioning systems.

From a statistical point of view, CRLB expresses the minimum variance value of any unbiased estimator of a deterministic parameter. In other words, the CRLB defines the minimum possible uncertainty associated with an estimation process.

$$var(\hat{\theta}) \geq \frac{1}{FIM} = \frac{1}{E\left[\left[\frac{\partial}{\partial x} ln\, f(X;\theta)\right]^2\right]} \tag{3.11}$$

In this equation, $\widehat{\boldsymbol{\theta}}$ is the unbiased estimator for the parameter of study, *FIM* is the Fisher Information Matrix, E the expectation value of the denominator function, X the parameter

measurement vector, θ is the parameter vector to be estimated, and *f (***X***;* $\boldsymbol{\theta}$*)* is the probability density function of **X** for the parameter $\boldsymbol{\theta}$.

Cramér-Rao Lower Bound has proved to be especially suitable in positioning. This is due to its definition based on a prior knowledge possibility of maximum reachable exactitude in terms of the architecture geometry, the environment modelling, and the intrinsic characteristics of measurement instruments. This maximum value reached by the position estimator would be valid as long as it is unbiased and efficient.

In this section, the CRLB is adapted to A-TDOA and D-TDOA architectures. Additionally, the noise variance model introduced in Section 3.3 is implemented in order to estimate the RMSE in the TS location estimation.

For a TDOA system, time measurements associated with the receivers are modelled by the addition of WGN. In a real environment, the variance associated with this phenomenon depends on the distance between emitter and receiver, inducing heteroscedasticity in data management. In this context, Kaune et al. [19] includes a model of the dependent parameter's variance in the calculation of the inverse of the Fisher Information Matrix (**J**).

$$J = \frac{1}{\sigma^2(X)}\left(\frac{\partial h(X)}{\partial X}\right)^T\left(\frac{\partial h(X)}{\partial X}\right) + \frac{1}{2}\frac{1}{\sigma^2(X)}\left(\frac{\partial \sigma(X)}{\partial X}\right)^T\left(\frac{\partial \sigma(X)}{\partial X}\right) \tag{3.12}$$

That can be expressed in matrix form as:

$$J_{mn} = \left(\frac{\partial h(X)}{\partial x_m}\right)^T R^{-1}(X)\left(\frac{\partial h(X)}{\partial x_n}\right) + \frac{1}{2}tr\left(R^{-1}(X)\left(\frac{\partial R(X)}{\partial x_m}\right)R^{-1}(X)\left(\frac{\partial R(X)}{\partial x_n}\right)\right) \tag{3.13}$$

where sub-indexes *m* and *n* refer to the respective row and column of **J**. The column matrix **h(X)** expresses the differences in the Euclidean distances among the TDOA measurements of each pair of receivers:

$$h_{A-TDOA} = \|TS - WS_i\| + \|TS - CS\| - \|WS_i - CS\| \qquad i = 1, \dots, M \tag{3.14}$$

$$h_{D-TDOA} = \|TS - WS_i\| + \|WS_i - CS\| - \|TS - CS\| \qquad i = 1, \dots, M \tag{3.15}$$

Finally, **R(x)** is the covariance matrix of the system, which is characterized by null off-

diagonal elements for both systems, due to the non-correlation among time measurements. The variance modelling was implemented according to the model explained in Section 3.3, with the following definition for the distances between each asynchronous TDOA system.

$$\begin{matrix} d_{A-TDOA\ i} = \|TS - WS_i\| + \|TS - CS\| \\ d_{A-TDOA\ j=1} = \|WS_i - CS\| \\ i = 1, \dots, M \end{matrix} \tag{3.16}$$

$$\begin{matrix} d_{D-TDOA\ i} = \|TS - WS_i\| + 2\|WS_i - CS\| \\ d_{D-TDOA\ j=1} = \|TS - CS\| \\ i = 1, \dots, M \end{matrix} \tag{3.17}$$

The uncertainty is evaluated in terms of RMSE, as shown in the following equation (three-dimensional location), where the sub-indexes refer to the diagonal elements of **J** matrix:

$$RMSE = \sqrt{J_{11} + J_{22} + J_{33}} \tag{3.18}$$

3.5. Simulation results

In this section, asynchronous TDOA systems A-TDOA and D-TDOA are compared for sensor network positioning. Firstly, a set of global communication parameters are defined in Table 3.1.

Table 3.1. Architecture parameters for CRLB study. Communication links amongst elements of A-TDOA and D-TDOA systems are restricted to these principal parameters. They were selected due to their utilization in similar tracking applications in the aerospace industry [26,27].

Parameter	Magnitude
Frequency of emission	1090 MHz
Bandwidth	100 MHz
Transmission power	400 W
Mean noise power	-94 dBm

In addition to these parameters, the comparison among architectures was carried out based on unity gain antennas in all system transceivers and on the assumption of full-duplex communication capacity among elements. Furthermore, an assumption of the receive-and-retransmit technique in transceivers operations and a unity frequency–time product in all the architectures' communications was considered.

The results were obtained based on simulations carried out on an irregular surface of 1 km^2 (1000 × 1000 m) with an elevation modelled by a normal distribution $N(15, 9)$ cm. The space analysis was limited to a height above ground level from 1 to 100 m. Under this assumption, the spatial discretization was 100 m for surface coordinates (Cartesian x and y) and 10 m for coordinate z. Additionally, the minimum height of sensor nodes (WS and CS) was restricted to 3 m with the objective of not inducing effects that were not considered by the Log-normal model (specially ground reflections and multipath). The maximum height was also limited to 13 m, but this restriction was related to the size of the supports (less than 10 m). Lastly, a path LOSs exponent value of 2.1 was selected as highly recommended in sub-urban environments with medium frequencies [27]. Due to the theoretical approach of the problem, the Free Space Propagation Model (FSPM) was used to obtain $PL(d_0)$.

The comparison among systems (in Table 3.2) was carried out with five random distributions of receivers, each one with a number of five sensors. This was the minimum number of nodes for a unique three-dimensional location in TDOA architectures. The best distributions for each system are illustrated in the following images, together with the CRLB evaluation in terms of RMSE at every point of the discretization.

Table 3.2. Node distributions in meters. Five random node distributions were defined in order to analyze the accuracy level of A-TDOA and D-TDOA architectures based on their CRLB system definition. CRLB evaluation does not require a classification of WS and CS nodes.

Distributions		x (m)	y (m)	z (m)
D.1	Sensor 1	249	242	3
	Sensor 2	254	759	4
	Sensor 3	576	500	3
	Sensor 4	811	124	13
	Sensor 5	879	819	13
D.2	Sensor 1	72	156	3
	Sensor 2	141	854	13
	Sensor 3	496	484	3
	Sensor 4	810	891	3
	Sensor 5	876	133	13
D.3	Sensor 1	78	911	13
	Sensor 2	244	241	13
	Sensor 3	516	539	3
	Sensor 4	624	655	13
	Sensor 5	810	891	3
D.4	Sensor 1	191	880	10
	Sensor 2	435	527	3
	Sensor 3	482	198	9

	Sensor 4	758	254	3
	Sensor 5	782	788	7
D.5	Sensor 1	148	313	3
	Sensor 2	469	621	13
	Sensor 3	550	500	3
	Sensor 4	750	218	13
	Sensor 5	783	944	3

As it can be seen in Figures 3.3 and 3.4, points that are close to the surface or nodes present a higher RMSE. This phenomenon is due to the relative location between nodes and these discretization points, that causes an increase of the influence of time measurements uncertainties in total positioning accuracy.

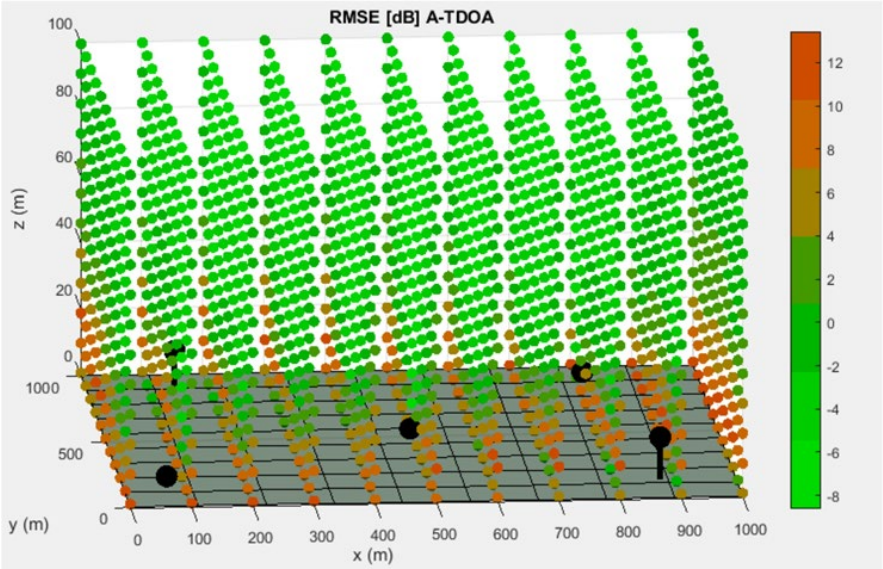

Figure 3.3. Best distribution of Worker Sensor (WS) and Coordinator Sensor (CS) nodes for the A-TDOA system. The base surface is presented as the grey hyperplane located at the bottom of the picture. The nodes are represented by black spheres with their correspondent holder that links them to the base surface. The CRLB evaluation of the discretization points is displayed according to the right-hand side legend.

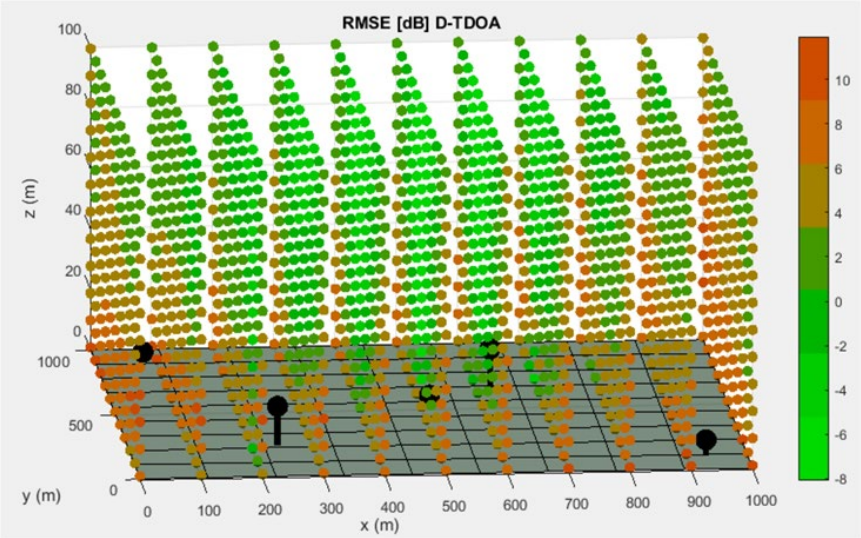

Figure 3.4. Best distribution of Worker Sensor (WS) and Coordinate Sensor (CS) nodes for the D-TDOA system. The base surface is presented as the grey hyperplane located at the bottom of the picture. The nodes are represented by black spheres with their correspondent holder that links them to the base surface. The CRLB evaluation of discretization points is displayed according to the right-hand side legend.

The final simulation results are presented in Table 3.3.

Table 3.3. RMSE distribution parameters for the five sensor distribution schemes in Table 3.2 are presented. These data were obtained based on the spatial discretization technique shown in Figures 3.3 and 3.4.

RMSE (dB)		**A-TDOA**	**D-TDOA**
D.1	Mean	-0.5791	2.1446
	Min	-9.3067	-8.2291
	Max	21.4022	19.1978
	SD	5.5552	4.6881
D.2	Mean	-0.9528	2.3131
	Min	-8.6153	-7.4459
	Max	13.4399	19.3637
	SD	4.6718	4.1344
D.3	Mean	0.0682	2.2769
	Min	-8.9972	-8.0968
	Max	13.2448	11.9421
	SD	4.9828	3.6965
D.4	Mean	0.2111	2.6452
	Min	-9.1009	-7.4856
	Max	17.3846	18.3655
	SD	5.7176	4.5620
D.5	Mean	0.2524	2.2070
	Min	-9.8805	-8.1964
	Max	13.3707	11.8791
	SD	5.0180	3.8402

Mean of Means RMSE	-0.2000	2.3174
Mean of SDs RMSE	5.1891	4.1842

Based on the results of the simulations, it was shown that the A-TDOA system presented a lower mean RMSE value in every distribution. The minimum RMSE values in each distribution were obtained by the A-TDOA method. In the case of maximum RMSE values, the tendency was not obvious. Finally, it can be observed that the standard deviation in every distribution was lower for the D-TDOA system, which implies a higher stability.

In terms of architecture complexity, A-TDOA systems require an initial step in the emission of the positioning pulses of the WS nodes in order to simultaneously start the process. In contrast, in D-TDOA systems, the first communication link exclusively depends on the target node emission. Energy consumption is another factor to be evaluated. Due to the lower energy requirements for amplifying the signal power at the retransmission stage in each node, A-TDOA architectures lead to better results than D-TDOA.

In summary, the A-TDOA system provides a higher accuracy than the D-TDOA method, but the latter presents a lower level of variation in the evaluation for sensor location. Although, A-TDOA architectures present more hardware complexity, they sport less energy consumption due to the reduction of the signal travel. On the basis of the information gathered, it can be concluded that the best method for multiple sensor locations is the A-TDOA system.

3.6. Discussion

The new asynchronous TDOA architectures have led to a major improvement as a consequence of the reduction of the complexity in sensor networks and the increasing accuracy of time measurements over the last few years. These methodologies have been experiencing a growing importance in LPS with particular application in robot indoor navigation and Unmanned Aerial Vehicles (UAVs).

Amongst the asynchronous architectures, A-TDOA and D-TDOA have taken special relevance, but their novelty assumed that no previous research on the suitability of these systems had been accomplished before. This means that these architectures have not been studied in an actual common environment in order to determine a comparison among their system errors that would allow us to select the best architecture under different conditions. The error bounds must be calculated through the Cramér–Rao Lower Bound estimator all over the domain. In this context, CRLB allows to determine the minimum achievable error

of a locating system with independence from the positioning algorithm used. With this parameter, the determination of the best asynchronous architecture could be done in a particular context. The extension of the usage of the LPS forces the design of an environment where CRLB must be derived in a 3D context for the first time.

This derivation includes a path-loss model propagation which depends on the distances between emitter and receiver of the positioning signal. This leads to heteroscedastic noise variances consideration that particularly fits with LPS.

The goal of this article has allowed for the development of a new methodology in order to select the best system in different contexts.

3.7. Conclusions

High accuracy requirements in modern applications lead to positioning systems where noise uncertainties must be minimized. New asynchronous positioning architectures have supposed a revolution where positioning errors have been considerably reduced. In this paper, a methodology to select the suitability of two asynchronous TDOA systems based on a CRLB evaluation under a 3D, real environment was accomplished for the first time to the best of our knowledge.

This analysis was performed based on a CRLB comparison where the uncertainties of time measurements originated by noise were distance dependent. This resulted in heteroscedasticity in the variance associated with sensor range estimation. This real model allowed us to determine the best TDOA asynchronous architecture with positioning algorithm independence.

The results showed that the A-TDOA system provided generally less uncertainty in the positioning, regardless of the node distributions. Nevertheless, the D-TDOA system achieved a better level of homogenization by reducing the RMSE standard deviation in the domain. On the basis of the information gathered, and taking into account the CRLB, it can be concluded that the best method for sensor location is the A-TDOA system.

These aspects are being treated in the current investigation, where the node distribution would be optimized for CRLB via genetic algorithms, attaining a RMSE minimization at all discretization points in future works.

3.8. References

1. D'Amico, A.A.; Mengali, U.; Taponecco, L. TOA Estimation with the IEEE

802.15.4a Standard. *IEEE Trans. Wirel. Commun.* **2010**, *9*, 2238–2247.

2. Shen, J.; Molisch, A.F.; Salmi, J. Accurate Passive Location Estimation Using TOA Measurements. *IEEE Trans. Wirel. Commun.* **2012**, *11*, 2182–2192.
3. Ho, K.C.; Lu, X.; Kovavisaruch, L. Source Localization Using TDOA and FDOA Measurements in the Presence of Receiver Location Errors: Analysis and Solution. *IEEE Trans. Signal Process.* **2007**, *55*, 684–696.
4. Xu, J.; Ma, M.; Law, C.L. Position Estimation Using UWB TDOA Measurements. In Proc. of the 2006 IEEE International Conference on Ultra-Wideband, Waltham, MA, USA, 24–27 September 2006.
5. Xu, J.; Ma, M.; Law, C.L. AOA Cooperative Position Localization. In Proc. of the IEEE Globecom 2008-2008 IEEE Global Telecommunications Conference, New Orleans, LA, USA, 30 November 2008.
6. Zhang, W.; Yin, Q.; Chen, H.; Gao, F. Distributed Angle Estimation for Localization in Wireless Sensor Networks. *IEEE Trans. Wirel. Commun.* **2013**, *12*, 527–537.
7. Wang, G.; Yang, K. A New Approach to Sensor Node Localization Using RSS Measurements in Wireless Sensor Networks. *IEEE Trans. Wirel. Commun.* **2011**, *10*, 1389–1395.
8. Weiss, A.J. On the Accuracy of a Cellular Location System Based on RSS Measurements. *IEEE Trans. Vehicular Technol.* **2003**, *52*, 1508–1518.
9. Patwari, N.; Ash, J.N.; Kyperountas, S.; Hero, A.O.; Moses, R.L.; Correal, N.S. Locating the Nodes. *IEEE Signal Process. Mag.* **2005**, *22*, 54–69.
10. D'Amico, A.A.; Mengali, U.; Taponecco, L. Joint TOA and AOA Estimation for UWB Localization Applications. *IEEE Trans. Wirel. Commun.* **2011**, *10*, 2207–2217.
11. Zou, Z.; Deng, T.; Zou, Q.; Sarmiento, D.; Jonsson, F.; Zheng, L.-R. Energy detection receiver with TOA estimation enabling positioning in passive UWB-RFID system. In Proc. of the 2010 IEEE International Conference on Ultra-Wideband, Nanjing, China, 20–23 September 2010.
12. Badorrey, R.; Hernandez, A.; Choliz, J.; Valdovinos, A.; Alastruey, I. Evaluation of TOA estimation algorithms in UWB receivers. In Proc. of the 14th European Wireless Conference, Prague, Czech Republic, 22–25 June 2008.
13. Ye, R.; Redfield, S.; Liu, H. High-precision indoor UWB localization: Technical

challenges and method. In Proc. of the 2010 IEEE International Conference on Ultra-Wideband, Nanjing, China, 20–23 September 2010.

14. Sundararaman, B.; Buy, U.; Kshemkalyani, A.D. Clock synchronization for wireless sensor networks: A survey. *Ad Hoc Netw.* **2005**, *3*, 281–323.
15. Sivrikaya, F.; Yener, B. Time synchronization in sensor networks: A survey. *IEEE Netw.* **2004**, *18*, 45–50.
16. Elson, J.; Estrin, D. Time Synchronization for Wireless Sensor Networks. In Proc. of the 15th International Parallel and Distributed Processing Symposium, San Francisco, CA, USA, 1–5 May 2000.
17. He, S.; Dong, X. High-Accuracy Localization Platform Using Asynchronous Time Difference of Arrival Technology. IEEE Trans. *Instrum. Meas.* **2017**, *66*, 1728–1742.
18. Zhou, J.; Shen, L.; Sun, Z. A New Method of D-TDOA Time Measurement Based on RTT. *MATEC Web Conf.* **2018**, *207*, 03018.
19. Kaune, R.; Hörst, J.; Koch, W. Accuracy Analysis for TDOA Localization in Sensor Networks. In Proc. of the 14th International Conference on Information Fusion, Chicago, IL, USA, 5 July 2011.
20. Jia, T.; Buehrer, R.M. A New Cramer-Rao Lower Bound for TOA-based Localization. In Proc. of the MILCOM 2008-2008 IEEE Military Communications Conference, San Diego, CA, USA, 16–19 November 2008.
21. Qi, Y.; Kobayashi, H. Cramér-Rao Lower bound for geolocation in non-line-of-sight environment. In Proc. of the 2002 IEEE International Conference on Acoustics, Speech, and Signal Processing, Orlando, FL, USA, 13–17 May 2002.
22. Chang, C.; Shai, A. Estimation Bounds for Localization. In Proc. of the 2004 First Annual IEEE Communications Society Conference on Sensor and Ad Hoc Communications and Networks, Santa Clara, CA, USA, 4–7 October 2004.
23. Huang, B.; Xie, L.; Yang, Z. Analysis of TOA Localization with Heteroscedastic Noises. In Proc. of the 33rd Chinese Control Conference, Nanjing, China, 28–30 July 2014.
24. Huang, B.; Xie, L.; Yang, Z. TDOA-Based Source Localization with Distance-Dependent Noises. *IEEE Trans. Wirel. Commun.* **2015**, *14*, 468–480.
25. Lanzisera, S.; Zats, D.; Pister, K.S.J. Radio Frequency Time-of-Flight Distance Measurement for Low-Cost Wireless Sensor Localization. *IEEE Sens. J.* **2011**, *11*,

837–845.

26. Yaro, A.S.; Sha'ameri, A.Z. Effect of Path LOSs Propagation Model on the Position Estimation Accuracy of a 3-Dimensional Minimum Configuration Multilateration System. *Int. J. Integr. Eng.* **2018**, *10*, 35–42.
27. Rappaport, T.S. Wireless Communications-Principles and Practice; Prentice Hall: Upper Saddle River, NJ, USA, 2002.

Chapter 4

Genetic algorithm approach to the 3D node localization in TDOA systems

This chapter has been published as:

Javier Díez-González, Rubén Álvarez, David González-Bárcena, Lidia Sánchez González, Manuel Castejón-Lima, Hilde Pérez

Sensors (2019)

DOI: 10.3390/s19183880

Abstract

Positioning asynchronous architectures based on time measurements are reaching growing importance in Local Positioning Systems (LPS). These architectures have special relevance in precision applications and indoor/outdoor navigation of automatic vehicles such as Automatic Ground Vehicles (AGVs) and Unmanned Aerial Vehicles (UAVs). The positioning error of these systems is conditioned by the algorithms used in the position calculation, the quality of the time measurements, and the sensor deployment of the signal receivers. Once the algorithms have been defined and the method to compute the time measurements has been selected, the only design criteria of the LPS is the distribution of the sensors in the three-dimensional space. This problem has proved to be NP-hard, and therefore a heuristic solution to the problem is recommended. In this paper, a genetic algorithm with the flexibility to be adapted to different scenarios and ground modelings is proposed. This algorithm is used to determine the best node localization in order to reduce the Cramér-Rao Lower Bound (CRLB) with a heteroscedastic noise consideration in each sensor of an Asynchronous Time Difference of Arrival (A-TDOA) architecture. The methodology proposed allows for the optimization of the 3D sensor deployment of a passive A-TDOA architecture, including ground modeling flexibility and heteroscedastic noise consideration with sequential iterations, and reducing the spatial discretization to achieve

better results. Results show that optimization with 15% of elitism and a Tournament 3 selection strategy offers the best maximization for the algorithm.

4.1. Introduction

Global Positioning Systems (GNSS) have been traditionally used to guide vehicle navigation in outdoor environments. However, the accuracy achieved by these systems has been insufficient for some tasks such as the navigation of AGVs, UAVs, precision agriculture, surveillance and espionage work, or indoor location of vehicles. For this reason, over the last few years, local positioning systems (LPS) have been developed where the proximity between their sensors and the positioning targets allows for the significant reduction of errors in positioning.

Both the GNSS and the LPS make measurements of certain parameters of the signals such as time [1], frequency [2], or power [3] in order to determine the location of the vehicles. From these models, the most popular are those based on temporary measurements because of their simplicity, robustness, accuracy, and ease of implementation. Among these temporary systems, it is possible to find the Time of Arrival (TOA) [4] and Time Difference of Arrival (TDOA) systems [5].

The TOA systems are based on the measurement of the absolute times of travel of the signal between the transmitter and the receiver. This requires synchronization between all the sensors involved in the calculation of the position, including the target. On the other hand, the TDOA systems are based on the measurement of the relative flight times of the signal reaching two different receivers. In this case, the synchronization of the sensors is optional since the computation of the time differences can be computed in a single clock in a coordinating sensor [6], as in the architecture A-TDOA [7]. The elimination of the synchronism in A-TDOA produces a global reduction of the positioning error and an increase in the stability of the position calculation over the time due to the elimination of the initial time offset and the drift [8], as these factors introduce errors in this methodology. Even though both TOA and TDOA systems can achieve better peaks of accuracy, the overall accuracy of these systems is reduced since the last synchronization of their clocks, showing the A-TDOA architecture better results and stability over the time. As a consequence, these asynchronous architectures are taking on a special relevance at present in applications that require high accuracy in positioning.

There is also a distinction in the systems according to the function of the target in the

processing of the positioning signal. The systems in which the position is calculated in a receptor of the vehicle, with the system nodes acting as emitters, are considered as direct or centralized methods, while the systems where the vehicle only sends the signal to the receiver nodes are considered as passive or decentralized methods. In this paper, the passive A-TDOA architecture has been selected according to its accuracy in highly demanded applications.

However, once the positioning architecture has been selected, along with the algorithms that allow for the calculation of the position [9–11], the only factor that allows the reduction of the global positioning error of the vehicles is the spatial distribution occupied by the sensors or satellites in space with respect to positioning targets. This spatial distribution strongly affects the system accuracy by increasing the positioning errors due to the changes in the geometric properties of the intersection of the surfaces containing the possible locations of the targets in the space [11] -spheres in TOA systems and hyperboloids in TDOA systems. An inappropriate sensor deployment can also produce an increase in the quantity of the noise received in the nodes and an increase of the multipath generated during the transmission. All these factors can be controlled through an optimized node localization.

This problem has been widely studied in recent years, although it differs significantly depending on the location of satellites in GNSS such as GPS, GLONASS, or Galileo and local positioning networks.

GNSS positioning systems seek global coverage as the main design requirement. This has led to the location of constellations of satellites that are at the same height above the earth's surface. As a consequence, the signals emitted by the satellites travel practically the same distance until they reach the positioning targets and their signals suffer distortions that could be considered homogeneous. In addition, the high cost of its satellites has promoted the search for the minimization of the deployment of satellites in space to reduce the overall costs of these systems. The satellites are all dependent on each other since the requirements of achieving a global synchronism of the positioning system significantly reduce the flexibility of the design.

On the other hand, LPS seek to maximize the accuracy in determining the position and thus they use an adequate number of sensors to reduce the errors in order to meet their needs. The altitudes in which the sensors are located are variable and highly dependent on the characteristics of the ground surface where they will be placed. The variability of the

distances between the target and the different sensors causes the heteroscedasticity of the noise measured in the sensors [12]. In addition, in LPS networks, sensors act in a more independent way since not all of them have to be interconnected with each other, and even asynchronous architectures are being developed [7,8] which increase the flexibility of these systems. As a consequence, it is necessary to establish a methodology to optimize the location of the beacons in LPS systems, considering the special characteristics of these architectures.

4.2. State of Art

The first studies on sensor location in Local Positioning Systems were focused on the minimization of the number of sensors displayed. Francis et al. [13] demonstrated that the initial linear models used to solve the node distribution problem were excessively complex. This hypothesis was supported in the large dimensionality of the solutions space, and it is the reason why he proposed a reduction of the complexity based on a grid model. Shoval et al. [14] modified the conception of the problem with the consideration of the C-N-LNR (Continuous non-linear) model in order to compute an optimization through a greedy-type algorithm. In this model, sensor location is defined between two main areas: maximum area (effective coverage of the sensor) and minimum area (where the least possible separation between sensors is considered). C-N-LNR aims for an optimization in the node distribution with special consideration of some critical points in the AGVs navigation.

The usage of heuristic methods has proven to be especially suitable for the sensor location problem. Tekdas et al. [15] and subsequently Yoon et al. [16] concluded that this distribution problem is NP-hard, which led to a heuristic method solution such as Genetic Algorithms (GA) [11,17–24], simulated annealing [25] or Tabu search methodologies [26].

The initial solutions of the problem through GA were based on Global Dilution of Precision (GDOP) as the factor to measure the quality of the sensor locations [27,28]. GDOP has been widely used in Global Positioning systems. GDOP consists of a measurement of the suitability of the relative position between the target and the sensor location, Position Dilution of Precision (PDOP), and the uncertainty of time measurements, Time Dilution of Precision (TDOP). While the TDOP depends on the measuring instruments, PDOP is a geometric factor which is determined by the calculation of the volume defined by the unitary vectors of the target with each sensor. The minimum value of the PDOP strongly depends on the number of sensors of the distribution [29].

Nevertheless, GDOP is constructed under the assumption of similar distances

between target and nodes, which happens only in satellite navigation. However, LPS can have variable distances in the target-node connection, leading to different noises in the signal receivers. Burke et al. [30] justified that noise variances can vary notably among sensors so that a heteroscedastic model in the time measurements must be considered to achieve practical results [31].

This model is evaluated in this paper through the CRLB, which is an unbiased estimator of the lowest uncertainty in a positioning system under Line-of-Sight (LOS) and Non-Line-of-Sight (NLOS) conditions [32].

A path LOSs propagation model is introduced in order to consider signal depreciation for an asynchronous positioning architecture (A-TDOA) for the first time. Furthermore, a 3D positioning of the automatic vehicles, both AGVs and UAVs, is considered in an LPS. This factor presents a novelty in comparison with the other papers considered in this revision, which are focused on 2D positioning. This consideration forces the introduction of a third coordinate as a new degree of freedom in the sensor location in the space.

In conclusion, this paper presents a 3D optimization in the sensor location of an asynchronous positioning architecture through the CRLB with heteroscedastic noises for the first time in the literature according to our best knowledge. An actual 3D environment has been defined to locate the sensors and to allow for navigation of the vehicles. The optimization process is performed via a genetic algorithm that will be presented in the paper.

The remainder of the article is organized as follows: In Section 4.3, an actual ground model is presented and the main area for navigation of the vehicles and location of the sensors are defined; in Section 4.4 the genetic algorithm characteristics are presented and its usage is justified. The evaluation of the quality of the node distributions in the genetic algorithm by means of CRLB is analyzed in Section 4.5. Section 4.6 shows the results that are then discussed in Section 4.7. And finally, Section 4.8 presents the conclusions related to the research reported in this paper.

4.3. Ground Model

The proposed GA allows the 3D optimization of the positioning sensor placement based on any base surface characterization, regardless of fluctuations in the elevation of the modeling environment. Additionally, this GA admits the generation of any optimization region at the base surface level (AGV modeling) or above it (UAV modeling).

The flexibility of the presented methodology is proven via the characterization of an

irregular 1000 × 1000 m base surface for all analysis optimizations. This modeling is defined by the projections of the ground curves on the x-z and y-z planes, which are shown in Figure 4.1. In addition, base surface elevation has been distorted with a normal distribution N(5, 1) meters.

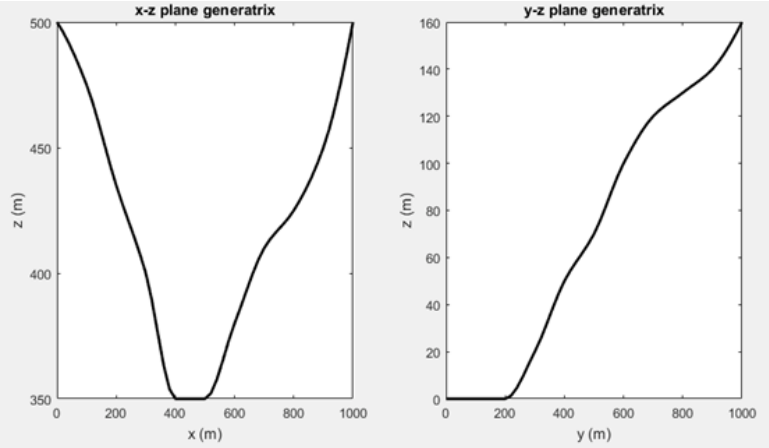

Figure 4.1. Base surface elevation profiles expressed in terms of x-z and y-z plane generatrix.

The characterization of the scenario is completely defined with two regions: Node Localization Environment (NLE) and Target Localization Environment (TLE). NLE is the space where nodes have free possible movement during genetic algorithm performance. The projection of the NLE to the base surface can have an area equal to or smaller than this, and there may be obstacle zones where the nodes cannot be located. Regarding elevation of the NLE, it is defined based on maximum and minimum elevations with respect to the modeling surface. The minimum pre-set elevation is 3 m with the aim of avoiding adverse phenomena originated by multipath trajectories that degrade the final position estimations. The maximum elevation of the nodes has been established as 10 m above the base surface, in order to limit the impact of the use of large supports to place the sensors.

TLE defines the entire space of possible locations of the targets that are going to be positioned. It is possible to perform its modeling both in the projection on the base surface and in elevation, which will be dependent on the type of optimization carried out. The lower limitation in height depends on the application to be optimized, while the upper limit will be as a general rule of 120 m (maximum flight height for UAVs).

Next, we present the two scenarios in which the final optimization of the sensor distribution will be based on the CRLB. The spatial discretization of the TLE region is 30 m

in Cartesian coordinates x-y and 5 m in the z-coordinate, in order to achieve the compromise solution between spatial resolution and processing time, taking advantage of the continuity of the accuracy results obtained when fine grids are implemented. In the case of the NLE, due to the adaptability of the length of chromosomes based on the region limits and the GA properties, the spatial resolution varies in the three coordinates from 0.5 to 1 m. In addition, if lower spatial resolutions are required, it could be achieved by the GA through the modification of the length of chromosomes to a higher value than initially determined.

Figure 4.2 shows the first of the scenarios submitted to the optimization process. The plan projection of the NLE and the TLE presents an area equal to the base surface, with the elevation limitations previously defined.

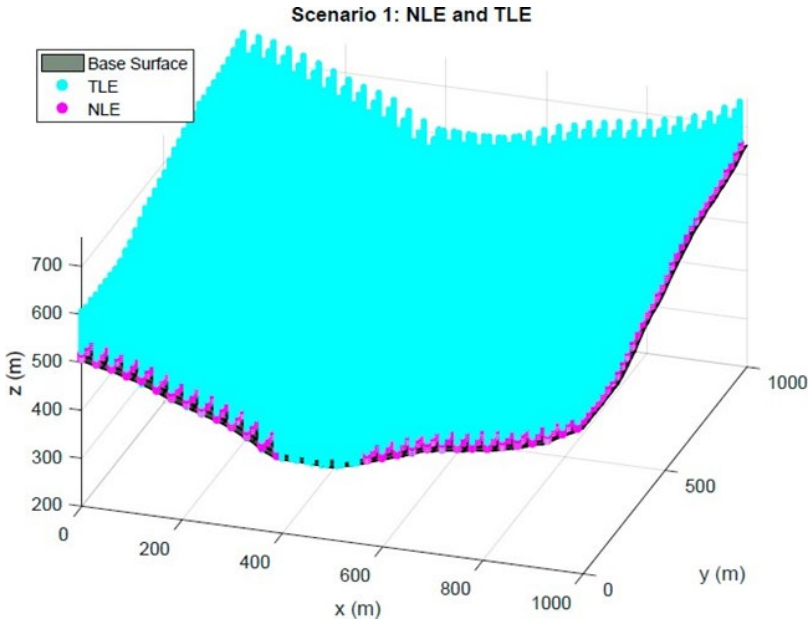

Figure 4.2. Scenario 1. First environment characterization for optimization with GA.

Figure 4.3 shows the second of the scenarios under analysis. In this case, the optimization is carried out for a TLE that extends to a bounded region of the base surface, fulfilling the limitations in elevation for Scenario 1. The NLE occupies the same volume as in Scenario 1, except for the space occupied by the TLE, which on this occasion cannot be used for the location of nodes inside it.

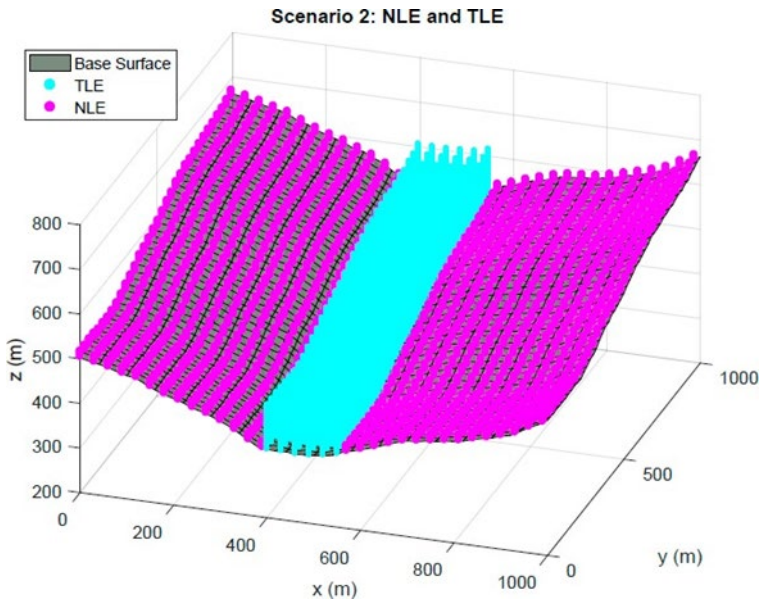

Figure 4.3. Scenario 2. Second environment representation for optimization with Genetic Algorithms–(GA). TLE region is limited to the center of the domain. NLE space extends all over the base surface, except for TLE region.

4.4. Genetic Algorithm

The total space of solutions of the optimization problem is dependent on the degree of spatial resolution required in the location of the nodes, which in turn will be determined by the spatial discretization developed on the NLE regions. For positioning of n sensors and with the spacings specified above, there will be 4624^n and 3944^n possible solutions to the problem in Scenario 1 and 2 respectively.

The magnitude of this search space prevents the use of exact resolution techniques that examine the entire spectrum of solutions to achieve the optimization of the problem in question. Additionally, greedy resolution techniques and those based on a recursive division [33] of the problem are discouraged due to the great joint dependence between the location of the different nodes and the final solution.

These aspects lead to the optimization of this problem being carried out through heuristic techniques [34]. Among them, genetic algorithms present multiple advantages, among which are great flexibility and robustness, use of non-derivable fitness functions, parallel treatment of solutions, and commitment between diversification and intensification in the search within the space of solutions. These characteristics set genetic algorithms as the final key for solving the node localization problem. Genetic algorithms are based on the hypothesis of the theory of evolution, where individuals better adapted to the environment

survive and generate descendants, who with the passing of generations will acquire better characteristics of adaptation to the environment than their predecessors [35]. In this way, this methodology starts from an initial set of random solutions whose aptitudes will be evaluated by means of a fitness function (problem optimization function). Subsequently, genetic selection, crossing, and mutation operators will be applied to generate new possible solutions to the problem from the best ones of the previous generation. This process will be repeated until the algorithm converges or until a predetermined number of generations, resulting in the final solution to optimize the problem.

4.4.1. Coding

The coding allows for the transformation of the variables of the problem to a system in which the genetic operators can be applied. The way in which it is carried out will determine to a large extent the search capacity in the solution space and the convergence of the algorithm.

The selected coding is of a binary type, facilitating the implementation of genetic operators and diversifying the search for solutions [35]. However, the evaluation of the individuals of the population must be carried out based on the Cartesian coordinates x, y, z of each of the nodes, these being expressed in real numbers.

Figure 4.4 shows an example of the transformation of the Cartesian coordinates of each node into a generic individual of the population. Real coordinates based on binary are obtained in two successive steps.

Figure 4.4. Binary coding in GA. Example of association between Cartesian node coordinates and their value in binary coding.

First, the direct conversion between binary digits and natural numbers is carried out, based on previously defined binary chain lengths. These can be invariant for all coordinates or determined based on the maximum magnitude differences possible in the scenario and for each of the coordinates. This last option is the one finally implemented because it allows for a greater homogeneity in the spatial resolution of the solutions in the three coordinates,

from 0.5 to 1 m, and total adaptability to the NLE region limits at every point of the environment.

Secondly, each of the coordinates of the nodes is transformed into natural numbers to the values in real numbers depending on the geometry of the environment. This conversion, which is called escalation, is done through the following relationship.

$$Coor_R = \frac{Coor_N}{2^L - 1}(N_{max} - N_{min}) + N_{max} \tag{4.1}$$

where $Coor_R$ is the Cartesian coordinate of the node scaled in real numbers $Coor_N$ is the Cartesian coordinate of the node expressed in natural numbers, L is the length of the binary chain associated with the coordinate in question, N_{max} is the maximum value of the coordinate in the scenario, and N_{min} is the minimum magnitude of the coordinate in the scenario.

This real-binary conversion must be carried out by means of a sequential calculation of the Cartesian coordinates of each of the nodes present in each individual of the population. In this way, first, the *x* coordinates of each node are scaled based on the knowledge of the maximum dimensions of the scenario (invariants for the *x* coordinate). Next, the coordinates are scaled and based on the spatial limitations for the direction and the scenario based on the previously scaled x coordinate. Finally, the z coordinates are scaled according to the maximum dimensions of the environment for the z-direction that is dependent on the previously scaled *x* and *y* coordinates.

The use of this methodology in any environment is linked to the implementation of some type of 1D interpolation for the scaling of the coordinates, as well as to the use of 2D interpolation for the scaling of the *z*-coordinates.

The real-binary transformation is governed by the same principles, with the proviso provision that the initial real coordinate must be a multiple of the step assigned to that scaling, where the step is expressed by the following equation:

$$Step = \frac{N_{max} - N_{min}}{2^L - 1} \tag{4.2}$$

4.4.2. Selection

The choice of genetic selection operator was based on a comparison between the most widespread in the literature: Tournament 2, Tournament 3, and Roulette [36]. In addition,

the comparative is completed with an analysis of elitism percentages for each selection procedure, searching for those that maximize the fitness function value while reducing the number of generations needed to reach convergence.

The results of the optimization are shown together with the number of generations needed in Scenarios 1 and 2, subject to the maximization of the fitness function and convergence criteria presented in Section 6. A number of 16 consecutive optimizations with the three operators has been performed in each scenario in order to avoid local maximums that could be achieved with this heuristic technique. This procedure allows for comparing the selection techniques in order to select the best fit for this problem.

Tables 4.1 and 4.2 show that the best results are obtained for a selection technique of Tournament 3 in Scenarios 1 and 2, being the option chosen for the final implementation of the GA. Tournament 2 presents more stability but does not reach the same maximum values which are the final objective of the optimization.

Table 4.1. Selection technique analysis. Mean and maximum fitness function values in Scenario 1 for Tournament 2, Tournament 3, and Roulette.

Selection Technique	Mean Fitness Function	Max Fitness Function
Tournament 2	646	656
Tournament 3	643	658
Roulette	618	649

Table 4.2. Selection technique analysis. Mean and maximum fitness function values in Scenario 2 for Tournament 2, Tournament 3, and Roulette

Selection Technique	Mean Fitness Function	Max Fitness Function
Tournament 2	757	776
Tournament 3	753	779
Roulette	708	758

Furthermore, the number of generations to reach the convergence of the algorithm is significantly reduced with Tournament 3, as can be seen in Figure 4.5, because a more competitive way in the selection of the individuals is performed. Roulette has been totally discarded because the number of generations suffers a notable increase which causes a computational time addition and the values of the optimization present more instabilities than in the other techniques.

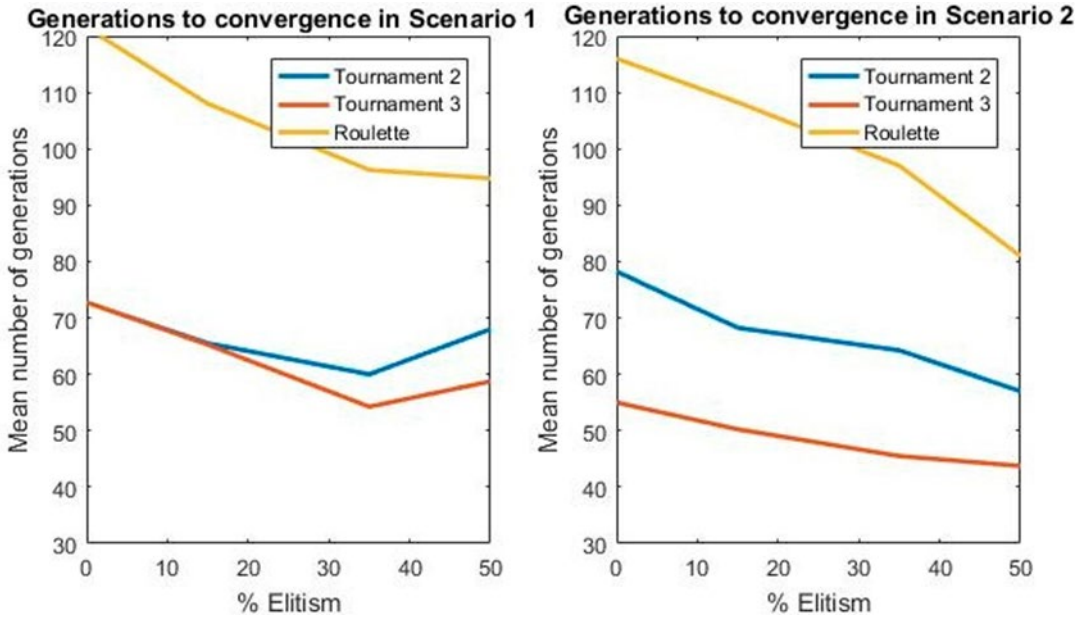

Figure 4.5. Convergence analysis in terms of elitism. In this picture, the number of generations that is needed to reach convergence is presented in Scenarios 1 and 2 in function of the percentage of elitism.

For these reasons, Tournament 3 was the final selection operator choice. Then, elitism had to be selected. Subsequently, a comparison was made for different percentages of elitism in the selected strategy, Tournament 3.

Based on Tables 4.1–4.3 it is possible to conclude that the genetic operator of selection most appropriate to this problem is Tournament 3 with 15% elitism, which is a compromise between a competitive selection and conservation of the best individuals that maximize the fitness function.

Table 4.3. Maximum fitness function representation for the best selection operator (Tournament 3) in terms of elitism percentage during population reproduction.

Elitism	Max Fitness Function Scenario 1	Max Fitness Function Scenario 2
0 %	655	778
15 %	658	779
35 %	649	752
50 %	647	749

4.4.3. Crossover and Mutation

The genetic operator of the selected crossing has been a single-point crossover. In conjunction with the selection strategy implemented, it provides an appropriate behavior as

a compromise between rapid convergence and the ability to prevent local optimums as final results. As for the mutation, a 4% probability has been selected to facilitate the initial diversification in the search for solutions without harming intensification in the optimal region of solutions.

4.5. Fitness Function and Algorithm Convergence

Genetic evolution of the generations is conditioned to an analysis of the beauty of each individual through a fitness function. In this problem, the CRLB estimator has been selected to perform the optimization of the sensor location in an asynchronous positioning architecture (A-TDOA) [6,7]. CRLB allows obtaining the minimum value of the global positioning error.

CRLB is an unbiased estimator of the lowest variance of a determining parameter. In positioning systems, CRLB determines the minimum error in the calculation of the position by any algorithm used under both LOS and NLOS conditions. CRLB estimates the variance of the position estimation by means of the Fisher Information Matrix (FIM):

$$var(\hat{\theta}) \geq \frac{1}{FIM} = \frac{1}{E\left[\left[\frac{\partial}{\partial x} ln\, f(X;\theta)\right]^2\right]} \tag{4.3}$$

Being $\widehat{\boldsymbol{\theta}}$, the unbiased estimator of the parameter under study, *E* the expectation value of the denominator function, $\boldsymbol{\theta}$ the parameter under study and $\mathbf{X}$ the measurements of this parameter that define a probability density function *f (*$\mathbf{X}$*;* $\boldsymbol{\theta}$*)*.

A White Gaussian Noise (WGN) is modeled with an association with the uncertainties of the time measurements. The variance of the WGN depends on the distance between the emitter and the receiver of the positioning signals. This leads to the heteroscedasticity of the noises. Huang et al. [31] defined a model in order to introduce all these parameters into the inverse of the FIM ($\mathbf{J}$):

$$J_{mn} = \left(\frac{\partial h(X)}{\partial x_m}\right)^T R^{-1}(X)\left(\frac{\partial h(X)}{\partial x_n}\right) + \frac{1}{2} tr\left(R^{-1}(X)\left(\frac{\partial R(X)}{\partial x_m}\right)R^{-1}(X)\left(\frac{\partial R(X)}{\partial x_n}\right)\right) \tag{4.4}$$

Matrix **h(X)** contains the information of the distance differences between the target and sensors, where m and n sub-indexes express the variables to estimate that are involved in the calculation of each FIM component. These differences are defined according to the

A-TDOA architecture [7] where the positioning signal travels from the Target Sensor (TS), Coordinator Sensor (CS)—where time differences are processed—and the Worker Sensors (WS)—where positioning signals are emitted to the Target Sensor [6]:

$$h_i = \|TS - WS_i\| + \|TS - CS\| - \|WS_i - CS\| \qquad i = 1, \dots, N_{WS} \tag{4.5}$$

where N_{WS} is the number of WS nodes. **R(X)** is the covariance matrix, where the CRLB variance definition is implemented according to a noise model characterization based on Log-normal path LOSs propagation model [37]:

$$\sigma_{ij}{}^2 = \frac{c^2}{B^2\left(P_T/P_n\right)} PL(d_0)\left[\left(\frac{d_i}{d_0}\right)^n + \left(\frac{d_{TS}}{d_0}\right)^n + \left(\frac{d_{CSi}}{d_0}\right)^n\right] \qquad i = 1, \dots, N_{WS} \tag{4.6}$$

where c is the signal propagation speed in m/s, B is the signal bandwidth in Hz, P_T is transmission power, P_n is the mean noise power that is modeled according to Johnson-Nyquist relation, n is the path loss exponent, d_0 is the reference distance between emitter and receiver from which Log-normal model is correctly implemented and $PL(d_0)$ is the path loss associated with d_0. Distances d_i, d_{TS} and d_{CS} are expressed by the following equations.

$$\begin{gathered} d_i = \|TS - WS_i\| \\ d_{TS} = \|TS - CS\| \\ d_{CSi} = \|WS_i - CS\| \\ i = 1, \dots, N_{WS} \end{gathered} \tag{4.7}$$

The Root Mean Square Error (RMSE) measures the uncertainty of the sensor location. In this model, RMSE can be obtained through the terms of the main diagonal of the inverse of the Fisher Information Matrix (**J**):

$$RMSE = \sqrt{trace(J^{-1})} \tag{4.8}$$

The analysis of the RMSE in each point of the TLE for Scenarios 1 and 2 has been defined as the fitness function in order to evaluate the quality of the sensor distributions in the A-TDOA architecture. The high amount of analysis points has led to a consideration of the mean values of the RMSE all over the TLE. The measure of the RMSE for each individual in the GA defines the best candidates to achieve the optimization, being the best

individuals directly conserved for the next generation through elitism principles defined in Section 4.2.

The converge criterion of the algorithm has been established by means of the stagnation of the maximum value of the fitness function in a number of consecutive generations. Furthermore, a number of coincidences among the individuals in the population of the last generation must be assured to stop the optimization process. This configuration allows a trade-off solution between the exploration in the space of solutions and the total processing time. Both Scenarios 1 and 2 present the best optimization results when a convergence criterion of the 80% of the individuals is considered.

4.6. Results

This section presents the results of optimizations for CRLB in an A-TDOA positioning system in Scenarios 1 and 2. Initially, a series of communication parameters linked to the positioning architecture have been defined in Table 4.4.

Table 4.4. A-TDOA system communication parameters for optimization. Their election has been made based on aeronautical tracking applications [38], with the objective of representing the use of generic technology in the CRLB analysis.

Parameter	Magnitude
Transmission power	400 W
Mean noise power	-94 dBm
Frequency of emission	1090 MHz
Bandwidth	100 MHz
Path LOSs exponent	2.1
Antennae gains	Unity
Time-Frequency product	1
Communication type	Full-duplex

The simulations presented below have been obtained based on an algorithm configuration with the Tournament 3 type selection strategy, elitism of 15%, single-point crossing, mutation probability of 4%, and binary coding with the scaling of individuals. All the optimizations have been made based on a total of 5 sensors to perform the position calculation, minimum necessary from the mathematical point of view [11] to perform 3D localization. The computational complexity of the algorithm is a polynomic order ($O(n^a)$) where super-index a is highly variable due to its dependency on the size of the TLE region, the GA population, and the number of generations to convergence. Algorithm coding and

representation have been implemented in the MATLAB platform.

First, in Figures 4.6 and 4.7, a CRLB evaluation in terms of dB in the TLE of Scenarios 1 and 2 is presented for node distributions optimized by the GA. Notable stability on the CRLB values can be observed and the results have supposed an improvement in system properties from initial random populations.

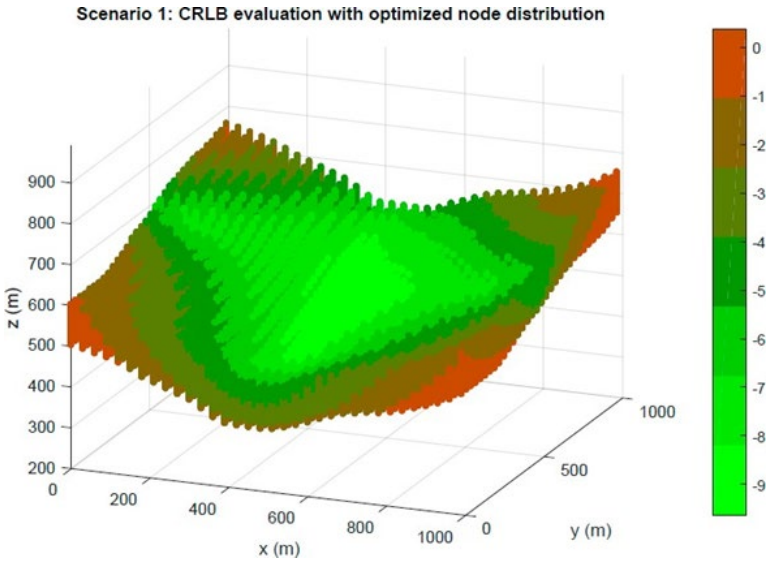

Figure 4.6. Optimization in Scenario 1. CRLB in meters for TLE region based on node location optimized by GA.

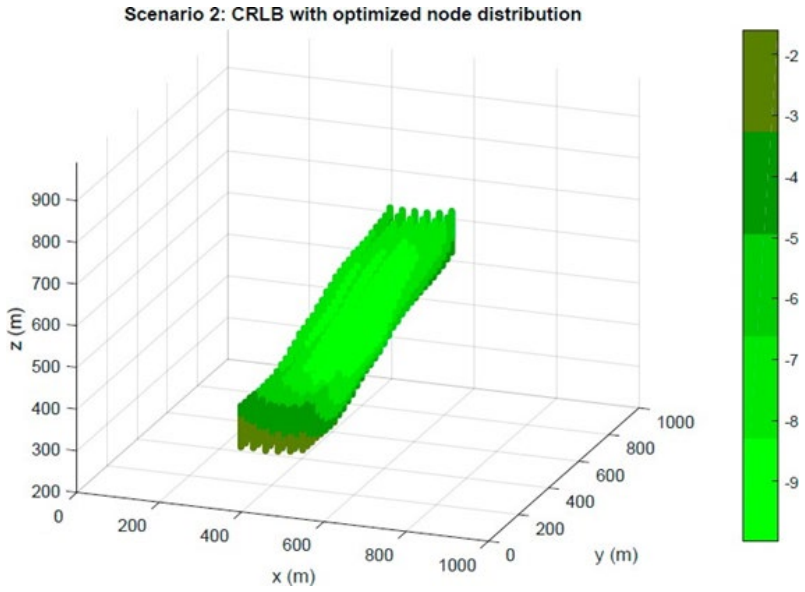

Figure 4.7. Optimization in Scenario 2. CRLB in meters for TLE region based on node location optimized by GA.

In the development of a set of optimizations with random initial populations for the

two scenarios, it has been observed, as in Figure 4.8, that whatever the initial starting population of the iterations, the convergence of each of the five beacons occurs in a very specific environment for each of them. This is due to the fact that the sensor positioning search region is very limited and shows the stability in the optimization of the genetic algorithm.

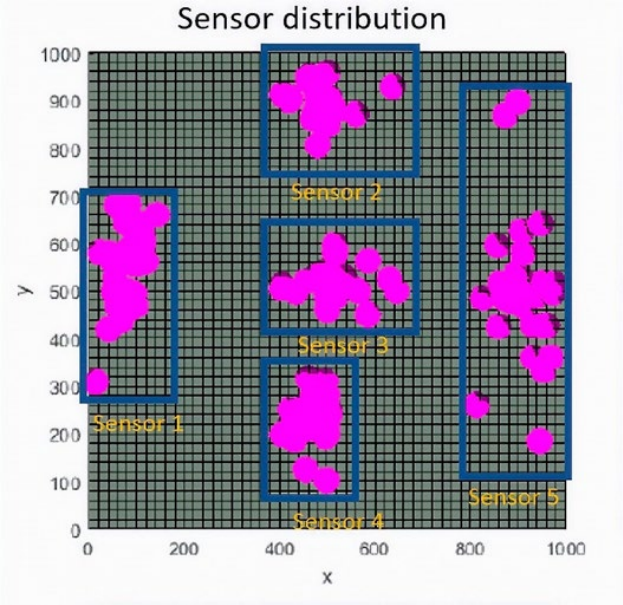

Figure 4.8. Sensor distribution in the x-y plane in meters. Each sensor defines an environment where convergence always happens during the optimization process with independence on the initial random population. In this figure the result of 48 different optimizations is represented.

With the optimization region delimited for each one of the sensors in Figure 4.8, the free movement zone of the beacons (NLE) is fixed to the environment delimited by the blue rectangles for each sensor. This way, the search space is reduced, and the convergence of the algorithm is achieved beforehand. In addition, the definition of this environment allows refining the spatial grid spacing in each coordinate, in order to obtain smaller steps and thereby obtain optimizations of the location of the sensors in the space with higher resolution and better properties.

Final results of this optimization with the new solution space properties previously defined are shown and compared with a random node distribution from the initial population of the GA in Tables 4.5 and 4.6.

Table 4.5. Final results. CRLB statistics in Scenario 1 for random and optimized node distributions of 5 A-TDOA sensors.

Scenario 1	Random Node Placement	Optimized Node Placement
Mean (m)	1.759	0.432
Max (m)	19.940	1.089
Min (m)	0.131	0.109
% < 0.5 m	11.44 %	65.43 %

Table 4.6. Final results. CRLB statistics in Scenario 2 for random and optimized node distributions of 5 A-TDOA sensors.

Scenario 2	Random Node Placement	Optimized Node Placement
Mean (m)	3.271	0.261
Max (m)	34.611	0.693
Min (m)	0.316	0.101
% < 0.5 m	6.54 %	94.56 %

These results show the possibility of using the methodology described as a sensor placement algorithm for applications with high accuracy needs in the positioning of objects. Likewise, a technique with a high degree of modularity is provided, which can be applied to any positioning architecture based on temporary measurements. Finally, the heteroscedastic characterization of the uncertainty associated with each of the temporary measurements of the system allows a high degree of correspondence with the reality, especially important in LPS systems.

4.7. Discussion

In the current article, we present the development of a genetic algorithm that allows the 3D localization of sensors in a local positioning system. This problem has special relevance since the error associated with the location of vehicles is very dependent on the spatial location of the sensors. Specifically, the sensor layout is the sole source of controllable error once the algorithms for calculating the position, the architecture of the system (A-TDOA) and the process of measuring the magnitude that allows locating times have been established.

In particular, the spatial distribution of the sensors determines the geometrical properties of the intersection of the hyperboloids in this problem [11], thus reducing the achievable error levels. For this reason, it has been shown in the state of the art that this

problem of the location of sensors has been widely studied in recent years. However, most of these articles address a two-dimensional location problem that in this article has also been extended to the third coordinate of the space to consider the flight of UAVs in local positioning systems.

In addition, these articles present very defined scenarios in indoor environments with ad-hoc resolutions for the environments designed. However, in this article, the problem-solving methodology is detailed in a generalized way for very different scenarios and contexts. This situation is particularized in two different scenarios where the modeling of the ground follows a randomness that brings the problem closer to a real context.

The studies carried out in these contexts allow us to optimize the spatial distribution of sensors for an asynchronous positioning architecture for the first time. To do this, the CRLB estimator is used to obtain the lowest error level achievable for any algorithm in the possible domain for locating the vehicles. For this reason, this article is especially relevant for locating vehicles in precision activities in outdoor environments and for indoor navigation of automatic vehicles (AGVs). The results achieved show the benefits of the selected techniques and the importance of the problem posed.

In future work, not only the optimization to reduce the CRLB but also the minimization of the number of sensors necessary for the location in a given context will be considered. For this, it will be necessary to analyze the properties of signals and receiver noises in LOS and NLOS communications, which will lead to a multivariable optimization that will improve the properties of the LPS to be studied.

4.8. Conclusions

The high accuracy requirements in the positioning system demanded in new applications such as autonomous vehicle navigation (AGVs and UAVs) or tracking of robots in industrial plants, have led to a huge increase in LPS based on asynchronous positioning architectures, as the A-TDOA. However, the intrinsic characteristics of the LPS systems cause a great dependence between the location of the sensors of the system and the degree of accuracy achieved in the positioning.

In this article, a genetic algorithm is presented for the sensor distribution in a 3D environment with total flexibility in both the definition of the optimization spaces for the location and the regions of possible location of the components of the positioning architecture. This technique has been applied to an LPS with A-TDOA architecture,

although its implementation is possible with any type of positioning system. The optimization carried out was based on the CRLB, with a WGN representation in the temporary measurements. This modeling allows heteroscedasticity in the variances associated with the temporal estimation of the sensors, which constitutes a fundamental factor in order to achieve a correct representation of reality in LPS systems.

The designed algorithm provides an optimal result for the solution of this problem since it defines a location environment for every sensor in the space of each executed simulation, showing great stability independently of the initial random population that is generated.

The definition of this solution space for each sensor allows us to reduce the search space of the solution, increasing the speed in the convergence and refining the discretization step in each coordinate in order to obtain a better resolution in the optimization.

4.9. References

1. D'Amico, A.; Mengali, U.; Taponecco, L. TOA Estimation with the IEEE 802.15.4a Standard. *IEEE Trans. Wirel. Commun.* **2010**, *9*, 2238–2247.
2. Khalife, J.J.; Kassas, Z.M. Receiver Design for Doppler Positioning with Leo Satellites. In Proc. of the ICASSP 2019—2019 IEEE International Conference on Acoustics, Speech and Signal Processing (ICASSP), Brighton, UK, 12–17 May 2019.
3. Wang, G.; Yang, K. A New Approach to Sensor Node Localization Using RSS Measurements in Wireless Sensor Networks. *IEEE Trans. Wirel. Commun.* **2011**, *10*, 1389–1395.
4. Shen, J.; Molisch, A.F.; Salmi, J. Accurate Passive Location Estimation Using TOA Measurements. *IEEE Trans. Wirel. Commun.* **2012**, *11*, 2182–2192.
5. Xu, J.; Ma, M.; Law, C.L. Position Estimation Using UWB TDOA Measurements. In Proc. of the 2006 IEEE International Conference on Ultra-Wideband, Waltham, MA, USA, 24–27 September 2006.
6. Álvarez, R.; Díez-González, J.; Alonso, E.; Fernández-Robles, L.; Castejón-Limas, M.; Pérez, H. Accuracy Analysis in Sensor Networks for Asynchronous Positioning Methods. *Sensors* **2019**, *19*, 3024.
7. He, S.; Dong, X. High-Accuracy Localization Platform Using Asynchronous Time Dierence of Arrival Technology. *IEEE Trans. Instrum. Meas.* **2017**, *66*, 1728–1742.
8. Zhou, J.; Shen, L.; Sun, Z. A New Method of D-TDOA Time Measurement Based

on RTT. In Proc. of the MATEC Web of Conferences, Jeju Island, Korea, 19–20 July 2018.

9. Mensing, C.; Plass, S. Positioning Algorithms for Cellular Networks Using TDOA. In Proc. of the 2006 IEEE International Conference on Acoustics, Speech, and Signal Processing, Toulouse, France, 14–19 May 2006.
10. Wu, P.; Su, S.; Zuo, Z.; Guo, X.; Sun, B.; Wen, X. Time Difference of Arrival (TDoA) Localization Combining Weighted Least Squares and Firefly Algorithm. *Sensors* **2019**, *19*, 2554.
11. Díez-González, J.; Álvarez, R.; Sánchez-González, L.; Fernández-Robles, L.; Pérez, H.; Castejón-Limas, M. 3D Tdoa Problem Solution with Four Receiving Nodes. *Sensors* **2019**, *19*, 2892.
12. Huang, L.X.; Yang, Z. Analysis of TOA Localization with Heteroscedastic Noises. In Proc. of the 33rd Chinese Control Conference, Nanjing, China, 28–30 July 2014.
13. Francis, R.L.; McGinnis, L.F.; White, J.A. *Facilities Layout and Location: An Analytical Approach*, 2nd ed.; Prentice-Hall: Englewood Cliffs, NJ, USA, 1992.
14. Sinriech, D.; Shoval, S. Landmark configuration for absolute positioning of autonomous vehicles. *IIE Trans.* **2000**, *32*, 613–624.
15. Tekdas, O.; Isler, V. Sensor Placement for Triangulation-Based Localization. *IEEE Trans. Autom. Sci. Eng.* **2010**, *7*, 681–685.
16. Yoon, Y.; Kim, Y.-H. An Effcient Genetic Algorithm for Maximum Coverage Deployment in Wireless Sensor Networks. *IEEE Trans. Cybern.* **2013**, *43*, 1473–1483.
17. Roa, J.O.; Jiménez, A.R.; Seco, F. Un método heurístico basado en algoritmos genéticos para optimizar la ubicación de balizas en sistemas de localización. In Proc. of the XXVII Jornadas Nacionales de Automática, Almería, Spain, 6–9 September 2006; pp. 120–129.
18. Galetto, M.; Pralio, B. Optimal sensor positioning for large scale metrology applications. *Precis. Eng.* **2010**, *43*, 563–577.
19. Qingli, Y.; Jianfeng, C. Node Placement Optimization for Distributed Sensor Network Using Adaptive Genetic Algorithm. In Proc. of the IEEE International Conference on Signal Processing, Communications and Computing, Hong Kong, China, 5–8 August 2016.
20. Jiang, N.; Jin, S.; Guo, Y. Localization of Wireless Sensor Network Based on Genetic

Algorithm. Int. J. *Comput. Commun. Control* **2013**, *8*, 825–837.

21. Peng, B.; Li, L. An improved localization algorithm based on genetic algorithm in wireless sensor networks. *Cogn. Neurodyn.* **2015**, *9*, 249–256.
22. Mnasri, S.; Thaljaoui, A.; Nasri, N.; Val, T. A genetic algorithm-based approach to optimize the coverage and the localization in the wireless audio-sensors networks. In Proc. of the IEEE International Symposium on Networks, Computers and Communications (ISNCC), Hammamet, Tunisia, 13–15 May 2015; pp. 1–6.
23. Domingo-Perez, F.; Lazaro-Galilea, J.L.; Wieser, A.; Martin-Gorostiza, E.; Salido-Monzu, D.; de la Llana, A. Sensor placement determination for range-difference positioning using evolutionary multi-objective optimization. *Expert Syst. Appl.* **2016**, *47*, 95–105.
24. Domingo-Perez, F.; Lazaro-Galilea, J.; Bravo, I.; Gardel, A.; Rodriguez, D. Optimization of the Coverage of an Indoor Positioning System with a Variable Number of Sensors. *Sensors* **2016**, *16*, 934.
25. Kammoun, S.; Pothin, J.B.; Cousin, J.C. Amélioration des performances de localisation en intérieur par optimisation du placement de balises. *Les Journ. Sci.* **2014**, *D'URSI*, 111–116.
26. Laguna, M.; Jiménez, A.R.; Seco, F. Diversified Local Search for the Optimal Layout of Beacons in an Indoor Positioning System. *IEEE Trans.* **2007**, *41*, 247–259.
27. Roa, J.O.; Jiménez, A.R.; Seco, F.; Prieto, C.; Ealo, J.; Ramos, F. Primeros resultados en la optimización de la ubicación de balizas para localización utilizando algoritmos genéticos. In Proc. of the XXVI Conference on Automation, Alicante, Spain, 7–10 September 2019; pp. 75–86.
28. Roa, J.O.; Jiménez, A.R.; Seco, F.; Prieto, J.C. Optimal placement of sensors for trilateration: Regular lattices vs meta-heuristic solutions. In Proc. of the International Conference on Computer Aided Systems Theory-EUROCAST 2007, Las Palmas de Gran Canaria, Spain, 12–16 February 2007; pp. 780–787.
29. Han, S.; Gui, Q.; Li, G.; Dulu, Y. Minimum of PDOP and its applications in inter-satellite links (ISL) establishment of Walker-δ constellation. *Adv. Space Res.* **2014**, *54*, 726–733.
30. Burke, M.; Bos, N. Optimal Placement of Range-only Beacons for Mobile Robot Localization. In Proc. of the 4th Robotics and Mechatronics Conference of South

Africa (RobMech 2011), CSIR International Conference Centre, Pretoria, South Africa, 23–25 November 2011.

31. Huang, B.; Xie, L.; Yang, Z. TDOA-Based Source Localization with Distance-Dependent Noises. *IEEE Trans. Wirel. Commun.* **2015**, *14*, 468–480.
32. Qi, Y.; Kobayashi, H. Cramér-Rao Lower bound for geolocation in non-line-of-sight environment. In Proc. of the 2002 IEEE International Conference on Acoustics, Speech, and Signal Processing, Orlando, FL, USA, 13–17 May 2002.
33. Karumanchi, N. *Algorithm Design Techniques: Recursion, Backtracking, Greedy, Divide and Conquer, and Dynamic Programming*; CareerMonk Publications: Bombay, India, 2018.
34. Simon, D. *Evolutionary Optimization Algorithms*; John Wiley & Sons: Hoboken, NJ, USA, 2013.
35. Goldberg, D.E. *Genetic Algorithms in Search, Optimization, and Machine Learning*; Addison-Wesley: Boston, MA, USA, 1989.
36. Shukla, A.; Pandey, H.M.; Mehrotra, D. Comparative Review of Selection Techniques in Genetic Algorithm. In Proc. of the IEEE International Conference on Futuristic Trends in Computational Analysis and Knowledge Management, Noida, India, 25–27 February 2015.
37. Rappaport, T.S. *Wireless Communications—Principles and Practice*; Prentice Hall: Upper Saddle River, NJ, USA, 2002.
38. Yaro, S.; Sha'ameri, A.Z. Effect of Path LOSs Propagation Model on the Position Estimation Accuracy of a 3-Dimensional Minimum Configuration Multilateration System. *Int. J. Integr. Eng.* **2018**, *10*, 35–42.

Chapter 5

Combined noise and clock CRLB error model for the optimization of node location in time positioning systems

This chapter has been published as:

Rubén Álvarez, Javier Díez-González, Lidia Sánchez González, Hilde Pérez

IEEE Access (2020)

DOI: 10.1109/ACCESS.2020.2973709

Abstract

The emergence of autonomous vehicles with high needs for accuracy in location has hardened the requirements of the positioning systems used for navigation. Local Positioning Systems (LPS) have shown an excellent adaptation to these conditions, thanks to stability and reduction in the levels of positioning uncertainty. The accuracy achieved by methodologies based on temporal measurements depends mainly on the uncertainties in the measurements of these systems. In this aspect, the presence of noise and the existence of temporary instabilities in measurement clocks, depending on the distribution of sensors in the environment, acquire great relevance. In this article, we introduce for the first time in the authors' best knowledge a Cramér-Rao Lower Bound (CRLB) model for the quantification of the global uncertainty in positioning systems caused by both noise and temporary instabilities in the measurement devices. Additionally, this technique is applied to the optimization of sensor distributions for Time of Arrival (TOA), Time Difference of Arrival (TDOA) and Asynchronous TDOA (A-TDOA) architectures using a Genetic Algorithm in a non-uniform 3D environment. Results show that A-TDOA methodology significantly overcomes synchronous architectures in terms of global accuracy and stability when noise and clock errors are considered in time measurements of LPS applications.

5.1. Introduction

The spatial location of objects in real-time has become one of the main factors of progress in current technological development. Its influence in relevant areas of modern society, such as transport, industry and security, is particularly noteworthy. Over the last few years, the emergence of autonomous vehicles has increased the accuracy and availability needs of the positioning systems as an essential part for the proper functioning and controlled navigation of these new devices through wireless communications. This dependence causes a remarkable hardening in the requirements of the positioning systems of these modern applications.

Traditionally, two main conceptions in the positioning systems design have been considered: a global coverage of the system through satellites in space trying to offer the maximum availability, or a local deployment of sensors looking for a particular adaptation to the characteristics of the environment and the positioning targets inside a known area.

Global Navigation Satellite Systems (GNSS) have represented a great advance in the history of humanity in terms of navigation. The deployment of constellations of satellites in space allows the global coverage of their signals extending even the use of the systems to difficult accessible environments. However, they present serious drawbacks when it comes to providing a stable navigation service with high accuracy services under real operating conditions. The reasons lie in the high probability of appearance of disruptive phenomena along the positioning signals path, due to the great distance between the satellites and the objects to be positioned.

The problem associated with GNSS is solved through Local Positioning Systems (LPS). These systems are built on the conception of an infrastructure of terrestrial sensors in charge of making the necessary measurements for the location. This approach entails a notable reduction in terms of the distance of the path of the positioning signal, favoring the reduction of harmful phenomena which may affect the accuracy of system measurements. Additionally, the flexibility in the location of sensors offers the advantage of adapting the system to the terrestrial orography taken into account the operating conditions of the environment, thereby increasing the position accuracy.

Regardless of the type of wireless system selected, GNSS or LPS, the location of objects requires the treatment of signals to define the position of any target in space. The systems act through the processing of signals emitted by the target, the satellites or nodes

[1]. If this signal is processed inside the target, the systems are classified as active or direct while if the signal is treated in the positioning infrastructure the systems are known as passive or indirect.

These systems depend on the acquisition of some measurements of signal and physical properties such as time, angle, power, frequency or phase to determine the location of the targets.

Time systems such as the Time of Arrival (TOA) [2] and Time Difference of Arrival (TDOA) [3] relies on the time-of- flight of the signal between an emitter and a receiver. Angle of Arrival (AOA) [4] measures the angle of an emission with respect to known position references. Received Signal Strength Indication (RSSI) [5] relies on the deterioration of the signal power in its propagation while acoustic Doppler- based systems [6] measure the differences in frequency of the signal among a set of receivers. Recent studies are also starting to combine these methods with sensor fusion [7] and including the use of multiple phase delays among the signals in Phase Difference of Arrival (PDOA) methods [8], [9].

Among all of these wireless methods, those based on temporary measurements -TOA and TDOA- stand out mainly due to their high ratio between accuracy, provided by the method- ology, and the complexity associated with architecture.

The main source of error comes from the necessary temporal synchronization between sensors in the TOA and TDOA architectures which acquires special relevance in LPS due to the higher sensitivity needs in the measurements and the increased accuracy requirements.

However, there is a difference between TOA and TDOA systems. While TOA systems require the synchronism of the clocks of every sensor involved in the localization process, TDOA systems do not require this synchronism as they mea- sure relative times of flight.

Nevertheless, the errors associated with the synchronization process in both systems are no longer negligible due to the reduction in the magnitude of the temporary measurement, making it difficult to implement these methodologies in applications with high location accuracy [10], [11].

The solution goes through the introduction of TDOA architectures of asynchronous typology, built on the basis of reduction or elimination of synchronization between the sensors of the system by centralizing all the system measurements in a single clock of a coordinator sensor. Within these systems, the Asynchronous TDOA (A-TDOA) [12] and Difference- time TDOA (D-TDOA) [13] architectures stand out. In one of our previous

works [14] we perform a comparison in terms of accuracy for these methodologies in 3D environments, obtaining the best overall results for the A-TDOA architecture. For this reason, in this article a comparison between synchronous (TOA and TDOA) and asynchronous temporal methods (A-TDOA) will be addressed. This will allow us to determine the influence of the synchronization process on the global positioning error of the systems.

However, in order to achieve valuable results, the synchronization error cannot be addressed separately from other error sources in a direct approach. Although the uncertainties linked to the temporal measurements are the main source of error in time positioning systems, this only happens when other factors are optimized. For instance, in the positioning design, the selection of the architecture and algorithms for the location determination lay down the first thresholds of uncertainty in the calculation of the position [15].

After this consideration, the attenuation of the signal power during its travel from the transmitter to the receiver due to the environment -noise errors-, the uncertainties caused by the instabilities of the measurement clocks and the occurrence of multipath must then be considered [16].

These errors are closely related to the spatial distribution of the system sensors, increasing the importance of this link in LPS. The minimization of these errors is a requirement in this article that allows the valuable comparison between synchronous and asynchronous positioning systems. Once its effects are minimized, the temporary measurements assume the greatest weight of the system error.

In this sense, the study of the optimized location of the sensors with the objective of minimizing these uncertainties in the calculation of the position has been fully studied recently. Tekdas and Isler [17] and subsequently Yoon and Kim [18] classified the problem of optimizing the distribution of sensors for positioning within the NP-hard category, which constitutes the absence of exact algorithms that resonate in polynomial time. This circumstance has directed research in this field towards the use of metaheuristic techniques, especially Genetic Algorithms (GA) [19]–[21].

The characteristics of robustness, flexibility, optimization of non-derivable and non-linear functions and space exploration of solutions have boosted the GA as the main methodology for optimizing the distribution of sensors in LPS. Historically, the

minimization of the uncertainty of the positioning was carried out based on the parameter Geometric Dilution of Position (GDOP) [22], governed by the adoption of homoscedastic noise models, where the variances have become invariants [23]. This hypothesis can be applicable in GNSS, where the distances between satellites and targets are similar. However, this does not occur in LPS where the distances traveled by the positioning signals may vary depending on the sensor receiver.

In this regard, the Cramér-Rao Lower Bound (CRLB) allows us to know the uncertainty of the positioning based on the heteroscedastic modeling of variances in temporal measurements [24]. This characterization of the error with noise consideration is made based on the models of signal propagation losses [25] and the positioning architecture in question which supposes a key fact due to the different paths of the signals in each system.

For this purpose, in one of our previous works, we have proposed the optimization of the sensor location of LPS systems in search of the minimization of the CRLB [26]. This methodology uses a GA to locate the components of the positioning system in any type of environment, regardless of its geometric characteristics and the predefined restrictions on the location of sensors.

This previous methodology contemplates one of the main causes of uncertainty in the calculation of the position as a result of the path traveled by the signals through the different locations of the system sensors. In this article, we will complete this error model with the contribution of errors caused by the temporary instabilities of the measurement clocks in the CRLB model.

This error characterization is mixing the uncertainties from the signal propagation, which are greater in A-TDOA rather than in TDOA and TOA systems as a consequence of the architecture design -the signal paths are greater-, and the clock errors which are reduced in A-TDOA systems rather than in TDOA and TOA as a consequence of the elimination of the synchronism. This fact promotes that only in scenarios where optimization has been performed, the time-based positioning systems accuracy achievable is comparable.

With this consideration, we apply for the first time in the authors' best knowledge a 3D optimization of the sensor location in any application environment for TOA, TDOA and A-TDOA architectures with the minimization of the positioning uncertainty induced by the combined effect of noise and system measurement clocks. We develop this methodology and this error modeling in order to be able to perform an a priori comparison of the suitability

of each architecture in a 3D complex environment and in order to show the effects of the synchronization process in the combined errors of each system.

The remainder of the article is organized as follows: in Section 5.2 the notation is introduced and the mathematical models of temporal instabilities of the measurement clocks for the TOA, TDOA and A-TDOA architectures are presented. Section 5.3 shows the construction of the CRLB to model the effects of noise and clock errors. Section 5.4 develops aspects related to the generation of the fitness function of the GA optimization required for the valuable comparison between architectures. Section 5.5 shows the results of the pro- posed methodology. Finally, sections 5.6 present the advances in innovation and the research conclusions.

5.2. Influence of clock errors in LPS

In this section, a characterization of time measurement errors induced by clocks in terms of positioning architectures is presented. The notation used throughout the study is described hereafter. Target Sensor (TS) indicates the target location. Coordinate Sensor (CS) represents every sensor of TOA, TDOA or A-TDOA methodologies that are capable of performing time measurements. In the case of TOA and TDOA architectures, all sensors will be CS, whereas in the A-TDOA technique [14] only one of them will possess the time measurement device. The term Worker Sensors (WS) refers to all architecture sensors without the capability of measure, acting as transponders. Lastly, NCS is the number of CS and NWS the number of WS. The described notation is presented in Figure 5.1 for TOA, TDOA and A-TDOA architectures.

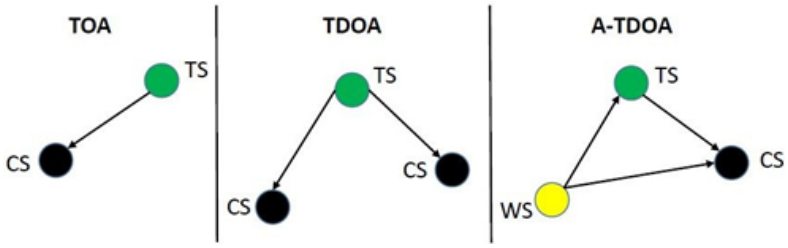

Figure 5.1. Sensor notation for TOA, TDOA and A-TDOA architectures.

Temporal instabilities in clocks originate from the appearance of additional uncertainties in time measurements during the location process. Zhou et al. [13] model clock errors according to two parameters: initial-time offset and clock drift. The initial-time offset points out the temporal delay between the reference clock used for synchronization and the

clock located in every CS of positioning architectures. Thus, this error only appears when a synchronization process is needed. The clock drift indicates the frequency deviation of the clocks, which introduces a cumulative error during time measurements. Conventionally, this clock instability is expressed in parts-per-million (ppm) or parts-per-billion (ppb).

The presence of initial-time offsets and/or clock drifts disturb time measurements in every time-based positioning methodology. However, their influence on final location accuracy depends on architecture characteristics, meaning that certain techniques are more vulnerable to these errors.

In the next paragraphs, an analysis of clock errors in time measurements of TOA ($\mathbf{T_{TOA}}$), TDOA ($\mathbf{T_{TDOA}}$) and A-TDOA ($\mathbf{T_{A\text{-}TDOA}}$) architectures is presented. This enables the modeling of these uncertainties and the collection of relationships between clock errors and the location of sensors in every architecture.

Zhou et al. [13] characterize the time measurement perturbed by clock instabilities as:

$$t = t' + U + \eta(t' - M) \tag{5.1}$$

where t indicates the clock measurement, t' indicates the ideal time measurement, U is the initial-time offset, η is the clock drift and M specifies the instant of the last process of synchronization.

Based on this error description, uncertainties in time measurements are obtained for each architecture on analysis. Firstly, relations that governed TOA methodology are presented:

$$\begin{gathered} T_{TOA_i} = t_i - t_0 \\ T_{TOA_i} = [t_i{}' + U_i + \eta_i(t_i{}' - M)] - [t_0{}' + U_0 + \eta_0(t_0{}' - M)] \\ i = 1, \dots, N_{CS} \end{gathered} \tag{5.2}$$

where the i sub-index refers to time measurements of each TOA sensor and the 0 sub-index indicates those measures carried out by the TS. Ideal time measurements are defined – t_i' and t_0' – in the following equations:

$$\begin{gathered} t_i{}' = t_0{}' + {\|TS - CS_i\|}/{c} = M + T_0 + T_i \\ t_0{}' = M + T_0 \end{gathered} \tag{5.3}$$

where T_0 is the interval between the end of the synchronization process and the instant of

the positioning pulse emission, and T_i is the amount of time required by the positioning signals to flight from the target to each CS of TOA architectures. In addition to the characterization of clocks instabilities, the temporal resolution of the implemented clocks must be considered. For this purpose, each TOA time measurement is truncated ($floor_{TR}$) based on the clock parameters of resolution.

$$\begin{aligned} T_{TOA_i} &= T_i + U_i - U_0 + T_0(\eta_i - \eta_0) + T_i\eta_i \\ CE_{TOA_i} &= \left|T_i - floor_{TR}(T_{TOA_i})\right| \end{aligned} \tag{5.4}$$

where $\mathbf{T_{TOA}}$ and $\mathbf{CE_{TOA}}$ are respectively the actual time measurement and the clock error in each TOA sensor. In the case of a TDOA architecture, time measurements with the effect of clock errors are characterized in terms of the next relations:

$$\begin{aligned} T_{TDOA_{ij}} &= (t_i - t_0) - (t_j - t_0) = t_i - t_j \\ T_{TDOA_{ij}} &= [t_i' + U_i + \eta_i(t_i' - M)] - [t_j' + U_j + \eta_j(t_j' - M)] \\ i &= 1, \dots, N_{CS} \\ j &= 1, \dots, N_{CS} \\ where\ i &\neq j \end{aligned} \tag{5.5}$$

where ideal time measurements in each sensor– t_i' and t_j'– are derived from the architecture characteristics:

$$\begin{aligned} t_i' &= t_0' + {\|TS - CS_i\|}/{c} = M + T_0 + T_i \\ t_j' &= t_0' + {\|TS - CS_j\|}/{c} = M + T_0 + T_j \end{aligned} \tag{5.6}$$

where $T_i$and T_j represent the time interval associated with the travel of the positioning signal from the target to each CS of TDOA architectures. Inserting (5.6) in (5.5) and adding the truncating effect derived from the deployment of clocks with finite time resolution:

$$\begin{aligned} T_{TDOA_{ij}} &= [T_i + U_i - U_0 + T_0(\eta_i - \eta_0) + T_i\eta_i] - [T_j + U_j - U_0 + T_0(\eta_j - \eta_0) + T_j\eta_j] \\ T_{TDOA_i} &= [T_i + U_i - U_0 + T_0(\eta_i - \eta_0) + T_i\eta_i] \\ T_{TDOA_j} &= [T_j + U_j - U_0 + T_0(\eta_j - \eta_0) + T_j\eta_j] \\ CE_{TDOA_{ij}} &= \left|T_i - floor_{TR}(T_{TDOA_i})\right| + \left|T_j - floor_{TR}\left(T_{TDOA_j}\right)\right| \end{aligned} \tag{5.7}$$

where $\mathbf{T_{TDOA}}$ and $\mathbf{CE_{TDOA}}$ represent the TDOA time measurement and the concerning error

in each TDOA measure. Time measurements uncertainties originated by clock errors in A-TDOA architecture [12], [14] are modeled by the following equations:

$$\begin{gathered} T_{A-TDOA_i} = (t_i - t_0) - (t_{CS} - t_0) = t_i - t_{CS} \\ T_{A-TDOA_i} = [t_i{}' + U_{CS} + \eta_{CS}(t_i{}' - M)] - [t_{CS}{}' + U_{CS} + \eta_{CS}(t_{CS}{}' - M)] \\ i = 1, \dots, N_{WS} \end{gathered} \tag{5.8}$$

where time measurements based on ideal conditions and in the absence of error – t_i' and t_{CS}'– are modeled through the following relations:

$$\begin{gathered} t_i{}' = t_0{}' + {\|TS - WS_i\|}/{c} + {\|TS - CS\|}/{c} = M + T_0 + T_i + T_{TS} \\ t_{CS}{}' = t_0{}' + {\|WS_i - CS\|}/{c} = M + T_0 + T_{CS_i} \end{gathered} \tag{5.9}$$

where T_i is the time of flight from the target to each WS of A-TDOA architectures, TTS is the duration that the positioning signal needs to complete the distance between the target and the CS, and T_{CSi} is referred to the period of time from the emission of the positioning signal in each WS to its reception in the CS. Combining (5.8) and (5.9) and including the time resolution effect on the measurements:

$$\begin{gathered} T_{A-TDOA_i} = (T_i + T_{TS} - T_{CS_i})(1 + \eta_{CS}) \\ CE_{A-TDOA_i} = \left|(T_i + T_{TS} - T_{CS_i}) - floor_{TR}(T_{A-TDOA_i})\right| \end{gathered} \tag{5.10}$$

where $\mathbf{T_{A\text{-}TDOA}}$ and $\mathbf{CE_{A\text{-}TDOA}}$ refer to the time measurement of each A-TDOA pair of sensors and the error introduced due to the clock instabilities.

Previous expressions reveal the key importance of the travel carried out by the positioning signal in the magnitude of the absolute error of time measurement uncertain- ties due to clock errors. However, their relativity on the final measure varies in function of the positioning architecture. This phenomenon is modeled by the Clock Relative Error (CRE) which is the ratio of absolute time error to ideal time measurement ignoring the time resolution. This is due to the independency of this factor with location methodologies:

$$CRE_{TOA_i} = \frac{\left|U_i - U_0 + T_0(\eta_i - \eta_0) + T_i\eta_i\right|}{T_i} \tag{5.11}$$

$$CRE_{TDOA_{ij}} = \frac{|U_i - U_0 + T_0(\eta_i - \eta_0) + T_i\eta_i|}{T_i} + \frac{\left|U_j - U_0 + T_0(\eta_j - \eta_0) + T_j\eta_j\right|}{T_j} \tag{5.12}$$

$$CRE_{A-TDOA_i} = \frac{|\eta_{CS}||T_i + T_{TS} - T_{CS}|}{|T_i + T_{TS} - T_{CS}|} = |\eta_{CS}| \tag{5.13}$$

These equations expose an important conclusion. CRE in A-TDOA architectures is constant and it only depends on CS clock frequency drift. In other words, the relativity of the clock errors in the final time measurement does not depend on sensors or target location. In contrast, in TOA and TDOA methodologies the impact of clock uncertainties is dependent on the signal travel and all clock instabilities.

Based on this analysis, the minimization of absolute temporal uncertainties and their influence on final measures is possible through an optimization of the distribution of the sensors of time-based positioning architectures. It is interesting to highlight that this effect is accomplished by the direct minimization of the time measurements performed by the CS clock in A-TDOA methodologies.

5.3. CRLB derivation with clock errors implementation

CRLB implementation in positioning enables the determination of the maximum accuracy of location when temporal measurements are perturbed. This tool has been widely adopted for LOS and NLOS conditions, as shown in [27]. The suitability of the CRLB, especially for LPS relies on the heteroscedasticity of variance models, heterogeneity in the sensor placement circumstances, and flexibility in the characterization of several operating conditions.

Conventionally, this technique has been used to characterize the reduction of accuracy in location due to time measurement errors induced by noise. The presence of noise in the communication channel has been traditionally modeled by a White Gaussian Noise (WGN) distribution [28]. Based on this assumption, Kaune et al. [29] develop a generic matrix form of the CRLB where time measurement uncertainties are dependent on target-sensor distance [14], [26].

$$J_{mn} = \left(\frac{\partial h(X)}{\partial x_m}\right)^T R^{-1}(X)\left(\frac{\partial h(X)}{\partial x_n}\right) + \frac{1}{2}tr\left(R^{-1}(X)\left(\frac{\partial R(X)}{\partial x_m}\right)R^{-1}(X)\left(\frac{\partial R(X)}{\partial x_n}\right)\right) \tag{5.14}$$

In this relation, **J** is the inverse of the Fisher Information matrix where *m* and *n* sub-indexes represent the parameters to estimate –TS Cartesian coordinates–. **h(TS)** vector indicates distance relationships between sensors and targets according to the positioning

signal travel in every architecture.

$$h_{TOA_i} = \|TS - CS_i\|, \quad i = 1, \dots, N_{CS} \tag{5.15}$$

$$h_{TDOA_i} = \|TS - CS_i\| - \|TS - CS_j\| \quad i = 1, \dots, N_{CS} \quad j = 1, \dots, N_{CS} \tag{5.16}$$

$$h_{A-TDOA_i} = \|TS - WS_i\| + \|TS - CS\| - \|WS_i - CS\| \quad i = 1, \dots, N_{WS} \tag{5.17}$$

The quantification of uncertainties in each time measurement is performed through the covariance matrix **R(TS)**.

In this paper, a combined model of noise effects and clock errors is presented based on the assumption of independence between these two factors. Reasons for this hypothesis rest in the absence of relation between the physical source of these disruptions.

The construction of the **R(TS)** matrix is subjected to significant differences according to positioning architectures. In the case of TOA and A-TDOA time measurements are independent of each other. In contrast, Z. Sahinoglu et al. proved in [30] that TDOA time differences measurements are correlated, which causes the presence of non-zero off-diagonal terms in the covariance matrix.

Noise components of variances in the **R(TS)** matrix is built based on a heteroscedastic model that is governed by a Log-normal path-loss propagation model. This characterization has been made under the assumption of uncorrelated measurement noise at different sensors [29].

Clock error terms in **R(TS)** matrix has been defined based on Monte-Carlo simulation of l iterations in order to correctly estimate each temporal variance associated with every positioning architecture. In addition, the time resolution is introduced in order to maximize clock uncertainty representation. The combined expressions of variances for noise and clock errors are presented in the following equations:

$$\sigma_{TOA_i}{}^2 = \frac{c^2}{B^2\left(P_T/P_n\right)} PL(d_0)\left[\left(\frac{d_i}{d_0}\right)^n\right] + \frac{1}{l}\sum_{k=1}^{l}\{CE_{TOA_i}c\}^2 \quad d_i = \|TS - CS_i\| \quad i = 1, \dots, N_{CS} \tag{5.18}$$

$$\sigma_{TDOA_{ij}}{}^2 = \frac{c^2}{B^2\left(P_T/P_n\right)} PL(d_0)\left[\left(\frac{d_i}{d_0}\right)^n + \left(\frac{d_j}{d_0}\right)^n\right] + \frac{1}{l}\sum_{k=1}^{l}\left\{CE_{TDOA_{ij}}c^2\right\}$$
$$d_i = \|TS - CS_i\| \tag{5.19}$$
$$d_j = \left\|TS - CS_j\right\|$$
$$i = 1, \dots, N_{CS} \quad j = 1, \dots, N_{CS} \quad where\ i \neq j$$

$$\sigma_{A-TDOA_i}{}^2 = \frac{c^2}{B^2\left(P_T/P_n\right)} PL(d_0)\left[\left(\frac{d_i}{d_0}\right)^n + \left(\frac{d_{TS}}{d_0}\right)^n + \left(\frac{d_{CS}}{d_0}\right)^n\right] + \frac{1}{l}\sum_{k=1}^{l}\left\{CE_{A-TDOA_i}c\right\}^2$$
$$d_i = \|TS - WS_i\| \tag{5.20}$$
$$d_{TS} = \|TS - CS\|$$
$$d_{CS_i} = \|WS_i - CS\| \quad i = 1, \dots, N_{WS}$$

where c is the signal propagation speed in m/s, B is the signal bandwidth is Hz, P_T is the transmission power in W, Pn is the mean noise level in W which is calculated based on Johnson-Nyquist relation, n is the path loss exponent, d_0 is the reference distance for the Log- normal model, $PL(d_0)$ is the path-loss related to reference distance.

Lastly, global accuracy in positioning is evaluated by means of the Mean Squared Error (MSE) of diagonal elements of matrix $\mathbf{J}^{-1}$. This enables an incremental penalization when the accuracy reduces its magnitude, which helps in the optimization process.

5.4. Fitness function modeling

In the previous sections, a combined clock and noise error model has been introduced in order to consider the uncertainties of the measurement devices and the signal deterioration in positioning systems. This model can be applied to achieve an optimized node distribution in TOA, TDOA and A-TDOA systems through the minimization of these uncertainties in each architecture. This is the main goal of this article and must guarantee the reduction of global positioning errors in any navigation environment for any type of vehicle.

The achievement of these objectives has led to the application of the positioning sensor layout proposed by J. Díez-González et al. [26]. This procedure is based on a Genetic Algorithm (GA) that allows the optimization of sensor placement in 3D irregular environments with free definitions of the reference surface and the region of optimization. For this purpose, the GA employs a methodology that allows the transformation of the cartesian coordinates of each individual in the population from binary to real digits –and vice versa– according to the local characteristics of the optimization environments. Additionally,

this GA provides freedom in the choice of: the selection technique –Tournament 2, Tournament 3, Roulette and Ranking–, the percentage of elitism and mutation, and the convergence criteria. Finally, a partial process of resolution allows the progressive reduction of the space of solution, stimulating the intensification in the search of the final solution.

Once the algorithm has been defined, the fitness function selection is the key factor to perform the optimization process. In this case, the fitness function must allow the combined reduction of the uncertainties introduced by noise and clock errors, with the aim of reaching the highest levels of accuracy for each positioning architecture. The equations defined in the Sections 2 and 3, show that a minimization of the signal travel, and the reduction of the time measurements in each clock -without null measurements- in order to minimize the influence of the clocks in the global error, allows the optimization of the global process with a concrete number of sensors.

This optimization methodology has led to the maximization of the inverse of the mean values of the Mean Squared Error (MSE) measured in each possible vehicle location in the optimization environment as follows. In addition, the fitness function penalizes forbidden sensor locations pre-determined based on environment characterization.

$$ff = \frac{1}{mean(MSE_{NT})} - C_P \frac{\sum_{i=1}^{N} R_i}{N} \tag{5.21}$$

where NT indicates the total number of evaluation points of the CRLB, N is the total number of architecture sensors, R_i represents the existence or not 1, 0 respectively- of sensors located in a banned area, and C_P is the weight associated to the penalization factor.

5.5. Results

In this section, the accuracy results after the optimization of sensors located in a 3D irregular environment for TOA, TDOA and A-TDOA architectures are presented.

Firstly, a 3D irregular scenario has been designed for the simulations. Area designations have followed the considerations of [26]. This simulation environment has been selected in order to exemplify a possible situation of optimization in real conditions. In this way, NLE is the Node Location Environment which indicates the extension free movement of the sensors during optimization, and TLE is the Target Location Environment which represents all possible locations of the positioning targets.

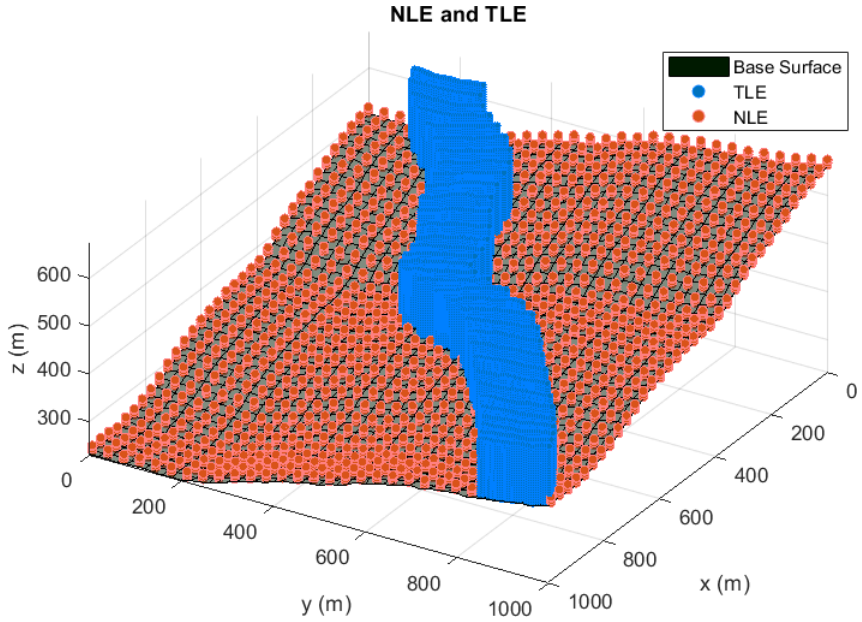

Figure 5.2. The scenario of the simulations. 3D irregular environment characterization for node optimization distribution of sensors in TOA, TDOA and A-TDOA architectures.

As can be observed in Figure 5.2, the NLE region spreads throughout the base surface with the exception of the zone corresponding to the TLE projection over the surface. In terms of elevation, the NLE minimum height is 1 meter - to prevent non-modeling events like multipath - and the maxi- mum elevation is pre-set to 15 meters to restrict sensor environment disruption. The NLE region resolution is contained in the interval [0.5,1] meters due to the adaptability of the length of the GA chromosomes based on the environment extension.

In the case of the TLE zone, limiting levels are 1 meter as the minimum and 120 meters as maximum. They have been selected to represent a joint aerial-ground accuracy maximization with maximum representativeness of the reality-based on pre-establish assumptions. The spatial discretization of the TLE region is 30 meters on x and y Cartesian coordinates, and 5 meters on z coordinate. This provides sufficient spatial resolution for the optimization, without reducing significantly the number of studied points.

Once the optimization scenario is selected, the next step is the determination of global configuration parameters that allow the comparison among time-based positioning architectures.

Table 5.1. TOA, TDOA and A-TDOA architectures parameters for optimization. Variables selection for noise modeling has been accomplished based on [31], whereas clock errors characterization is in reliance

with [13].

Parameter	**Value**
Transmission power	400 W
Mean noise power	- 94 dBm
Frequency of emission	1090 MHz
Bandwidth	100 MHz
Clock frequency	1 GHz
Frequency-drift	$U\{-10, 10\}$ ppm
Initial-time offset	$U\{15, 30\}$ ns
Time from synchronization	1 μs
Path LOSs exponent	2.1
Antennae gains	Unity
Time-Frequency product	1
Communication type	Full-duplex

Lastly, the GA configuration parameters selected are Tournament 3 as selection procedure, 7 % of elitism, single-point crossover and mutation probability of 3 %. This election provides the best relation between fitness function maximization and convergence speed. It must be stressed that TDOA and A-TDOA optimization have been carried out with five sensors in order to deploy the minimum number of them to accomplish and univocal 3D positioning. In the case of TOA architecture, the optimization process has been performed with four and five sensors to facilitate the comparison and the acquisition of conclusions.

The importance of the sensor placement for any positioning architecture is proved in Figure 5.3, where the CRLB is obtained for a random distribution of 5 sensors for TOA architecture.

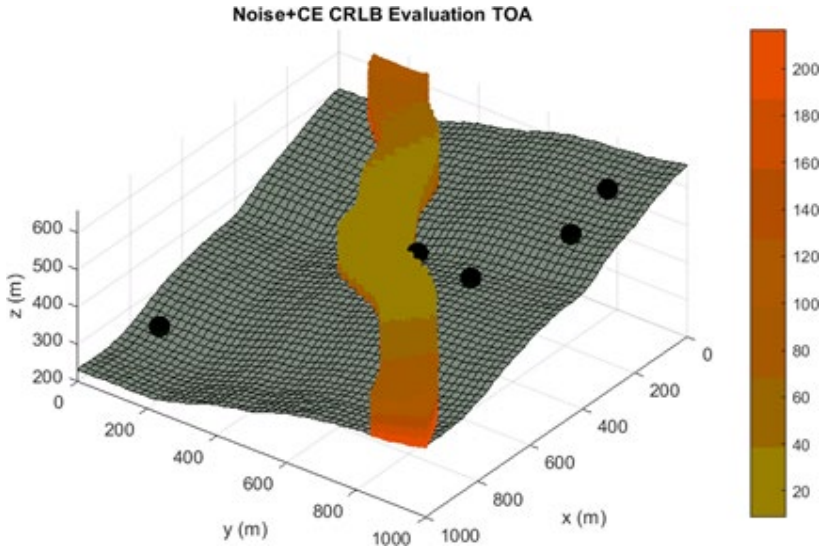

Figure 5.3. RMSE analysis in terms of noise and clock errors for TOA architecture with 5 sensors. The distribution of sensors is not optimized via GA. The reference surface is presented in grey tones. Black spheres symbolize the localization of each sensor.

As shown, a non-optimized location of sensors is the major contribution to the increase in the uncertainty of positioning. The accuracy evaluation after the optimization of sensor location for TOA, TDOA and A-TDOA architectures with noise and clock error uncertainties, is presented hereafter. Results are shown together with the localization of the optimized sensor placement in the environment.

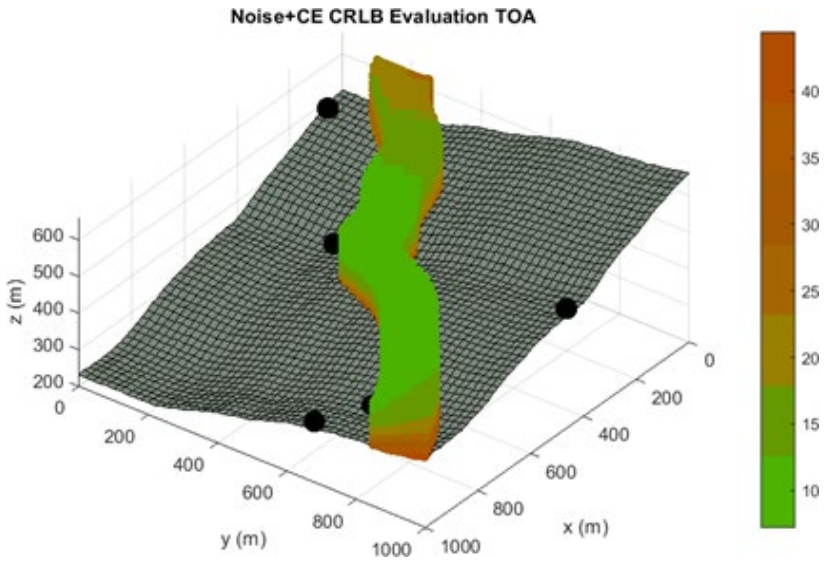

Figure 5.4. RMSE analysis in terms of noise and clock errors for TOA architecture with an optimized node distribution of 5 sensors.

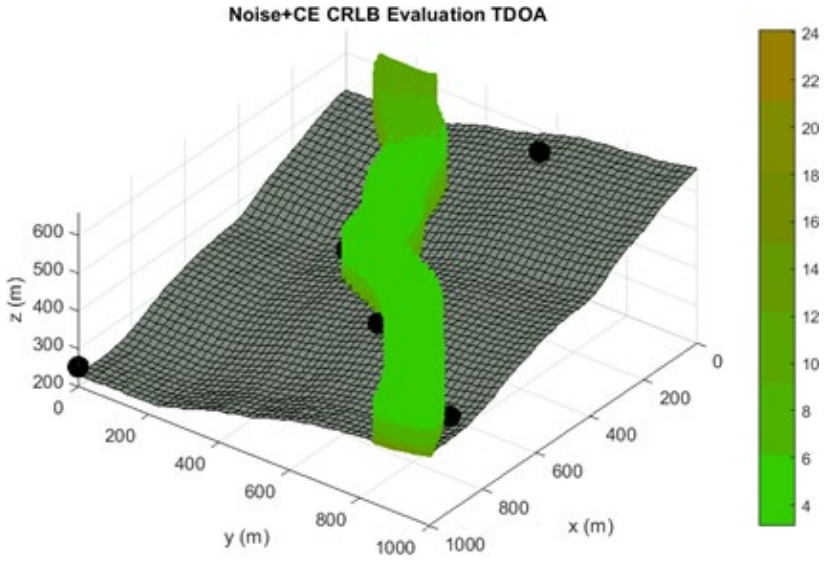

Figure 5.5. RMSE analysis in terms of noise and clock errors for TDOA architecture with an optimized node distribution of 5 sensors.

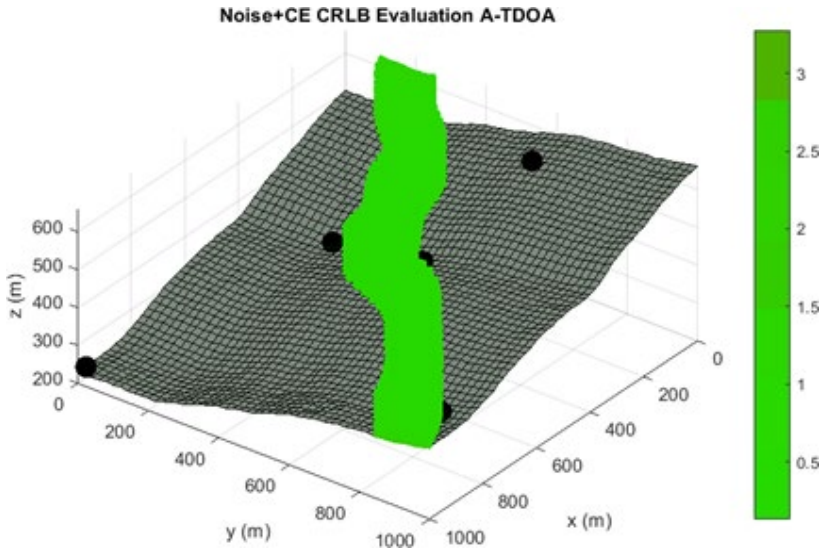

Figure 5.6. RMSE analysis in terms of noise and clock errors for A-TDOA architecture with an optimized node distribution of 5 sensors.

A comparative in terms of accuracy is displayed in Tables 5.2 and 5.3 for all positioning methodologies on analysis. These values have been obtained based on five different optimizations for each architecture with the objective of avoiding peak results due to the random initialization of the GA. Firstly, results are shown when only noise effects affect the

time measurements.

Table 5.2. Accuracy analysis for TOA, TDOA and A-TDOA architectures after sensor location optimization when noise uncertainties are present. Values in parentheses indicate the number of sensors in the distribution.

CRLB: Noise	**TOA (4)**	**TOA (5)**	**TDOA (5)**	**A-TDOA (5)**
Mean (m)	0.336	0.253	0.303	0.640
Max (m)	2.204	0.774	1.964	2.352
Min (m)	0.147	0.053	0.091	0.119
% < 0.5 m	84.74	92.16	84.06	52.47

Secondly, accuracy estimation with noise and clock error uncertainties is evaluated for positioning architectures.

Table 5.3. Accuracy analysis for TOA, TDOA and A-TDOA methodologies after sensor location optimization when noise and clock error uncertainties are considered. Values in parentheses indicate the number of sensors in the distribution.

CRLB: Noise + Clock errors	**TOA (4)**	**TOA (5)**	**TDOA (5)**	**A-TDOA (5)**
Mean (m)	19.993	17.962	8.152	0.704
Max (m)	77.377	44.480	24.129	3.277
Min (m)	8.761	7.177	3.124	0.130
% < 0.5 m	0	0	0	44.80
% Clock /Total errors	97.86	98.22	95.72	34.74

Tables 5.2 and 5.3 reveal important information about the performance of the architectures in the analysis for an LPS application. Synchronous methodologies –TOA and TDOA- provide better accuracy than asynchronous (A-TDOA) if only noise disturbance is modeled. This aspect is directly related to the reduction of the travel distance of positioning signal which is typical of TOA and TDOA methods.

However, when clock instabilities are added to noise as uncertainty factors in time measurements, the performance of A-TDOA architecture is far significantly higher than synchronous methodologies. This is mainly induced by the elimination of initial time-offset and cumulative errors that are introduced in the time measurements as a consequence of the time-lapse from the last synchronization. In addition, A-TDOA architectures could reduce, through the sensor distribution, the amount of the time measurements thanks to the TDOA

methodology employing one common sensor (CS) for all measures. Clock error models have shown that this aspect directly reduces the uncertainties induced in the final measurement, and the errors in the final positioning. The relation of these magnitudes with the global accuracy for TOA, TDOA and A-TDOA architectures are presented hereafter:

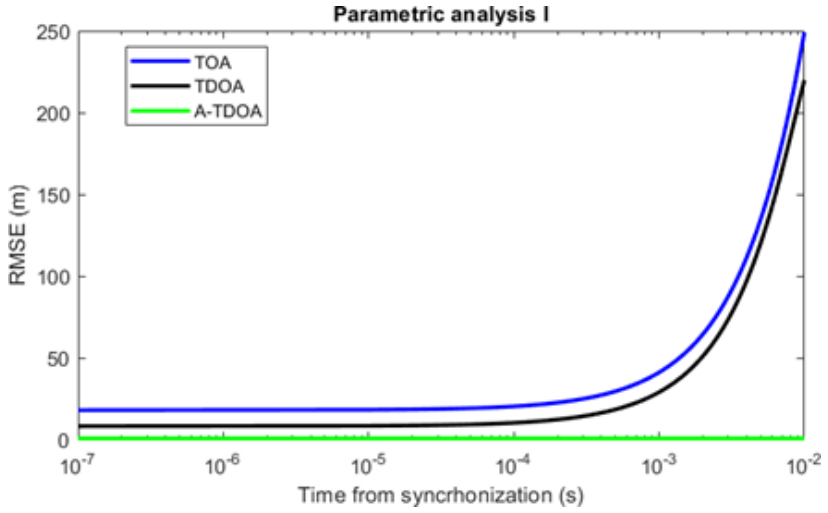

Figure 5.7. Parametric analysis of the time from synchronization in TOA, TDOA and A-TDOA architectures with an optimized distribution of 5 sensors. Variables for the analysis are derived from Table 5.1.

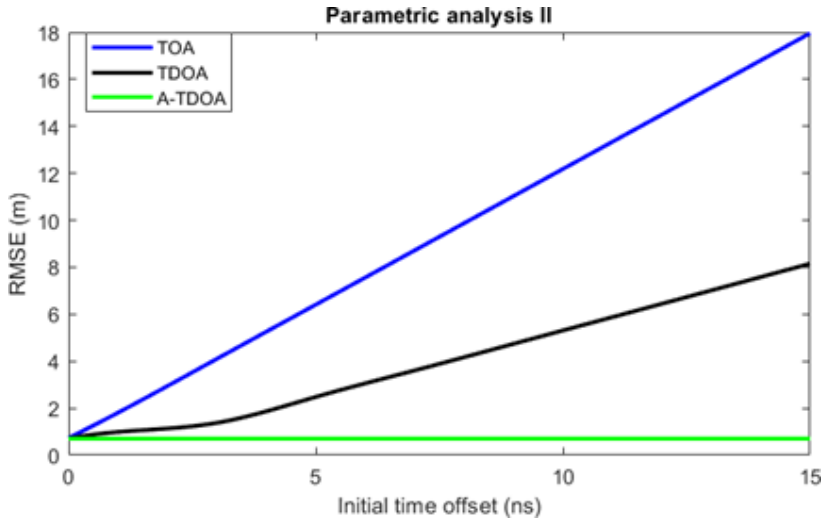

Figure 5.8. Parametric analysis of initial time offset for TOA, TDOA and A-TDOA architectures with an optimized distribution of 5 sensors. Variables for the analysis are derived from Table 5.1.

Figures 5.7 and 5.8 reveals that TOA and TDOA architectures would provide the same accuracy level if their sensors initial- time offset were null and the time from synchronization was less than 1 μs, which is nearly impracticable with actual technology. Based on these

results, the better candidate in terms of accuracy and performance stability for LPS applications are the asynchronous time-based architectures.

5.6. Conclusion

The LPS have emerged as the most adequate systems for high-performance applications in terms of accuracy and stability in the target localization. This has been achieved through the reduction of the uncertainties related to the measurements in these architectures and the flexibility to locate the sensor distribution in the space.

In this paper, we have developed for the first time in the authors' best knowledge a model to consider the uncertain- ties introduced by the navigation environment and the clock instabilities in the time measurements of the CRLB matrix. This methodology has been derived for the TOA, TDOA and A-TDOA architectures, with the aim of evaluating their performance based on a set of global communication parameters under a 3D-real environment. This error characterization shows the necessary process to minimize these measurement instabilities and jointly reduce the influence of the signal travel.

It must be highlighted that it has been shown that the Clock Relative Error (CRE) in A-TDOA architectures has a constant factor that is independent of the signal positioning travel and it only depends on the clock drift of its coordinate sensor which produces great stability in the accuracy results of this methodology. This fact has special relevance in LPS where distances between target and sensors are highly heterogeneous.

The minimization of the error uncertainties requires an optimized sensor distribution for each architecture in order to make the results comparable and to achieve practical results. This is a consequence of the influence of the sensor deployment in the signal paths of each architecture as well as time lapses to be measured. In optimized sensor distributions signal paths are reduced in TOA systems from TDOA systems which in turn are smaller than A-TDOA as a result of the architecture design. But, in these systems, the path degradation of the signals can be offset by less affected clock errors. For this reason, this article studies the combined effect of these error sources under optimized node deployments for each time-based positioning architecture.

We apply a heuristic optimization for each system with the minimum number of sensors to achieve an unequivocal target location. This optimization has been achieved by means of a genetic algorithm with total independence from the space surface to locate sensors, the target possible localizations and the adoption of crossing, selection and mutation

techniques. Results show that A-TDOA provides significantly better performance in terms of accuracy and stability than TOA and TDOA architectures. The influence of the time since the last synchronization and initial time offset on clock errors have been demonstrated through a parametric analysis. A-TDOA architectures accuracy is more stable due to the elimination of uncertainties related to the synchronism process and the combined minimization of positioning signal path and time measures made by sensor clocks.

5.7. References

1. K. W. Kolodziej and J. Hjelm, *Local Positioning Systems: LBS Applications and Services*. Boca Raton, FL, USA: CRC Press, 2017.
2. A. A. D'Amico, U. Mengali, and L. Taponecco, "TOA estimation with the IEEE 802.15.4a standard", *IEEE Trans. Wireless Commun.*, vol. 9, no. 7, pp. 2238–2247, Jul. 2010.
3. T.-K. Le and N. Ono, "Closed-form and near closed-form solutions for TDOA-based joint source and sensor localization", *IEEE Trans. Signal Process.*, vol. 65, no. 5, pp. 1207–1221, Mar. 2017.
4. J. Xu, M. Ma, and C. L. Law, "AOA cooperative position localization", in *Proc. IEEE Global Telecommun. Conf. (GLOBECOM)*, New Orleans, LO, USA, Nov./Dec. 2008, pp. 1–5.
5. G. Wang and K. Yang, "A new approach to sensor node localization using RSS measurements in wireless sensor networks", *IEEE Trans. Wireless Commun.*, vol. 10, no. 5, pp. 1389–1395, May 2011.
6. D. Lindgren, G. Hendeby, and F. Gustafsson, "Distributed localization using acoustic Doppler", *Signal Process.*, vol. 107, pp. 43–53, Feb. 2015.
7. L. Taponecco, A. A. D'Amico, and U. Mengali, "Joint TOA and AOA estimation for UWB localization applications", *IEEE Trans. Wireless Commun.*, vol. 10, no. 7, pp. 2207–2217, Jul. 2011.
8. B. Sackenreuter, N. Hadaschik, M. Fassbinder, and C. Mutschler, "Low- complexity PDoA-based localization", in *Proc. Int. Conf. Indoor Positioning Indoor Navigat. (IPIN)*, Alcalá de Henares, Spain, Oct. 2016, pp. 1–6.
9. Y. Ma, B. Wang, S. Pei, Y. Zhang, S. Zhang, and J. Yu, "An indoor localization method based on AOA and PDOA using virtual stations in multipath and NLOS environments for passive UHF RFID", *IEEE Access*, vol. 6, pp. 31772–31782, 2018.

10. B. Sundararaman, U. Buy, and A. D. Kshemkalyani, "Clock synchronization for wireless sensor networks: A survey", *Ad Hoc Netw.*, vol. 3, no. 3, pp. 281–323, May 2005.
11. J. Y. D. Elson Estrin, "Time synchronization for wireless sensor net- works", in *Proc. 15th Int. Parallel Distrib. Process. Symp., San Francisco*, CA, USA, 2000, p. 1.
12. S. He and X. Dong, "High-accuracy localization platform using asynchronous time difference of arrival technology", *IEEE Trans. Instrum. Meas.*, vol. 66, no. 7, pp. 1728–1742, Jul. 2017.
13. J. Zhou, L. Shen, and Z. Sun, "A new method of D-TDOA time measurement based on RTT", in *Proc. MATEC Web Conf.*, vol. 207, 2018, Art. no. 03018.
14. R. Álvarez, J. Díez-González, E. Alonso, L. Fernández-Robles, M. Castejón-Limas, and H. Perez, "Accuracy analysis in sensor networks for asynchronous positioning methods", *Sensors*, vol. 19, no. 13, p. 3024, Jul. 2019.
15. P. Wu, S. Su, Z. Zuo, X. Guo, B. Sun, and X. Wen, "Time difference of arrival (TDoA) localization combining weighted least squares and firefly algorithm", *Sensors*, vol. 19, no. 11, p. 2554, Jun. 2019.
16. S. Lanzisera, D. Zats, and K. S. J. Pister, "Radio frequency time-of-flight distance measurement for low-cost wireless sensor localization", *IEEE Sensors J.*, vol. 11, no. 3, pp. 837–845, Mar. 2011.
17. O. Tekdas and V. Isler, "Sensor placement for triangulation-based localization", *IEEE Trans. Autom. Sci. Eng.*, vol. 7, no. 3, pp. 681–685, Jul. 2010.
18. Y. Yoon and Y.-H. Kim, "An efficient genetic algorithm for maximum coverage deployment in wireless sensor networks", *IEEE Trans. Cybern.*, vol. 43, no. 5, pp. 1473–1483, Oct. 2013.
19. J. O. Roa, A. R. Jiménez, F. Seco, C. Prieto, J. Ealo, and F. Ramos, "Primeros resultados en la optimización de la ubicación de balizas para localización utilizando algoritmos genéticos", in *Proc. 24th Jornadas Automática*, 2005, pp. 75–86.
20. J. O. Roa, A. R. Jiménez, and F. Seco, "Un método heurístico basado en algoritmos genéticos para optimizar la ubicación de balizas en sistemas de localización", in *Proc. 24th Jornadas de Automática*, 2006, pp. 120–129.
21. J. Díez-González, R. Álvarez, L. Sánchez-González, L. Fernández-Robles, H. Pérez, and M. Castejón-Limas, "3D Tdoa problem solution with four receiving nodes",

Sensors, vol. 19, no. 13, p. 2892, Jul. 2019.

22. W. Huihui, Z. Xingqun, and Z. Yanhua, "Geometric dilution of precision for GPS single-point positioning based on four satellites", *J. Syst. Eng. Electron.*, vol. 19, no. 5, pp. 1058–1063, Oct. 2008.
23. N. Rajagopal, S. Chayapathy, B. Sinopoli, and A. Rowe, "Beacon placement for range-based indoor localization", in *Proc. Int. Conf. Indoor Positioning Indoor Navigat.* (IPIN), Alcalá de Henares, Spain, Oct. 2016, pp. 1–8.
24. B. Huang, L. Xie, and Z. Yang, "TDOA-based source localization with distance-dependent noises"*, IEEE Trans. Wireless Commun.*, vol. 14, no. 1, pp. 468–480, Jan. 2015.
25. T. S. Rappaport, *Wireless Communications—Principles and Practice*. Upper Saddle River, NJ, USA: Prentice-Hall, 2002.
26. J. Díez-González, R. Álvarez, D. González-Bárcena, L. Sánchez-González, M. Castejón-Limas, and H. Perez, "Genetic algorithm approach to the 3D node localization in TDOA systems", *Sensors*, vol. 19, no. 18, p. 3880, Sep. 2019.
27. Y. Qi and H. Kobayashi, "Cramér–Rao lower bound for geolocation in non-line-of-sight environment", in *Proc. IEEE Int. Conf. Acoust. Speech Signal Process.*, May 2002, pp. III-2473–III-2476.
28. B. Huang, L. Xie, and Z. Yang, "Analysis of TOA localization with heteroscedastic noises", in *Proc. 33rd Chin. Control Conf., Nanjing*, China, Jul. 2014, pp. 327–332.
29. R. Kaune, J. Hörst, and W. Koch, "Accuracy analysis for TDOA localization in sensor networks", in *Proc. 14th Int. Conf. Inf. Fusion*, Chicago, IL, USA, Jul. 2011, pp. 1–8.
30. Z. Sahinoglu, S. Gezici, and I. Gvenc, *Ultra-Wideband Positioning Systems*. New York, NY, USA: Cambridge Univ. Press, 2008.
31. A. S. Yaro and A. Z. Sha'ameri, "Effect of path LOSs propagation model on the position estimation accuracy of a 3-dimensional minimum configuration multilateration system", *Int. J. Integr. Eng.*, vol. 10, no. 4, pp. 35–42, 2018.

Chapter 6

Multi-objective optimization for asynchronous positioning systems based on a complete characterization of ranging errors in 3D complex environments

This chapter has been published as:

Rubén Álvarez, Javier Díez-González, Nicola Strisciuglio, Hilde Pérez

IEEE Access (2020)

DOI: 10.1109/ACCESS.2020.2978336

Abstract

High-accuracy positioning is fundamental for modern applications of autonomous agent navigation. The accuracy and stability of predicted locations are key factors for evaluating the suitability of positioning architectures that have to be deployed to real-world cases. Asynchronous TDOA (A-TDOA) methodologies in Local Positioning Systems (LPS) are effective solutions that satisfy the given requirements and reduce temporal uncertainties induced during the synchronization process. In this paper, we propose a technique for the combined characterization of ranging errors –noise, and Non-Line-of-Sight (NLOS) propagation – through the Cramér-Rao Bound (CRB). NLOS propagation effects on signal quality are predicted with a new ray-tracing LOS/NLOS algorithm that provides LOS and NLOS travel distances for communication links in 3D irregular environments. In addition, we propose an algorithm for detecting multipath effects of destructive interference and disability of LOS paths. The proposed techniques are applied to sensor placement optimization in 3D real scenarios. A multi-objective optimization (MOP) process is used

based on a Genetic Algorithm (GA) that provides the Pareto Fronts (PFs) for the joined minimization of location uncertainties (CRB) and multipath effects for a variable number of A-TDOA architecture sensors. Results show that the designed procedure can determine, before real implementation, the maximum capacities of the positioning system in terms of accuracy. This allows us to evaluate a trade-off between accuracy and cost of the architecture or support the design of the positioning system under accuracy demands.

6.1. Introduction

Local Positioning Systems (LPS) received a growing interest from engineering community in recent years as candidates for navigation applications with high-accuracy requirements, such as Automatic Ground Vehicles (AGVs) and Unmanned Aerial Vehicles (UAVs). The justification lies in the small location uncertainties originated during data acquisition and the stability that these systems provide, due to their capability of reducing the distances between targets and architecture sensors.

All positioning systems require estimating the location of targets. Among them, the most popular techniques are based on measuring time delays [1], [2], received power [3], or angles of incidence [4]. Time-based architectures have become predominant due to their trade-off between hardware complexity, accuracy, and adaptability to complex environments of operation [5].

Historically, time-based positioning architectures were designed under the obligation of synchronization between targets and sensors, i.e. Time-Of-Arrival (TOA) [6], or architecture sensors, i.e. Time-Difference-of-Arrival (TDOA) [7]. This factor induces a substantial instability in the magnitude of the nominal accuracy of localization, due to the time measurement uncertainties induced during the synchronization process [8], [9]. High location accuracy is mandatory in autonomous navigation in which positioning service must remain stable in time, which is difficult to attain with TOA and TDOA conventional methods.

The asynchronous TDOA (A-TDOA) architecture [10], [11] eliminates the synchronism between sensors through a positioning methodology where time measurements are performed at only one clock located in a specific sensor of the architecture. This fact substantially reduces time measurement uncertainties with respect to TOA and TDOA techniques.

Once the time-based positioning architecture is determined, the major contributions

to its accuracy are the algorithm implemented, and the errors on time measurements, i.e. ranging errors. Under the assumption of an efficient estimator for the location, maximum capabilities of the positioning architecture could be predicted a priori based on the effects of ranging uncertainties: noise, clock errors, Non-Line-Of- Sight (NLOS) propagation and multipath [12]. These factors are essentially influenced by sensor placement [13]–[15] and this affection is crucial in LPS, where the localization performance is maximized through an optimization of the distribution of sensors.

The optimization of sensor placement for LPS has been subjected to analysis in the past decades. First studies focused on the reduction of the dimensionality of the problem [16]. Greedy-type algorithms were implemented in [17] and [18] for computing the optimization of sensor positioning through a linearization process. Recent approaches try to solve the problem without simplifications, leading to NP-hard resolutions [19], [20]. At this point, heuristic methods became pre- dominant, with special relevance of Genetic Algorithms (GA) [21]–[24]. Multi-objective optimizations (MOP) performed by [25], [26] provide optimization for multiple criteria, enabling compromise solutions. However, these works are not able to perform a 3D optimization in real environments, and the fitness function implemented only consider some of the factors that cause location errors, which are mainly noise and some cases where NLOS propagation is present.

The accuracy estimation of positioning has also been widely studied. Originally, accuracy was evaluated through the Geometric Dilution of Precision (GDOP), where ranging variances are assumed homoscedastic [27], [28]. However, this model is valid only for homogenous distances between targets and sensors, which is infeasible for LPS [29]. This leads to a heteroscedastic treatment of time measurement variances [30], [31], which is accomplished via the Cramér- Rao Lower Bound (CRLB). Martínez et al. provide in [32] a cLOSed-form expression for the CRLB in 2D and 3D environments. Similarly, Isaacs et al. applied in [33] the CRLB to a TDOA architecture. Previous works are related to Line-Of-Sight (LOS) conditions, where NLOS is introduced in the CRLB derivation in [34] and [35]. However, observed models depend on several pre-established parameters and can only be applied in certain environments. Earlier studies only characterized the accuracy of the positioning based on the presence of noise in the environment. This assumption compromises the application of these models in actual 3D situations, where NLOS propagation are induced in time measurements. Linked to this, multipath effects due to the

presence of obstacles have not been addressed in the literature in order to minimize their impact in 3D environments, which further weakens the representativeness of the described methods in complex conditions of operations.

This paper is built on our previous work of the authors [36], where sensor placement is optimized in 3D irregular scenarios via GA. The aim of this article is the 3D optimization of a variable number of sensors for the A-TDOA architecture in 3D real scenarios with a complete characterization of ranging errors. For this purpose, we develop algorithms for LOS/NLOS ray-tracing and multipath detection which allow the detection of obstacles that obstruct positioning signals and/or create destructive interference, leading to degradation or cancelation of the LOS paths. In addition, we implement a new characterization of the Cramér-Rao Bound (CRB) which includes noise and NLOS propagation. The combination of CRB and multipath identification enables a MOP process for estimating a priori maximum capabilities of A-TDOA architecture in 3D complex environments in terms of accuracy and stability. We propose a method for multi-objective optimization (MOP) that allows the minimization of the effect of adversarial factors and the adaptability of time-based positioning architectures to 3D environments. In addition, the combination of the new CRB model with the multipath detection algorithm provides a trade-off of these parameters, especially in indoor and urban areas, where the sensor placement could be optimized for maximizing the architecture accuracy and stability.

The remainder of this article is organized as follows. In section 6.2, we present a LOS/NLOS ray-tracing algorithm for measuring LOS and NLOS emitter-receiver distances together with a multipath detection algorithm for 3D environments. Section 6.3 presents the derivation of the CRB for A-TDOA architecture for the combined presence of noise and NLOS propagation. In Section 6.4, we discuss the configuration of the MOP with the definition of the designed fitness function. In Section 6.5 we report and discuss the results of the application of the techniques and models described in the article for the optimization of sensor distribution in a 3D irregular scenario. Finally, section 6.6 concludes the paper.

6.2. LOS/NLOS ray-tracing and multipath detection algorithms

The presence of objects in the proximity of emitter-receiver links could lead to over-reduction of the signal power that reaches the receptor, originated by NLOS conditions [37],

and/or the generation of different paths which adversely affect the detection process and could generate destructive interference, i.e. multipath [38]. These effects significantly

deteriorate the accuracy of positioning and, consequently, they must be detected and quantified.

We propose two algorithms to characterize the properties of communication channels in 3D complex environments, where NLOS conditions and multipath are present. Firstly, we implement a ray-tracing algorithm that estimates the LOS and NLOS distances associated with a generic communication link between an emitter and a receiver. We develop this technique under the requirements of 3D applications in complex irregular environments.

The algorithm is based on the spatial discretization of the emitter-receiver link for each communication of the positioning architecture, i.e. we divide the line between emitter and receiver in a number of evaluation points. For each of these points, the algorithm compares the height of the line that join the emitter and the receiver with the elevation of the surface and/or obstacles in the environment. If the subtraction of link heights and surface/obstacles elevation is positive, any object interferes with the emitter-receiver link in that point. Otherwise, some object is obstructing the positioning signal. The application of this evaluation for every point of the discretization in each positioning link allows not only the detection of obstructions, but also the quantification of the LOS and NLOS distances associated with each link. The description of the ray-tracing LOS/NLOS algorithm is shown in Figure 6.1.

Algorithm 1 3D LOS/NLOS ray-tracing Algorithm

```
Characterize in cartesian coordinates the base surface
Construct 3D Line between emitter and receiver
Define spatial resolution in the emitter-receiver
direction
Divide the 3D Line based on the spatial resolution
Initialize LOS and NLOS distances
for points=1,2, … do
    Calculate the height of 3D Line in each point
    Interpolate the base surface elevation in each point
    if 3D Line height < Base surface elevation
        NLOS detection
    end if
end for
Sum of NLOS distance detection for consecutive
points, and reduce spatial resolution and recalculate
Algorithm 1 when NLOS detection occurs after a LOS
detection (reducing spatial resolution)
```

Figure 6.1. 3D LOS/NLOS ray-tracing algorithm.

The only parameters needed to initialize the algorithm are the emitter and receiver

locations, the base/ground surface elevation and the spatial resolution required for the analysis. This methodology allows the calculation of LOS and NLOS distances, which directly impacts on the uncertainties of time measurements and the global accuracy of the positioning process.

The second algorithm proposed is a new technique that enables the identification and evaluation of all regions that could potentially produce adverse multipath effects in receivers. The presence of multipath leads to two problems in receivers: the appearance of destructive interferences that cancel the communications signal and the introduction of multiple signals that overlap preventing the detection of the LOS path [38].

Destructive interferences are modeled by the Fresnel zone, which is defined in 3D space as the ellipsoid where any object located totally or partially inside generates a reflected signal that nullifies the original transmission. The ellipsoid is built based on the emitter and receiver locations –the focus of the ellipsoid- and the radius at any point of the communications link is calculated as follows [39]:

$$R_{Fr} = \sqrt{\frac{n_{Fr}\lambda d_E d_R}{d_E + d_R}} \tag{6.1}$$

where R_{Fr} is the Fresnel zone radius at the point at study, n_{Fr} is the nth Fresnel zone radius, λ is the wavelength of the communication signal, d_E indicates the distance between the emitter and the point at analysis, and d_R represents the distance between the receiver and the point which radius is being calculated.

In multipath environments, reflected multiple signals might reach the receptor antenna with certain delays. This phenomenon is characterized based on the delay spread (τ_{ds}), which defines the maximal mutual delay between signals of different paths. The delay spread is closely related to the signal correlation spread ($\tau_c \approx 1/B$) which characterizes the negligibility of resemblance in the time domain between two time-shifted copies of the same signal [38]. Thus, if consecutive multipath signals arrive at the receptor in a period of time lower than the delay spread, which is equal to the correlation spread in the most critical case, they will overlap and the signals cannot be distinguished. This feature is critical during the discrimination of the first signal, LOS path, in positioning systems where multipath is involved. Every reflected path with a travel distance lower than LOS path distance plus the correlation spread distance ($\tau_c c$) cause a multipath fading and the impossibility of employing

this communication link for positioning [38].

Similarly to the Fresnel zone, it is possible to generate a 3D region in space where any object located inside could originate paths that are not distinguished from the LOS path, Minimum NLOS path zone. Formally, this is represented as an ellipsoid where the emitter and the receiver act as the ellipsoid focus, defined as:

$$R_{12path} = \sqrt{{d_{12\_min}}^2 \left[1 - \left(\frac{{d_P}^2}{{d_{LOS}}^2 + {d_{12\_min}}^2}\right)\right]} \qquad (6.2)$$

$$d_{12\_min} = d_{LOS} + \tau_c c \approx d_{LOS} + \frac{c}{B}$$

where R_{12_path} is the radius of the multipath ellipsoid section, d_{12_min} is the minimum distance of the reflected paths below which they are not discernible from LOS path, d_{LOS} indicates the direct distance in LOS conditions between emitter and receiver, d_P is the distance between the center of the ellipsoid and the point of analysis, c is the signal propagation velocity, and B is the signal bandwidth.

Based on these two factors, we propose an algorithm to detect the presence of obstacles that could generate destructive interference and/or non-discriminated minimum reflected paths. This technique relies on the evaluation of the Fresnel and Minimum NLOS path ellipsoids. Figure 6.2 illustrates the proposed methodology. Firstly, both ellipsoids are obtained through the calculation of their semi-major and semi-minor axis. Based on the larger ellipsoid, corresponding to the most critical condition of multipath, the algorithm discretized its semi-major axis with a similar procedure to that of the ray-tracing algorithm. In each of these points, a perpendicular plane section to the major axis is performed in order to obtain an ellipsoid section based on the radius of Eq. 6.1 or 6.2, depending on the selected ellipsoid. This ellipsoid section is discretized (e.g. black spheres in Figure 6.2) and projected onto the base surface for obtaining the region of the base surface/obstacles that could interfere with the ellipsoid. Once this zone is delimited, a set of extra evaluation points are defined in the base surface/obstacles to complete the multipath analysis points (e.g. brown spheres in Figure 6.2). The elevation of these points is compared with the height of the plane that contain the ellipsoid section (e.g. green and red spheres in Figure 2). In the case of higher point elevation than ellipsoid section high, the algorithm detects an obstacle that could create adverse multipath effects in the system. The complete multipath algorithm is presented in

Figure 6.3.

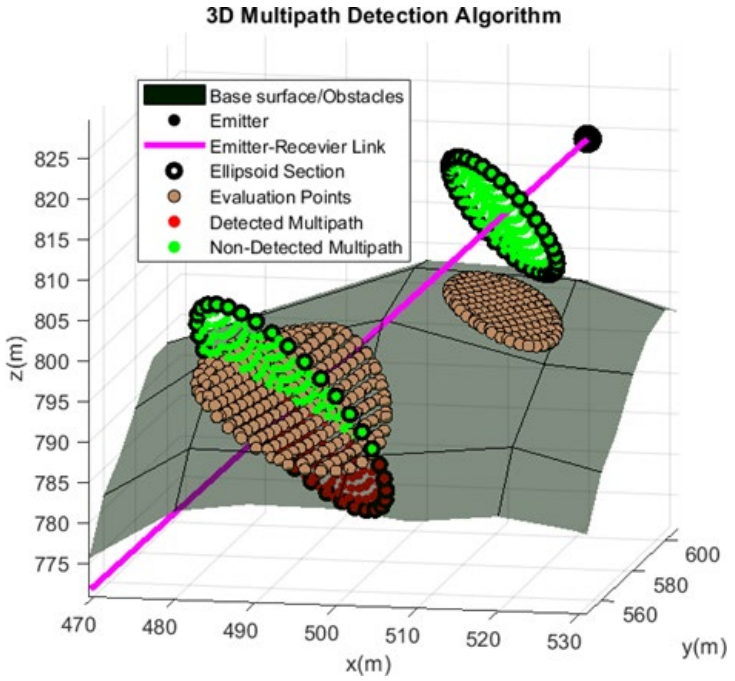

Figure 6.2. Graphical operation of the 3D Multipath detection Algorithm. Example of multipath analysis for two distinct ellipsoid sections of an emitter-receiver link. Obstacles zones are characterized through grey tones, symbolizing in this case the ground surface.

Algorithm 2 3D Multipath detection Algorithm

Model in cartesian coordinates of the base surface
Construct the largest major axis of ellipsoids of Fresnel and Minimum NLOS path zones for emitter-receiver link
Define spatial resolution for major axis, circumference section, and generation of internal points to the base surface projection
Divide the major axis based on spatial resolution pre-selected (Z points)
Initialize multipath detection
for points = 2, … , Z-1 **do**
    Generate a perpendicular plane to the major axis of the ellipsoid
    Construct two orthogonal vector contents in the plane
    Generate the circumference points, based on the spatial resolution predefined for the circumference section
    Project circumference points onto the base surface
    Generate additional points in the interior region of the projected area, based on the predetermined spatial resolution

```
    if Circumference point heights < Base surface
        Multipath detection
    end if
end for
Sum of multipath detected points in each point of the
discretization of the major axis of the largest
multipath ellipsoid
```

Figure 6.3. 3D Multipath detection algorithm.

The multipath algorithm inputs are the emitter and receiver location, the spatial resolution required and the principal parameters needed for modeling Fresnel and Minimum NLOS path zones. An example of the combined operation of LOS/NLOS ray-tracing and multipath detection algorithms is displayed in Figure 6.4.

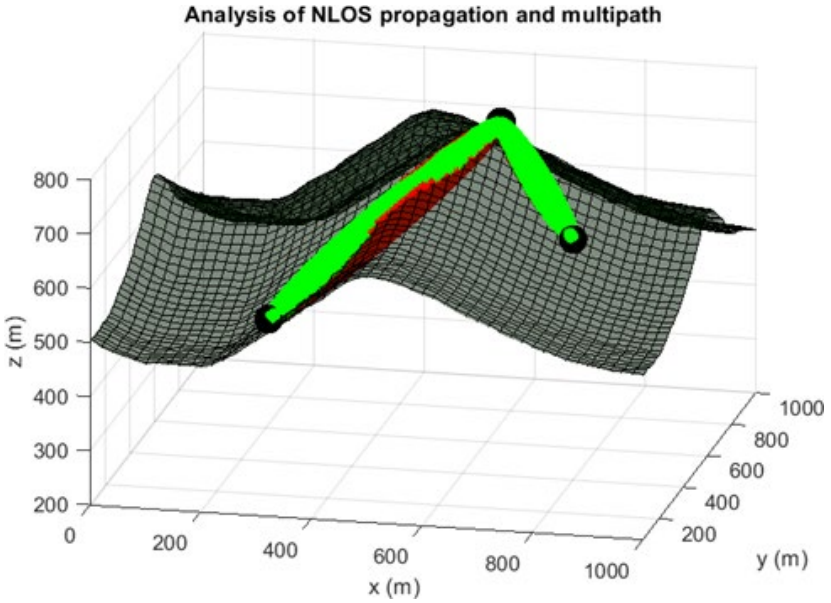

Figure 6.4. Ray-tracing and Multipath detection algorithms application. Red zones indicate the presence of objects that could induce multipath. The reference surface in presented in grey tones. Black spheres indicate the location of the sensors.

The methodologies proposed to detect disruptive phenomena on positioning signals are valid for any irregular 3D region, as they only depend on the discretized points of the environment and the definition of the set of hyper-parameters relative to the demanded spatial resolution for the solution of the task at hand. They do not require extra characterization of the given environment. This fact is mandatory for the optimization of the location of LPS sensors in complex environments.

6.3. CRB derivation with LOS/NLOS implementation for A-TDOA architecture

The CRB allows for the determination of the minimum values of variance associated with any unbiased estimator of a deterministic parameter. In the positioning context, it is widely applied, especially as an indicator of the maximum achievable location accuracy according to the characteristics of the positioning systems employed [40]. CRB has been traditionally implemented in the estimation of uncertainties induced by the presence of White Gaussian Noise (WGN) in the communication channel [31]. However, noise is only one of the main sources of ranging uncertainties [12], becoming particularly important clock error measurements [41] and Non-Line-Of-Sight (NLOS) propagation in the deployment of LPS.

The objective of this section is the generation of a generic CRB model that estimates 3D location accuracy when noise and NLOS propagation are considered. In this work, the CRB derivation is applied to an A-TDOA architecture, as the best candidate in terms of accuracy, stability and complexity for an LPS application, due to the elimination of clock errors caused by synchronism between sensors. Target Sensor (TS) represents the position of the object to locate. Coordinate Sensor (CS) refers to the A-TDOA sensor that is capable of accomplishing time measurements. Worker Sensors (WS) encompass every transponder sensor of A-TDOA architectures without internal clocks for time estimation.

Due to the diversity of target-sensor distance typical of LPS, the derivation of the CRB is subjected to a heteroscedastic treatment of the process estimation variances [30]. In this regard, regard, in [42] a distance-dependent modeling for a generic matrix form of the CRB was proposed:

$$J_{mn} = \left(\frac{\partial h(X)}{\partial x_m}\right)^T R^{-1}(X)\left(\frac{\partial h(X)}{\partial x_n}\right) + \frac{1}{2}tr\left(R^{-1}(X)\left(\frac{\partial R(X)}{\partial x_m}\right)R^{-1}(X)\left(\frac{\partial R(X)}{\partial x_n}\right)\right) \tag{6.3}$$

FIM is the Fisher Information matrix where *m* and *n* sub-indexes are the parameters to estimate –TS Cartesian coordinates-. Distance relations among sensors and targets are expressed by the **h(TS)** vector, the construction of which depends on the positioning architecture implemented. In the case of an A-TDOA architecture:

$$h_{A-TDOA_i} = \|TS - WS_i\| + \|TS - CS\| - \|WS_i - CS\| \qquad i = 1, \dots, N_{WS} \tag{6.4}$$

$$\frac{\partial h_{A-TDOA_i}}{\partial TS_m} = \frac{TS_m - WS_{i_m}}{\|TS - WS_i\|} + \frac{TS_m - \mathrm{CS}_m}{\|TS - \mathrm{CS}\|} \tag{6.5}$$

where N_{WS} is the number of WS in the architecture. The covariance matrix –**R(TS)**- introduced all factors that con- tribute to the generation of uncertainties during the positioning process. In the case of A-TDOA architecture, time measurements are uncorrelated [10] and off-diagonals matrix elements are null.

Noise and NLOS propagation are joined together based on a Log-normal path loss propagation model with different characteristics for LOS and NLOS signals [43], based on the assumption of uncorrelated noise measurements at different sensors [42]. In the following equations, the variances expressions for noise and NLOS propagation effects are computed:

$$\begin{aligned}
\sigma_{A-TDOA_i}{}^2 = \frac{c^2}{B^2\left(P_T/P_n\right)} \frac{PL(d_0)}{d_0{}^{n_{LOS}}} \left[\left(d_{i_{LOS}} + d_{i_{NLOS}}{}^{x}\right)^{n_{LOS}} + \left(d_{TS_{LOS}} + d_{TS_{NLOS}}{}^{x}\right)^{n_{LOS}}\right. \\
\left. + \left(d_{CS_{LOS}} + d_{CS_{NLOS}}{}^{x}\right)^{n_{LOS}}\right] \\
d_{i_{LOS}} = \|TS - WS_i\|_{LOS} \\
d_{i_{NLOS}} = \|TS - WS_i\|_{NLOS} \\
d_{TS_{LOS}} = \|TS - \mathrm{CS}\|_{LOS} \\
d_{TS_{NLOS}} = \|TS - \mathrm{CS}\|_{NLOS} \\
d_{CS_{i_{LOS}}} = \|WS_i - CS\|_{LOS} \\
d_{CS_{i_{NLOS}}} = \|WS_i - CS\|_{NLOS} \\
x = n_{NLOS}/n_{LOS} \\
i = 1, \ldots, N_{WS}
\end{aligned} \tag{6.6}$$

$$\frac{\partial {\sigma_{A-TDOA_i}}^2}{\partial TS_m} = \frac{c^2}{B^2\left({P_T}/{P_n}\right)} \frac{PL(d_0)}{{d_0}^{n_{LOS}}} n_{LOS} \left\{ \left[\left({d_{i_{LOS}}} + {d_{i_{NLOS}}}^{x} \right)^{n_{LOS}-1} \left(\frac{TS_m - WS_{i_m}|_{LOS}}{\|TS - WS_i\|_{LOS}} \right. \right. \right.$$
$$\left. + x {d_{i_{NLOS}}}^{x-1} \frac{TS_m - WS_{i_m}|_{NLOS}}{\|TS - WS_i\|_{NLOS}} \right) \Bigg] \tag{6.7}$$
$$+ \left[\left({d_{TS_{LOS}}} + {d_{TS_{NLOS}}}^{x} \right)^{n_{LOS}-1} \left(\frac{TS_m - \mathrm{CS}_m|_{LOS}}{\|TS - \mathrm{CS}\|_{LOS}} \right. \right.$$
$$\left. \left. \left. + x {d_{TS_{NLOS}}}^{x-1} \frac{TS_m - \mathrm{CS}_m|_{NLOS}}{\|TS - \mathrm{CS}\|_{NLOS}} \right) \right] \right\}$$

where P_T is the transmission power, P_n is the mean noise level calculated based on Johnson-Nyquist equation, d_0 is the reference distance for the Log-normal path loss model, $PL(d_0)$ is the path loss referred to d_0, n_{LOS} and n_{NLOS} are the path loss exponents for the LOS and NLOS conditions respectively, and N_{WS} is the number of A-TDOA WS. Every distances d_{LOS} and d_{NLOS} are calculated through the LOS/NLOS ray-tracing algorithm proposed in Section 6.2.

Lastly, the global accuracy is computed based on the Root Mean Squared Error (RMSE) of the diagonal components of the inverse of the FIM (**J**). This metric is widely applied in positioning systems [30], [31] due to the direct knowledge of the radius of global uncertainty in the final target location induced by each Cartesian component of the estimation.

$$RMSE = \sqrt{tr(\mathbf{J})} = \sqrt{\sigma(\widehat{TS})} \tag{6.8}$$

6.4. Multi-objective optimization

The global accuracy of time-based positioning architectures can be maximized in any environment through the optimization of the sensor distribution. Based on the combined model presented in Sections 2 and 3 for estimating time measurement uncertainties, we can perform this optimization for 3D irregular scenarios in the presence of noise, NLOS propagation and multipath. The 3D irregular scenario is designed with a random definition of Node Location Environment (NLE) and Target Location Environment (TLE) [36], to simulate general real scenarios. This allows the optimization of the node deployment in the NLE and the determination of the vehicle navigation areas in the TLE separately.

This is achieved with the Genetic Algorithm (GA) developed in [36], which allows maximum flexibility during the deployment of architecture sensors. The GA introduced a

binary codification of individuals with a scaling technique for achieving 3D adaptation to the NLE region, partial optimizations for reducing grid resolution and free decision in selection techniques (i.e. Tournament, Roulette and Ranking), elitism and mutation.

This optimization of the node deployment in A-TDOA architectures with noise, NLOS propagation and multipath uncertainties must provide an effective connection between the TS and at least four WSs and one CS to determine the target location. The appearance of critical multipath effects and cancelation of LOS paths causes the unavailability of the necessary number of sensors to determine TLE points. Thus, the introduction of more WSs and CSs is required in these cases. The use of a higher number of sensors increases the overall costs of the architecture while also increasing the accuracy.

The main objective of this article is the determination of the best sensor distribution for the combined minimization of noise and NLOS uncertainties and the multipath disruptive effects for multiple number of sensors.

Consequently, a MOP process has been adopted. There are two general approaches in performing MOP [44]: the combination of individual functions with methods to characterize the optimization preferences into a single objective, and the determination of entire Pareto Fronts (PFs) where the final decision is carried out based on a trade-off between crucial parameters [26]. In practice, Pareto optimal sets are preferred to single solutions due to the complexity of the weight selection in the combination of functions and their capability of representing all the spectrum of optimal solutions, which is typical in real-world problems. We refer at [26] and [44] for extensive details on the mathematical framework of the deployed Genetic Algorithm.

For these reasons, we performed a MOP based on the characterization of the PF for the combined minimization of CRB and multipath effects. This process has been accomplished for a different number of sensors, each of them with their own PF. The fitness function *ff* of the GA MOP is based on a maximization approach:

$$ff = c_1 ff_1 + c_2 ff_2 \mp (c_1 + c_2) ff_3 \tag{6.9}$$

where c_1 and c_2 are vectors of coefficients for obtaining PF and individual fitness functions are expressed through the following relations. The sum of c_1 and c_2 components guarantees the limitations and the accomplishment of the objectives of the optimization regardless of the environment and the characterization of the MOP process. ff_1 introduces global accuracy

in the MOP fitness function:

$$ff_1 = \frac{\left(RMSE_{ref} - \frac{\sum_{k=1}^{K_{TLE}} RMSE_k}{K_{TLE}}\right)^4}{RMSE_{ref}{}^4} \tag{6.10}$$

where K_{TLE} indicates the number of analyzed points in the TLE region, $RMSE_k$ is the RMSE of the point of the discretization of TLE in which accuracy is being analyzed, and $RMSE_{ref}$ is the RMSE fixed as accuracy reference for the optimization. The $RMSE_{ref}$ parameter controls three aspects: a) the confinement of all values of the ff_1 function in the interval [0,1] for alluring subsequent MOP process, b) the provision of a mode for a progressive penalization in ff_1 function as RMSE values become higher, and c) the characterization of all conditions where the minimum number of sensors for a univocal positioning in an A-TDOA architecture is not available. These aspects are accomplished through the definition of a value of the $RMSE_{ref}$ larger than the maxi- mum expected in the environment for any sensor distribution. In this case, previous studies showed that 100 meters are the optimum value for the $RMSE_{ref}$ parameter for guaranteeing a correct incremental penalization for low accuracy sensor placements, and this error bound is not reachable in any circumstances of operation (in different scenarios, this value should be adjusted).

The term ff_2 represents the contribution of the multipath effect, which is introduced in the main fitness function as:

$$ff_2 = \frac{\sum_{k=1}^{K_{TLE}} \left(1 - \frac{\sum_{j=1}^{3N_{WS}+1} M_j}{3N_{WS}+1}\right)}{K_{TLE}} \tag{6.11}$$

where N_{WS} is the total number of WS, and M_j indicates the ratio between multipath detected points (1 positive, 0 negative) and the total number of analyzed points for each communication link associated to A-TDOA architecture – N_{WS} links target-WS, N_{WS} links WS-CS and $N_{WS}+1$ links target-CS–. This evaluation is based on the assumption of one CS for the A-TDOA architecture deployed. The possible values for ff_2 are contained in the interval [0,1], where higher quantities indicate less presence of multipath effects.

The component ff_3 of the MOP fitness function expresses the penalization factor associated with forbidden censoring regions, i.e. inner zone to NLE region limits, or incapacity of 3D positioning when less than five sensors received the positioning signals with

a power that exceeds the sensibility of the receivers (SNR_{min}), resulting in the unavailability for positioning in each point of the TLE region. The component ff_3 also allows the reward in *ff* values when sensors are situated in certain regions of interest or the sensors configuration presents homogeneity in the number of sensors for the TLE region. The component ff_3 is expressed as:

$$ff_3 = \frac{\sum_{i=1}^{N} R_i}{N} + \frac{\sum_{k=1}^{K_{TLE}} \left(P_{CS_k} + P_{WS_k} - \frac{Dif_k}{100} \right)}{K_{TLE}}$$

$$Dif_k = \begin{cases} 1 - \left[\frac{\left(\frac{1}{4}\right) - \left(\frac{1}{Md_k}\right)}{\left(\frac{1}{4}\right)} \right] & if \quad \frac{\sum_{k=1}^{K_{TLE}} P_{WS_k}}{K_{TLE}} = 0 \\ 0 & if \quad \frac{\sum_{k=1}^{K_{TLE}} P_{WS_k}}{K_{TLE}} \neq 0 \end{cases} \tag{6.12}$$

$$Md_k = max(P_{WS}) - min(P_{WS})$$

where R_i indicates if penalization is applied or not (value of 1 or 0, respectively) for each sensor location in the case of forbidden sensor placement. P_{CS} represents the penalization due to the unavailability of CS in every point k of the TLE region. In this way, P_{CS} indicates the penalization at each point of the TLE when at least four complete links (i.e. 1 CS and 4 WS, assuming a "receive and retransmit" technique for the A-TDOA system [10]) are not accomplished. Lastly, *Dif* relates the difference between the maximum and the minimum number of possible positioning links in the TLE region, applied if P_{WS} is null in every point of the TLE zone. The *Dif* parameter acquires a special relevance, since it penalizes sensor distributions with high heterogeneity in the number of possible links for each point of the TLE region. This circumstance induces stagnations in the accuracy value in the GA optimization, leading to reach sub-optimal sensor distributions. Therefore, the minimization of the *Dif* magnitude is accomplished by sensor placements where the number of possible positioning links in each point of the TLE region is comparable (and adaptable to the environment conditions). The combined ff_3 function ensure the progressive penalization of individuals, facilitating the learning process of the GA and enabling a correct exploration of the possible solutions space. All the variables of the ff_3 function are confined in the interval [0,1].

The focus on the interval of possible values of individual fitness functions allows the adequate characterization of c_1 and c_2 weight vectors. This enables the attainment of a proper

PF for every number of sensors involved in the positioning architecture.

6.5. Results

The configuration parameters for the modeling of the noise presence and NLOS propagation is reported in Table 6.1. Their selection has been made on an attempt of representing a LPS.

Table 6.1. Parameters selected for the combined model for noise, clock errors and NLOS propagation. Values selected are based on [41], [43], [45].

Parameter	Magnitude
Frequency of emission	1090 MHz
Bandwidth	100 MHz
Transmission power	400 W
Mean noise power	- 94 dBm
Receptor sensibility	- 90 dBm
Time-Frequency product	1
Antennae gains	Unity
LOS Path LOSs exponent	2.1
NLOS Path LOSs exponent	4.1

The configuration variables of the multipath detection algorithm are shown in Table 6.2. The selection of the parameter values reported in Table 6.1 and Table 6.2 are an example of configuration according to the environment characteristics and a generic positioning technology. The proposed technique could be adapted to the analysis of any 3-D irregular environment and the simulation of distinct operating conditions through the modification of the hyper-parameters presented in Tables 6.1 and 6.2. In this sense, the positioning technology implemented and the parameters for modeling LOS/NLOS environments are defined based on Table 6.1 magnitudes. The estimation and characterization of multipath phenomena is provided through the calibration of Table 6.2 parameters according to the environment particularities.

Table 6.2. Parameters and magnitudes selected for the multipath detection algorithm.

Parameter	Magnitude
Fresnel Zone	First
Obstacle Clearance Fresnel Zone	60%
Relative spatial resolution of the	10 %

emitter-receiver link	
Angle discretization in the ellipsoid section	10 °
Relative spatial resolution in the surface projection	5 %

For the values of the parameters related to the ellipsoid discretization process, we took into account the trade-off between spatial resolution and processing time. It should be pointed out that the multipath detection remains practically the same with finer relative spatial resolutions than presented in Table 6.2.

For the configuration of the GA we chose Tournament 2 as selection procedure, single-point crossover, and 2% of elitism. Due to the complexity of the optimization environment and the proclivity to local maxima, a highly mutation percentage of 7% has been set. This characterization grants the maximization of the MOP fitness function with minimum number of generations to converge, a situation that is reached when the maximum value of the fitness function remains unchanged for three generations and at least 80% of individuals are similar.

The characteristics of this optimization, where the environment causes that a great number of solutions are not valid, leads to the application of a pre-processing during the construction of the initial population of the GA. In this regard, we use a random search based on seeking solutions where the value of ff_1 is higher than 0 for constructing the initial population. This guarantees the correct progressive improvement of the quality of the individuals and the avoidance of local optimizations.

We constructed a 3D scenario for simulations, where NLE and TLE regions are defined as presented in Figure 6.5.

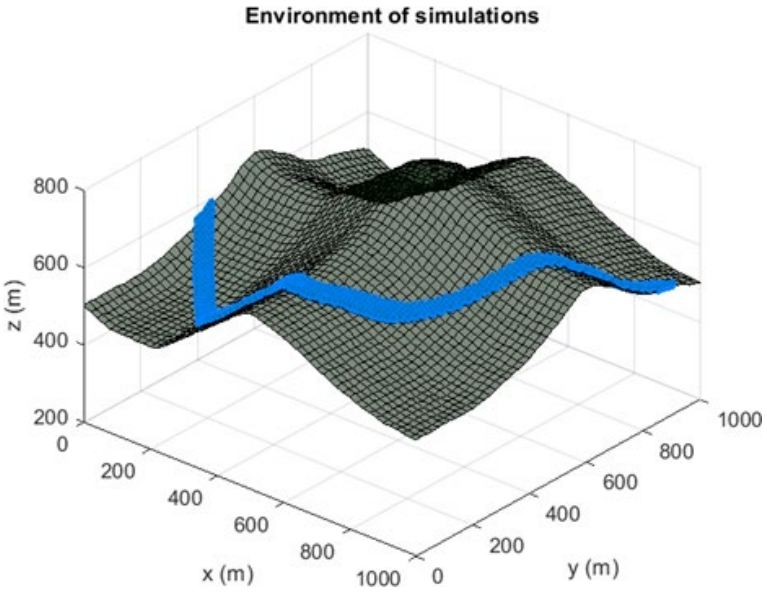

Figure 6.5. Environment of optimization. TLE region is represented in blue color.

The TLE region height modeled is of size from 1 to 10 meters with regards to the base surface elevation. The spatial discretization of the TLE is 10 meters in *x-y* cartesian coordinates and 2 meters in z coordinate. The resolution selected provides a correct evaluation of sensor distribution properties without the need of analyzing an excessive number of points. This is due to the continuity of accuracy and multipath conditions which are characteristic for finer grids than selected. In regard to the NLE region, the GA coding [36] enables the adaptation of the length of chromosomes to region limits. This factor provides a spatial resolution that varies in the range of 0.5 to 1 meters, depending on the specific local characteristics of the environment. In terms of elevation, the NLE region has a limited minimum height of 3 meters for reducing multipath and interference effects and a restricted maximum magnitude of 15 meters in order to reduce the size of sensor supports.

The results achieved for the optimization of the PFs for a distinct number of sensors are shown in Figure 6.6.

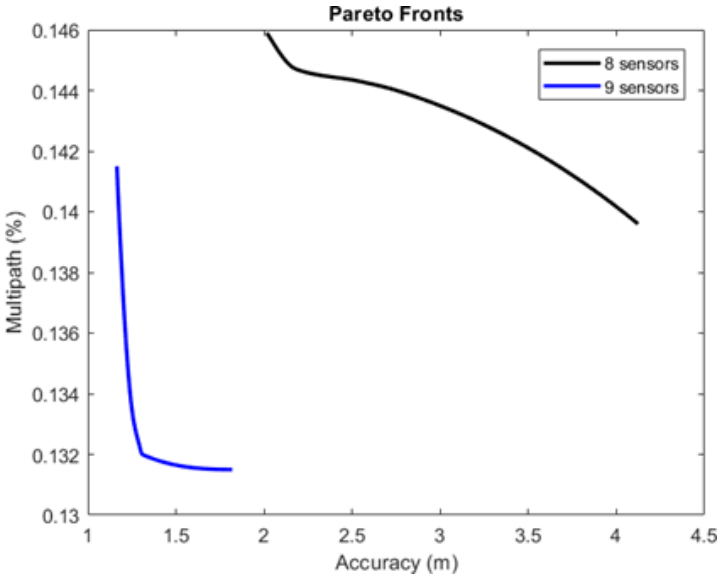

Figure 6.6. Pareto Fronts for 8 and 9 sensors.

On the one hand, an increase in the number of sensors deployed in the scenario directly leads to a reduction in the location uncertainties and in adverse multipath phenomena. On the other hand, the architecture cost expressed via the number of spread sensors also enhances. Table 3 shows the relation between optimization parameters for the PF of 8 sensors in terms of MOP fitness function components ff_1 and ff_2:

Table 6.3. Example of individual fitness functions in the PF in the case of 8 sensors.

Ponderation ($ff_1 - ff2$)	**Value ff_1**	**Value ff_2**
1-10	0.9462	0.8604
3.25 - 7.75	0.9638	0.8560
5.5 – 5.5	0.9665	0.8557
7.75 – 3.25	0.9712	0.8553
10 - 1	0.9734	0.8541

In Figures 6.7 and 6.8, we report the accuracy evaluation and multipath analysis for 5 A-TDOA sensors. The selected distribution is relative to an equal weighting of MOP parameters for CRB and multipath.

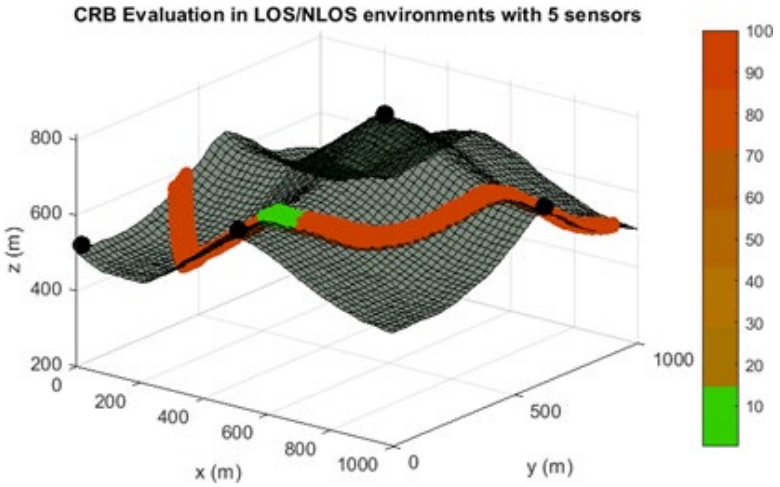

Figure 6.7. CRB 5 sensors for MOP with equal coefficient for CRB and Multipath. Grey tones indicate the reference surface and black spheres the location of the A-TDOA architecture sensors.

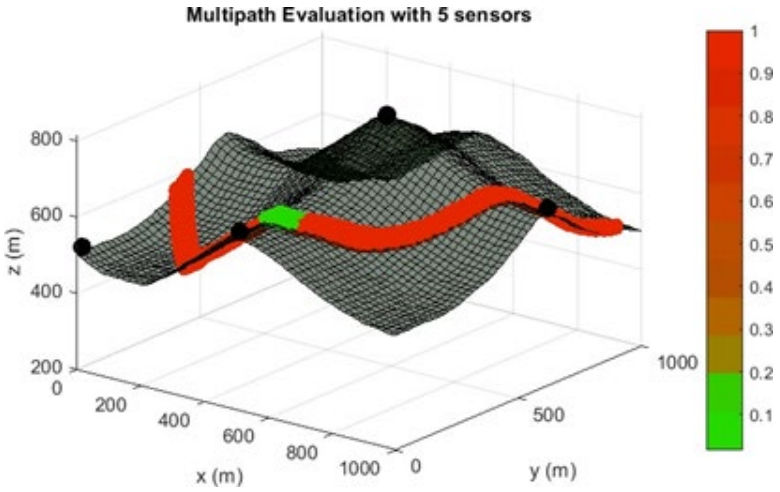

Figure 6.8. Multipath evaluation for 5 sensors in the case of MOP with equal coefficient for CRB and Multipath. Values represent the ratio between multipath detected points and total analyzed points for each zone in the TLE region.

It is observed in Figure 6.7 that 5 sensors cannot provide high-accuracy positioning for the complete TLE region. This is due to the unavailability of at least 5 sensors in coverage for each analyzed point in the scenario of simulations (ff_3 value do not exceed zero). Multipath adverse effects shown in Figure 6.6 present a similar behavior, where multipath impacts cannot be minimized in the entire domain, especially at communication links between targets and sensors. Problems associated with the deployment of 5 A-TDOA sensors can be overcome with the introduction of additional sensors, as shown in Figures

6.9 and 6.10, where the CRB and multipath evaluation for an A-TDOA architecture with 9 sensors are displayed (in this configurations ff_3 value exceed zero and the homogeneity term -*Dif*- is applied to the GA optimization).

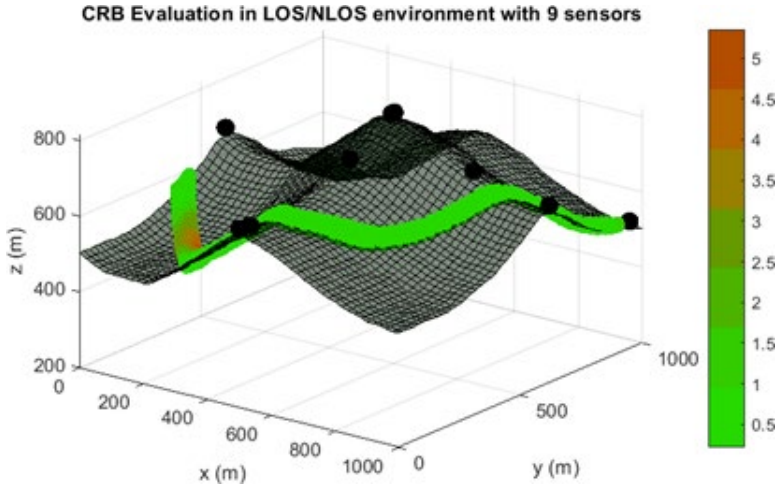

Figure 6.9. CRB 9 sensors for MOP with equal coefficient for CRB and Multipath.

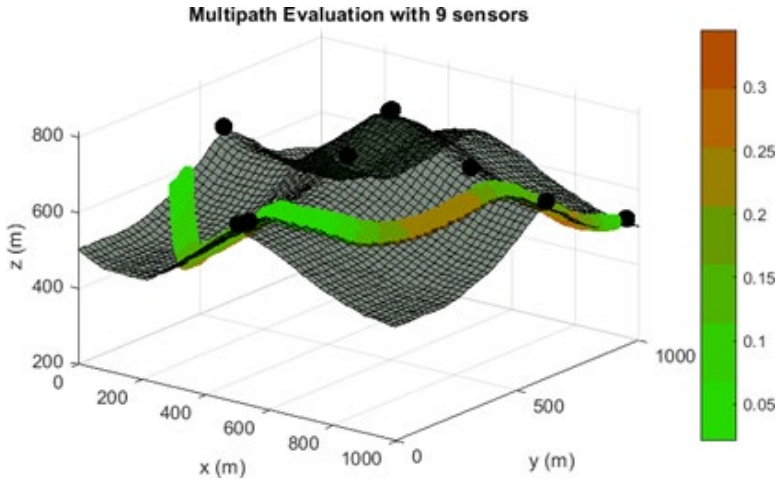

Figure 6.10. Multipath evaluation for 9 sensors in the case of MOP with equal coefficient for CRB and Multipath.

Lastly, the results shown in Figures 6.7, 6.8, 6.9 and 6.10 indicate that the location of the CS for the A-TDOA architecture, and all systems with at least one centralized sensor for performing time measurements, is critical for accurate operation of the positioning system. The methodology presented in this manuscript provides a real-based estimation of the capabilities of the positioning architectures in 3D real environments prior to its real

implementation.

6.6. Conclusion

In this paper, we propose a new combined model for measuring positioning architectures accuracy, where the effects of noise and NLOS propagation are quantified in the CRB. For that purpose, we implemented a ray-tracing LOS/NLOS algorithm for determining LOS and NLOS distances in each communication link in 3D environments. In addition, the most critical multipath effects, i.e. destructive interference and inability to distinguish LOS path, are detected by means of a novel algorithm that operates in the 3D space.

We implemented this characterization of principal ranging errors in the A-TDOA architecture, developing a MOP process for optimizing sensor placement based on the combined minimization of ranging errors and multipath impacts. This optimization has been performed in a 3D real scenario for a variable number of architecture sensors.

The results that we achieved show that the designed methodology provides a method for estimating a priori the maximal accuracy capabilities of the A-TDOA architecture in 3D complex environments. In addition, the procedure allows to determine the minimum number of sensors to achieve a required accuracy demand, taking into account a trade-off between accuracy, multipath presence and cost of the system.

6.7. References

1. J. Shen, A. F. Molisch, and J. Salmi, "Accurate passive location estimation using TOA measurements", *IEEE Trans. Wireless Commun.*, vol. 11, no. 6, pp. 2182–2192, Jun. 2012.
2. C. Mensing and S. Plass, "Positioning algorithms for cellular networks using TDOA", in *Proc. IEEE Int. Conf. Acoust., Speech, Signal Process.*, Toulouse, France, May 2006, p. 5,
3. A. J. Weiss, "On the accuracy of a cellular location system based on RSS measurements", *IEEE Trans. Veh. Technol.*, vol. 52, no. 6, pp. 1508–1518, Nov. 2003.
4. D. Niculescu and B. Nath, "Ad hoc positioning system (APS) using AOA", in *Proc. 22nd Annu. Joint Conf. IEEE Comput. Commun. Soc. (INFOCOM)*, San Francisco, CA, USA, Mar. 2003, pp. 1734–1743.
5. D. Ni, O. A. Postolache, C. Mi, M. Zhong, and Y. Wang, "UWB indoor positioning

application based on Kalman filter and 3-D TOA localization algorithm", in *Proc. 11th Int. Symp. Adv. Topics Electr. Eng. (ATEE)*, Bucharest, Romania, Mar. 2019, pp. 1–6.

6. A. A. D'Amico, U. Mengali, and L. Taponecco, "TOA estimation with the IEEE 802.15.4a standard", *IEEE Trans. Wireless Commun.*, vol. 9, no. 7, pp. 2238–2247, Jul. 2010.
7. J. Xu, M. Ma, and C. Law, "Position estimation using UWB TDOA measurement", in *Proc. IEEE Int. Conf. Ultra-Wideband*, Waltham, U.K., Sep. 2006, pp. 605–610.
8. B. Sundararaman, U. Buy, and A. D. Kshemkalyani, "Clock synchronization for wireless sensor networks: A survey", *Ad Hoc Netw.*, vol. 3, no. 3, pp. 281–323, May 2005.
9. V. Djaja-Josko and J. Kolakowski, "A new transmission scheme for wireless synchronization and clock errors reduction in UWB positioning system", in *Proc. Int. Conf. Indoor Positioning Indoor Navigat. (IPIN)*, Alcala de Henares, Spain, Oct. 2016, pp. 1–6.
10. S. He and X. Dong, "High-accuracy localization platform using asynchronous time difference of arrival technology", *IEEE Trans. Instrum. Meas.*, vol. 66, no. 7, pp. 1728–1742, Jul. 2017.
11. R. Álvarez, J. Díez-González, E. Alonso, L. Fernández-Robles, M. Castejón-Limas, and H. Perez, "Accuracy analysis in sensor networks for asynchronous positioning methods", *Sensors*, vol. 19, no. 13, p. 3024, Jul. 2019.
12. S. Lanzisera, D. Zats, and K. S. J. Pister, "Radio frequency time-of-flight distance measurement for low-cost wireless sensor localization", *IEEE Sensors J.*, vol. 11, no. 3, pp. 837–845, Mar. 2011.
13. G. Han, C. Zhang, L. Shu, and J. J. P. C. Rodrigues, "Impacts of deployment strategies on localization performance in underwater acoustic sensor networks", *IEEE Trans. Ind. Electron.*, vol. 62, no. 3, pp. 1733–1752, Mar. 2015.
14. J. O. Roa, A. R. Jiménez, F. Seco, J. Ealo, and F. Ramos, "Optimal placement of sensors for trilateration: Regular lattices vs meta-heuristic solutions", in *Proc. Int. Conf. Comput. Aided Syst. Theory (EUROCAST)*, 2007, pp. 780–787.
15. D. Moreno-Salinas, A. Pascoal, and J. Aranda, "Optimal sensor placement for multiple target positioning with range-only measurements in two-dimensional scenarios", *Sensors*, vol. 13, no. 8, pp. 10674–10710, Aug. 2013.

16. R. L. Francis, L. F. McGinnis, and J. A. White, *Facilities Layout and Location: An Analytical Approach*, 2nd ed. Englewood Cliffs, NJ, USA: Prentice-Hall, 1992.
17. D. Sinriech and S. Shoval, "Landmark configuration for absolute positioning of autonomous vehicles", *IIE Trans.*, vol. 32, no. 7, pp. 613–624, Jul. 2000.
18. M. Shamaiah, S. Banerjee, and H. Vikalo, "Greedy sensor selection: Lever- aging submodularity", in *Proc. 49th IEEE Conf. Decis. Control (CDC)*, Atlanta, GA, USA, Dec. 2010, pp. 2572–2577.
19. O. Tekdas and V. Isler, "Sensor placement for triangulation-based localization", *IEEE Trans. Autom. Sci. Eng.*, vol. 7, no. 3, pp. 681–685, Jul. 2010.
20. Y. Yoon and Y.-H. Kim, "An efficient genetic algorithm for maximum coverage deployment in wireless sensor networks", *IEEE Trans. Cybern.*, vol. 43, no. 5, pp. 1473–1483, Oct. 2013.
21. J. Díez-González, R. Álvarez, L. Sánchez-González, L. Fernández-Robles, H. Pérez, and M. Castejón-Limas, "3D tdoa problem solution with four receiving nodes", *Sensors*, vol. 19, no. 13, p. 2892, Jun. 2019.
22. S. Joshi and S. Boyd, "Sensor selection via convex optimization", *IEEE Trans. Signal Process.*, vol. 57, no. 2, pp. 451–462, Feb. 2009.
23. B. Peng and L. Li, "An improved localization algorithm based on genetic algorithm in wireless sensor networks", *Cognit. Neurodyn.*, vol. 9, no. 2, pp. 249–256, Jan. 2015.
24. N. Jiang, S. Jin, Y. Guo, and Y. He, "Localization of wireless sensor network based on genetic algorithm", *Int. J. Comput. Commun. Control*, vol. 8, no. 6, pp. 825–837, 2013.
25. F. Domingo-Perez, J. L. Lázaro-Galilea, E. Martín-Gorostiza, D. Salido-Monzú, and A. Wieser, "Evolutionary optimization of sensor deployment for an indoor positioning system with unknown number of anchors", in *Proc. Ubiquitous Positioning Indoor Navigat. Location Based Service (UPINLBS)*, Corpus Christ, TX, USA, 2014, pp. 195–202.
26. F. Domingo-Perez, J. L. Lázaro, I. Bravo, A. Gardel, and D. Rodríguez, "Optimization of the coverage and accuracy of an indoor positioning system with a variable number of sensors", *Sensors*, vol. 16, no. 6, p. 934, Jun. 2016.
27. J. Chaffee and J. Abel, "GDOP and the Cramer-Rao bound", in *Proc. IEEE Position, Location Navigat. Symp. (PLANS)*, Las Vegas, NV, USA, Apr. 1994, pp. 663–668.
28. J. O. Roa, A. R. Jiménez, F. Seco, C. Prieto, J. Ealo, and F. Ramos, "Primeros

resultados en la optimización de la ubicación de balizas para localización utilizando algoritmos genéticos", in *Proc. 26th Jornadas Automática*, 2005, pp. 75–86.

29. M. Burke and N. Bos, "Optimal placement of range-only beacons for mobile robot localization", in *Proc. 4th Robot. Mechatronics Conf. South Africa*, Pretoria, South Africa, 2011, pp. 1–6.
30. B. Huang, L. Xie, and Z. Yang, "Analysis of TOA localization with heteroscedastic noises", in *Proc. 33rd Chin. Control Conf.*, Nanjing, China, Jul. 2014, pp. 327–332.
31. B. Huang, L. Xie, and Z. Yang, "TDOA-based source localization with distance-dependent noises", *IEEE Trans. Wireless Commun.*, vol. 14, no. 1, pp. 468–480, Jan. 2015.
32. S. Martínez and F. Bullo, "Optimal sensor placement and motion coordination for target tracking", *Automatica*, vol. 42, no. 6, pp. 661–668, 2006.
33. J. T. Isaacs, D. J. Klein, and J. P. Hespanha, "Optimal sensor placement for time difference of arrival localization", in *Proc. 48h IEEE Conf. Decis. Control (CDC) Held Jointly 28th Chin. Control Conf.*, Shanghai, China, Dec. 2009, pp. 7878–7884.
34. K. Papakonstantinou and D. Slock, "Cramer-Rao bounds for hybrid localization methods in LOS and NLOS environments", in *Proc. IEEE 21st Int. Symp. Pers., Indoor Mobile Radio Commun. Workshops*, Instanbul, Turkey, Sep. 2010, pp. 213–217.
35. B. T. Sieskul, F. Zheng, and T. Kaiser, "A hybrid SS–ToA wireless NLOS geolocation based on path attenuation: ToA estimation and CRB for mobile position estimation", *IEEE Trans. Veh. Technol.*, vol. 58, no. 9, pp. 4930–4942, Jun. 2009.
36. J. Díez-González, R. Álvarez, D. González-Bárcena, L. Sánchez-González, M. Castejón-Limas, and H. Perez, "Genetic algorithm approach to the 3D node localization in TDOA systems", *Sensors*, vol. 19, no. 18, p. 3880, Sep. 2019.
37. R. M. Vaghefi and R. M. Buehrer, "Cooperative localization in NLOS environments using semidefinite programming", *IEEE Commun. Lett.*, vol. 19, no. 8, pp. 1382–1385, Aug. 2015.
38. V. P. Ipatov, *Spread Spectrum and CDMA: Principles and Applications*. Hoboken, NJ, USA: Wiley, 2005.
39. H. D. Hristov, *Fresnel Zones in Wireless Links, Zone Plate Lenses and Antennas*. Norwood, MA, USA: Artech House, 2000.
40. S. Cavassila, S. Deval, C. Huegen, D. van Ormondt, and D. Graveron-Demilly,

"Cramér-Rao bounds: An evaluation tool for quantitation", *NMR Biomed.*, vol. 14, no. 4, pp. 278–283, Jun. 2001.

41. J. Zhou, L. Shen, and Z. Sun, "A new method of D-TDOA time measurement based on RTT", in *Proc. MATEC Web Conf.*, Sep. 2018, p. 03018.
42. R. Kaune, J. Hörst, and W. Koch, "Accuracy analysis for TDOA localization in sensor networks", in *Proc. 14th Int. Conf. Inf. Fusion*, Chicago, IL, USA, Jul. 2011, pp. 1–8.
43. T. S. Rappaport, *Wireless Communications: Principles And Practice*. Upper Saddle Rive, NJ, USA: Prentice-Hall, 2002.
44. A. Singh, "A comprehensive review on multi-objective optimization using", *Int. J. Comput. Techn.*, vol. 3, no. 2, pp. 1–8, 2016.
45. A. S. Yaro and A. Z. Sha'ameri, "Effect of path loss propagation model on the position estimation accuracy of a 3-dimensional minimum configuration multilateration system", *Int. J. Integr. Eng.*, vol. 10, no. 4, pp. 35–42, Aug. 2018.

Chapter 7

Conclusions and future research

7.1. Conclusions

Modern and future high-demanding applications in positioning services, such as autonomous navigation, require novel approaches and methodologies to successfully provide on-demand superior accuracy in location, stability, and robustness during actual operation, and realistic cost estimations for architectures deployment. All of these conditions can be accomplished through the optimization of architecture sensor distributions of Local Positioning Systems (LPS), which is the aim that guides this dissertation. In this sense, the concluding remarks of this thesis are outlined hereunder:

- The Genetic Algorithm (GA) with the new scaling technique for node codification allows the optimization of sensor distributions of time-based positioning systems with a free definition of Node Location Environments (NLE) and Target Location Environments (TLE). Besides, the proposed methodology increases the flexibility in the analysis of the solutions space, enables on-demand optimizations with variable spatial resolutions, and empowers trade-offs between representativeness of simulations and GA processing time.
- The new adaptation of the Cramér-Rao Lower Bound (CRLB) for noised modeling shows that the Asynchronous Time-Difference of Arrival (A-TDOA) architecture provides the best performance in terms of principal statistical metrics for accuracy than the Difference Time-Difference of Arrival (D-TDOA) systems. This behavior is directly promoted by the minimization of the total path of positioning signals for generating each time-difference measurement.
- The novel CRLB model for noise and clock errors combined uncertainties in

time-based positioning systems and the GA optimization with scaling technique, allow the comparison among location architectures and the obtainment of multiple conclusions:

- The stability of time measurement uncertainties only depends on the clock drift of the Coordinate Sensor (CS) for A-TDOA architectures, unlike TOA and TDOA systems, where the instability is encouraged due to synchronism errors, clock drift, and positioning signals paths. This fact has special relevance in LPS where distances between target and sensors are highly heterogeneous.

- For environments where clock error uncertainties are practically neglected in comparison to noise effects, as in Global Navigation Satellite Systems (GNSS), TOA techniques show better throughput in terms of accuracy for optimized sensor distributions, followed by TDOA and A-TDOA architectures. The reason lies in the minimization of noise-induced uncertainties in global accuracy due to the diminution in total absolute signal distance travels for each time measurement to compute in the architecture.
- For conditions where clock error uncertainties cannot be ignored, characteristic of LPS, A-TDOA architectures significantly outperform the rest of time-based positioning due to the reduction of clock uncertainties in global accuracy. This is mainly supported in the elimination of synchronism errors –initial time offset and time from the last synchronization– while maintaining noise uncertainties. Besides, this behavior benefits the stability and robustness of A-TDOA systems, becoming a potential candidate for high-demanding LPS applications.

- The new LOS/NLOS ray-tracing and multipath detection algorithms, in combination with the GA optimization with scaling in codification and the Cramér-Rao Bound (CRB) for modeling NLOS conditions in time-based positioning systems, provide a novel method for estimating a priori the maximal performance of architecture before implementation in 3D complex

scenarios.

Besides, multi-objective optimizations for obtaining Pareto-Fronts (PFs) among accuracy, multipath, number of deployed sensors, and cost of the system are achieved thanks to the presented models and algorithms.

7.2. Future research areas

The advent of autonomous vehicles, in terrestrial and aerial variants, together with current and future applications with high-demands in location accuracy, requires new approaches in positioning systems where location service must be not only high-accurate also remarkably robust and stable in all the expected areas of operations of the objects to locate. The understanding of these necessities is essential for the safe deployment of these modern applications. In this sense, the work presented in this dissertation is only the beginning of the future research of this study scope, being the most representative investigation lines presented in the following paragraphs:

Experiments in outdoor and indoor conditions must be conducted to validate and enhance the quality of uncertainty models of noise, clock errors, and NLOS conditions, for different positioning technologies. Concretely, Ultra-Wide Band (UWB) communications are a very promising technique for high-accuracy location in indoor environments. For outdoor scenarios, a plethora of new different technologies based on *pulse compression* signals with Non-Orthogonal Multiple Access (NOMA) techniques for multiplexing can be tested for high-demanding applications. The obtainment of experimental data enables the adoption of supervised techniques of Artificial Intelligence (AI) to build complex uncertainty models with more representativeness for closing the gap between simulations and reality.

GAs are perfectly adapted techniques to solve the Node Location Problem (NLP). However, like the rest of heuristic methodologies, are exposed to local optimizations, convergence problems, and difficult transitions between intensification and diversification stages. In this regard, potential improvements can be achieved by increasing the robustness of the GA when optimizing discrete environments subjected to NLOS discontinuities. Other performance improvements can be achieved with the adoption of new optimization procedures that allows the reduction of stagnation periods, thanks to the combination of different genetic operators or the association with other heuristics/exacts optimization procedures. Lastly, studies about the fitness function characteristics would allow future "translations" to more solvable functions with less susceptibility to fall into local

optimizations.

Finally, more investigation should be carried out in A-TDOA architectures, as the most promising architecture in terms of accuracy, stability, and robustness for modern high-demanding applications such as autonomous navigation. Particularly, A-TDOA systems present distinct types of sensors, where Coordinate Sensors (CS) play a critical role during positioning. In this sense, availability analysis and optimization for normal and failure conditions should be performed for future implementations of these systems. Also "receive and retransmit" strategies of these architectures should be modeled in the accuracy and availability ambits, as the point of difference with traditional time-based positioning systems.

Annex I

Synthesis in Spanish

En virtud del cumplimiento del punto 3º del artículo 19 del Reglamente de las enseñanzas Oficiales de Doctorado y el Título de Doctor por la Universidad de León, debido a que el idioma de la tesis es diferente del castellano, se adjunta un resumen de cada uno de los capítulos de esta tesis doctoral para su adopción a trámite.

Resumen

El desarrollo e implementación de futuras aplicaciones construidas sobre tecnologías de navegación autónoma está fuertemente conectado a sistemas de posicionamiento de altas prestaciones que puedan localizar objetivos con gran exactitud, estabilidad y robustez en entornos con condiciones de operación severas.

Los Sistemas de Posicionamiento Locales (LPS) se erigen como tecnologías prometedoras para acometer estos requerimientos, gracias a la implementación adaptable de múltiples sensores de la arquitectura de posicionamiento seleccionada en las proximidades de los objetos a los que proporcionar el servicio de localización, disminuyendo con ello los efectos adversos sobre las señales de posicionamiento y maximizando el rendimiento global del sistema. Sin embargo, el comportamiento de los LPS es directamente dependiente de la ubicación de los sensores de las arquitecturas de posicionamiento, estando este problema de optimización caracterizado dentro de la categoría NP-Hard, siendo imposible alcanzar soluciones exactas en tiempo polinómico.

La tecnología de posicionamiento implementada en los LPS también afecta masivamente al rendimiento global del sistema. Los sistemas basados en mediciones temporales se han extendido universalmente gracias a su solución de compromiso entre exactitud, efectividad, estabilidad, flexibilidad, robustez y ratio entre coste y comportamiento del sistema deseado. Se han utilizado predominantemente las arquitecturas TOA, TDOA y TDOA asíncronas. No obstante, no existen modelos para establecer comparativas entre el rendimiento de cada arquitectura para aplicaciones de altos requerimientos en LPS.

El objetivo y motivación de esta tesis doctoral es el desarrollo de un procedimiento novedoso para optimizar la colocación de sensores de sistemas de posicionamiento basados en mediciones temporales para aplicaciones de LPS de altas prestaciones en entornos tridimensionales complejos. Unido a ello, en esta disertación se aborda la generación de nuevos modelos para caracterizar las principales fuentes de error en los sistemas basados en mediciones temporales. A partir de la metodología propuesta, se establecen comparativas

entre las arquitecturas de posicionamiento, maximizando el rendimiento de cada una de ellas en el entorno en cuestión, y permitiendo el diseño bajo demanda de LPS y la estimación de sus capacidades con anterioridad a su implementación real.

Para completar este objetivo, el primer paso fue el desarrollo de una herramienta heurística basada en Algoritmos Genéticos (GA) para optimizar distribuciones de sensores de sistema de posicionamiento de acuerdo a un conjunto de requerimientos predefinidos. En esta tesis se presenta un nuevo GA con una codificación de tipo "scaling" capaz de realizar optimizaciones tridimensionales en entornos complejos, con independencia de la definición de las posibles localizaciones de los sensores de la arquitectura de posicionamiento (NLE) y de los objetivos a ubicar (TLE).

El segundo paso es la creación de modelos de exactitud basados en la cota-inferior de Cramér-Rao (CRLB) para estimar las máximas capacidades de sistemas de posicionamiento basados en mediciones temporales, independientemente del algoritmo de posicionamiento utilizado. La principal ventaja de este método es su cimentación sobre la flexibilidad a la hora de caracterizar comportamientos heterocedásticos en las varianzas asociadas a los factores que componen el problema de estimación. Este factor es especialmente importante en LPS, donde cada sensor de la arquitectura está sometido a condiciones de operación diferentes. Inicialmente, se presenta una nueva adaptación de la CRLB para incertidumbres introducidas por ruido en las mediciones temporales para arquitecturas TDOA asíncronas. Convencionalmente, los modelos de ruido han sido aplicados a sistemas TOA y TDOA, donde los trayectos de las señales de posicionamiento son directos entre objetivos y sensores. Para sistemas TDOA asíncronos, las técnicas de retransmisión deben ser embebidas dentro del modelo, junto con la caracterización de las pérdidas de propagación introducidas. Entre los sistemas asíncronos, las simulaciones demuestran que las arquitecturas A-TDOA superan en rendimiento al resto en términos de exactitud.

A continuación, los errores de los relojes presentes en los instrumentos de medición y las incertidumbres generadas por el ruido fueron modelizados conjuntamente en base a una nueva caracterización de la CRLB. Con este modelo y la optimización mediante GA con codificación de tipo "scaling" se estableció un banco de pruebas para comparar las arquitecturas TOA, TDOA y A-TDOA en entornos tridimensionales. Después de las optimizaciones, la arquitectura A-TDOA superó considerablemente al resto de sistemas debido a la eliminación de los errores relacionados con el sincronismo –desviación inicial de

sincronización y lapso temporal desde la última sincronización– y la reducción de las incertidumbres inducidas por trayectos de las señales más extensos que en el resto de sistema, convirtiéndose en la única arquitectura candidata para ser implementada en LPS de altas prestaciones.

Finalmente, las condiciones de operación NLOS fueron modelizadas en la CRB para estimación de exactitud. La nueva propuesta utiliza un nuevo algoritmo de rastreo para cuantificar las condiciones NLOS en cada uno de los enlaces de comunicación para las diferentes arquitecturas de posicionamiento en entornos complejos tridimensionales. Adicionalmente, se desarrolló un novedoso enfoque para detectar y cuantificar los efectos adversos del multipath debido a la presencia de objetos en la zona de Fresnel y la zona de Minimum Line-of-Sight path para cada enlace de comunicaciones. La combinación de las todas técnicas propuestas permite la realización de optimizaciones multiobjetivo para exactitud, multipath, y coste en estos sistemas de posicionamiento.

Como apunte adicional, los resultados y explicaciones de este resumen están ampliamente detallados, justificados y validados en el contenido en el idioma original de la tesis doctoral. Este resumen es solamente un documento de apoyo, para más información consulte el resto del documento.

Sección A.1

Objetivos y organización de la tesis

A.1.1. Objetivos

El objetivo de esta disertación es la generación de una nueva metodología que optimice la distribución de sensores en sistemas de posicionamiento local (LPS) en escenarios 3D complejos para aplicaciones de altas prestaciones en la localización, como es el caso de la navegación autónoma. Para afrontar este problema, nos es posible elaborar la siguiente lista de objetivos específicos:

- Investigación sobre los algoritmos genéticos (GA) como las principales técnicas heurísticas para la resolución del problema de localización de nodos (NLP), el cual que se encuentra categorizado dentro de la categoría NP-Hard de problemas matemáticos.
- Desarrollo de un nuevo método para combinar las diferentes codificaciones de diferentes técnicas heurísticas, principalmente para los GA, logrando así la aplicación de estos procesos en escenarios 3D complejos.
- Cuantificar las incertidumbres producidas por la existencia de ruido en el entorno de operación del sistema de posicionamiento, y desarrollo de modelos de estimación derivados de las principales tecnologías de posicionamiento basadas en mediciones temporales.
- Generación de un nuevo modelo para caracterizar la incertidumbre de la localización ocasionada por inestabilidades del reloj y errores de sincronismo en los instrumentos de adquisición de datos de los sistemas de posicionamiento más expandidos basados en mediciones temporales.
- Investigación en los efectos de las distorsiones NLOS en la exactitud para las señales de posicionamiento en situaciones complejas de operación.
- Diseño de técnicas para detectar y minimizar el fenómeno del multipath que induce degradaciones en la señal, así como la incapacidad para diferenciar las

emisiones con línea de visión (LOS) de las diferentes emisiones reflejadas por el escenario.

A.1.2. Contribuciones principales

Una sinopsis de las principales contribuciones de esta disertación se presenta a continuación:

I. Una adaptación de la Cota Inferior de Cramér-Rao (CRLB) para la caracterización de las incertidumbres de ruido a través de un modelo de propagación Log-normal para arquitecturas de posicionamiento asíncronas - Asynchronous Time-Difference of Arrival (A-TDOA) – y diferenciales - Difference Time-Difference of Arrival (D-TDOA).

II. Una nueva técnica para implementar GA en el NLP para escenario 3D complejos basados en un factor de escalamiento en la trasformación a codificación binaria y en operadores genéticos

III. Un novedoso modelo del CRLB para estimación de la precisión en sistemas de posicionamiento basados en mediciones de tiempo, fundamentado en la caracterización de las incertidumbres en las mediciones temporales inducidas por las inestabilidades de ruido y relojes.

IV. Un nuevo algoritmo LOS/NLOS basando en la tecnología ray-tracing para la medición de distancias recorridas por la señal en enlaces de comunicación para el posicionamiento en escenarios 3D complejos.

V. Un novedoso algoritmo multipath para la identificación y cuantificación de inferencia destructiva y para la medición de distancia LOS en comunicaciones para sistemas de posicionamiento basados en mediciones de tiempo para escenarios 3D complejos.

VI. Una nueva cota de Cramér-Rao (CRB) para estimación de la precisión de sistemas de posicionamiento basados en mediciones de tiempo operado en escenarios 3D adversos, con condiciones LOS y NLOS combinadas.

VII. La serie completa de técnicas y algoritmos presentados en esta disertación ofrece un procedimiento para determinar las capacidades máximas de exactitud y alusión de efectos multipath para sistemas de posicionamiento basados en mediciones de tiempo previa implementación real. Esto permite la persecución

de estrategias que valoren la exactitud y el coste de la implementación de estos sistemas, así como soportar la aplicación bajo demanda de esos sistemas para casos particulares.

A.1.3. Organización de la tesis

Esta disertación es estructurada en los siguientes capítulos. En el Capítulo 2 se ofrece una introducción sobre los aspectos generales de la disertación. Concretamente, muestra el estado del arte de los sistemas de posicionamiento junto a las principales técnicas de localización basadas en mediciones temporales. Adicionalmente, se ofrece un análisis de las técnicas de posicionamiento más significantes, remarcando la utilización de metodología heurística y especialmente GA dada su idoneidad para la resolución del NLP.

El Capítulo 3 introduce un nuevo modelo CRLB para la caracterización de la precisión para estimar incertidumbres debido a la presencia de ruido en el escenario para arquitecturas asíncronos. Además, una comparativa en términos de prestaciones se ofrece en escenario 3D con condiciones LOS.

En el Capítulo 4, se presenta un nuevo GA para optimizar la distribución de sensores de sistemas de posicionamiento en entornos complejos 3D. Esta nueva metodología se basa en una nueva etapa de escalado que permite transformar coordenadas cartesianas –expresadas en números reales– en codificación binaria para la aplicación de los operadores genéticos, a partir de las propiedades locales del entorno. Además, los principales operadores genéticos son investigados y comparados para una optimización de una arquitectura A-TDOA en un entorno LOS 3D.

El Capítulo 5 introduce un nuevo modelo CRLB para estimar conjuntamente las incertidumbres inducidas por el ruido y los errores de reloj generadas por el entorno de funcionamiento para las arquitecturas de posicionamiento basadas en el tiempo más ampliamente extendidas –TOA, TDOA, A-TDOA–. La combinación de este modelado con la optimización GA descrita en el Capítulo 4 permite la comparación entre sistemas de posicionamiento basados en mediciones temporales para aplicaciones LPS de alta prestaciones.

En el Capítulo 6 se estudian los fenómenos disruptivos causados por obstrucciones en el entorno de las señales de posicionamiento. Para las condiciones NLOS, se presenta un nuevo modelo CRB para arquitecturas de posicionamiento basadas en mediciones

temporales en combinación con un nuevo algoritmo de trazado de trayectorias LOS / NLOS para caracterizar los enlaces de señales de posicionamiento. Para los fenómenos de multipath, se proporciona una nueva técnica para cuantificar estos fenómenos adversos inducidos por la presencia de objetos en la zona de Fresnel y la zona de trayectoria mínima NLOS. El modelado CRB y la cuantificación multipath se aplican en un proceso de optimización multiobjetivo (MOP) con la GA descrita en el Capítulo 4 para optimizar las distribuciones de sensores de arquitecturas A-TDOA en entornos 3D con condiciones de funcionamiento LOS y NLOS.

Por último, el Capítulo 7 resume las conclusiones de la tesis doctoral y ofrece una visión general de las futuras investigaciones vinculadas a esta disertación.

A.1.4. Marco de investigación

Las investigaciones de esta disertación se han desarrollado bajo la supervisión de la Dra. Hilde Pérez en el grupo de investigación SINFAB. La investigación ha sido financiada por las becas del Ministerio de Economía, Industria y Competitividad de España números DPI2016-79960-C3-2-P y PID2019-108277GB-C21.

Sección A.2

Introducción general

A.2.1. Sistemas de Posicionamiento

El posicionamiento en tiempo real es uno de los soportes sobre los que se asientan gran parte de los desarrollos tecnológicos pasados y existentes en la actualidad. Su influencia va en aumento incluso en los avances tecnológicos futuros, especialmente en todos los relacionados con la navegación autónoma y las aplicaciones derivadas de ella, como robots industriales colaborativos, agricultura de alta precisión, navegación interior y aterrizajes de precisión.

El advenimiento de las tecnologías de navegación autónoma ha endurecido los requisitos de los servicios de localización proporcionados por los sistemas de posicionamiento. Concretamente, estas novedosas aplicaciones exigen un gran rendimiento en términos de exactitud, estabilidad y robustez durante su funcionamiento en entornos hostiles, como escenarios urbanos o interiores.

Tradicionalmente, los sistemas globales de navegación por satélite (GNSS) se han extendido universalmente para aplicaciones de posicionamiento que ofrecen servicios precisos de cobertura global. Asimismo, el despliegue de constelaciones de satélites permite realizar posicionamientos en zonas de difícil acceso, lo que representa un gran avance en el proceso de navegación. Sin embargo, las técnicas GNSS están sujetas a fenómenos ionosféricos adversos que degradan las señales de posicionamiento, haciéndolas vulnerables a fenómenos terrestres hostiles, como la degradación de la señal por las pérdidas de propagación, maximizado con la presencia obstrucciones en durante el trayecto de las señales, y la aparición de multipath. Estos factores inducen grandes incertidumbres durante el posicionamiento, provocando una baja precisión y limitando gravemente la estabilidad y robustez de los GNSS. Las técnicas de augmentación satelitales pueden implementarse localmente para impulsar el rendimiento GNSS en entornos predefinidos, sin embargo, los rendimientos obtenidos de estabilidad y robustez dificulta su uso en aplicaciones de navegación autónoma, independientemente del problema previamente expuesto de la localidad de estas técnicas.

Los sistemas de posicionamiento local (LPS) pueden abordar los requisitos de alta exigencia típicos de las tecnologías de navegación autónoma. Esto es debido a la concepción de estos sistemas, que tienen como piedra angular la reducción de la distancia entre la ubicación de los vehículos y los sensores de la arquitectura de posicionamiento. La disminución del número de trayectorias de las señales de posicionamiento, junto con la flexibilidad y adaptabilidad de la ubicación de los sensores de posicionamiento, permite la reducción de los efectos adversos en las señales de posicionamiento durante condiciones de funcionamiento hostiles y, por lo tanto, lo que trae consigo un aumento en rendimiento del sistema en términos de exactitud, y especialmente en estabilidad y robustez.

GNSS y LPS realizan el posicionamiento basándose en la recopilación de determinadas medidas de propiedades físicas, como el tiempo, la frecuencia, el ángulo, la potencia o una combinación de las técnicas anteriores.

Los sistemas de posicionamiento basados en mediciones temporales se han convertido en predominantes debido a su compromiso entre la complejidad del hardware, precisión, escalabilidad, efectividad, solidez y flexibilidad para distintos requisitos operativos. Las arquitecturas basadas en ángulos se destacan por su precisión y solidez en la obtención de la ubicación, sin embargo, su implementación depende de condiciones restricciones operativas, lo que conduce a aplicaciones con carácter local. Las técnicas de frecuencia son especialmente adecuadas para obtener velocidades del vehículo, pero la precisión es generalmente escasa y su escalabilidad es también limitada. Por último, el posicionamiento basado en potencia está muy extendido para aplicaciones de precisión con baja exigencia debido a su costo de implementación, efectividad y escalabilidad.

Según la descripción anterior, las arquitecturas de posicionamiento basadas en medidas temporales son las metodologías más prometedoras para lograr rendimientos de alta exigencia. Dentro de ellas, existen tres principales topologías, dependiendo del tipo de medición temporal realizado.

Las técnicas de tiempo de llegada (TOA) calculan el posicionamiento basándose en los tiempos de viaje absolutos de las señales de posicionamiento entre el transmisor y el receptor. En este sentido, la sincronización entre todos los componentes del sistema (es decir, objetivos y sensores de arquitectura) es necesaria para obtener medidas temporales. Geométricamente, los objetivos están situados en circunferencias o esferas (posicionamiento 2D o 3D) de posibles localizaciones alrededor de cada sensor de arquitectura TOA. Para el

posicionamiento 3D, se necesitan al menos cuatro sensores TOA para determinar unívocamente la ubicación del objetivo, debido a las propiedades no lineales del problema de posicionamiento.

Las arquitecturas de diferencia de tiempo de llegada (TDOA) realizan el posicionamiento mediante la medición de las diferencias entre los lapsos de tiempo de las señales del objetivo y un par de sensores de arquitectura. En este caso, la sincronización solo se exige entre los componentes del sistema. De esta manera, para proporcionar el servicio de ubicación, los objetivos no es necesario sincronizarlos. Desde el punto de vista geométrico, los objetos a localizar se pueden ubican en todas las posiciones determinadas por las hipérbolas o hiperboloides (posicionamiento 2D o 3D respectivamente) donde cada uno de los sensores del par TDOA se ubica en los correspondientes focos. A diferencia de los sistemas TOA, se requiere un mínimo de cinco sensores TDOA para resolver de forma unívoca el cálculo de posicionamiento.

Las metodologías TDOA asíncronas se basan en la medición de lapsos de tiempo desde pares de sensores al objetivo correspondiente, como en el caso de arquitecturas TDOA, pero evitando el sincronismo entre sensores del sistema (y también con el/los objetivo/s). Esto se puede lograr mediante la concentración de todas las mediciones de tiempo en un solo sensor coordinador (CS) por zona y asignando al resto las funciones de retransmisión de las señales de posicionamiento. Dependiendo de las rutas de las señales de posicionamiento, se han desarrollado diferentes tecnologías en los últimos años.

El desarrollo de LPS unido a la implementación de arquitecturas de posicionamiento basadas en toma de mediciones temporales fomenta un gran impulso en el rendimiento de estos sistemas necesario para futuras aplicaciones de alta prestaciones en la localización. Sin embargo, surgen serias dificultades a la hora de diseñar su despliegue: en primer lugar, la optimización de las distribuciones de los sensores LPS, y, en segundo lugar, la generación de modelos que permitan efectuar estimaciones realistas del rendimiento de estas arquitecturas en entornos complejos.

A.2.2. Técnicas heurísticas: Algoritmos Genéticos

Además de la tecnología de implementada y el algoritmo de posicionamiento seleccionado, las incertidumbres de ubicación están directamente influenciadas por la distribución de los sensores de arquitectura, lo que comúnmente se conoce como el problema de ubicación de nodos (NLP). El NLP ha sido clasificado como problema matemático NP-

Hard debido a la ausencia de algoritmos exactos para resolverlo en tiempo polinomial

Las metodologías heurísticas pueden proporcionar una solución aproximada al problema de la NLP, basada en una exploración efectiva del espacio de soluciones. Sin embargo, estas metodologías no pueden asegurar matemáticamente la obtención de la solución global del problema.

Además de esto, la optimización de las distribuciones de los sensores de posicionamiento suele estar sujeta a funciones objetivo no derivables, discontinuidades severas durante el proceso de optimización e inmensos espacios de búsqueda relacionados con el grado de resolución espacial deseada, el número de sensores desplegados y la magnitud del área de optimización.

Estos factores juegan un papel determinante durante la selección del procedimiento de optimización heurística para resolver cada tipo de NLP. En las últimas décadas se han presentado muchas metodologías heurísticas basadas en comportamientos estocásticos de la naturaleza: recocido simulado, técnicas evolutivas, algoritmos genéticos, algoritmos de colonias de hormigas, algoritmos de luciérnagas, y algoritmos de enjambre de delfines, son algunos ejemplos de ellos. Además, en los últimos años las estrategias de búsqueda local diversificadas y las búsquedas tabú se han vuelto populares para resolver este tipo de problemas.

En esencia, todos los métodos heurísticos presentan dos etapas distintas durante la exploración del espacio de soluciones. En primer lugar, se realiza una fase de diversificación donde los algoritmos intentan examinar múltiples zonas de los espacios de soluciones, aplicando todos los recursos al descubrimiento de una posible área con máximos/mínimos globales. Posteriormente, una etapa de intensificación permite explorar en profundidad estas áreas más prometedoras para encontrar la solución global. En este punto se localiza la complejidad de los métodos heurísticos, ya que durante la exploración de las soluciones los algoritmos espaciales deben escapar de las optimizaciones locales, sin ninguna fuente externa de información que ayude al proceso.

En base a esto, la selección del procedimiento heurístico depende de la adecuación de las etapas de diversificación y exploración al problema correspondiente. Para la resolución de NLP, los GA presentan gran flexibilidad para modelar problemas complejos, optimizaciones con funciones objetivo no derivables, robustez y posibilidad de paralelización durante el proceso de optimización, y control sobre las etapas de diversificación e

intensificación, aprovechando con ello todos los beneficios de los enfoques heurísticos.

Los GA se fundamentan en los paradigmas de la teoría de la evolución de Darwin, donde la adaptabilidad de los individuos al medio es el factor que determina su supervivencia y la posibilidad de engendrar descendientes con mejores aptitudes que sus antecesores, expuestos a comportamientos estocásticos en forma de mutaciones. En base a esto, los GA se basan en la definición inicial de una población aleatoria de individuos (es decir, posibles soluciones al problema de optimización). Su adaptación al entorno se evalúa a través de la función de adaptación, que caracteriza el problema de optimización. Posteriormente, se aplica un conjunto de operadores genéticos de selección, reproducción y mutación para generar una nueva población de individuos. Las soluciones finales se obtienen mediante la repetición de este proceso (es decir, generaciones), con la mejora progresiva del valor de la función de adecuación de los individuos de las nuevas poblaciones, hasta las condiciones de convergencia (predefinidas para cada optimización) o un prefijo se alcanza el número de generaciones.

Los GA deben implementar una técnica de codificación que transforme las variables del problema de optimización a una forma específica para aplicar los operadores genéricos (especialmente reproducción y mutación). En el manuscrito original del GA, se introdujo la codificación binaria para garantizar la máxima flexibilidad para diseñar operadores genéricos específicos para cada problema y controlar así el proceso de optimización. Sin embargo, este enfoque no se puede aplicar a todos los problemas de optimización y aparecieron nuevas técnicas de codificación.

A.2.3. Modelos de exactitud en sistemas de posicionamiento temporales

La estimación de la exactitud en los sistemas de posicionamiento, y en particular en las arquitecturas basadas en el tiempo, ha recibido una gran atención de investigación durante las últimas décadas. Históricamente, los modelos de precisión estuvieron dominados por el estimador de Dilución Geométrica de Posición (GDOP). Esta métrica asume homocedasticidad en las varianzas asociadas con cada medición temporal, lo que conduce a modelos en los que las distribuciones de probabilidad entre los sensores de arquitectura eran invariantes (es decir, independientes de las condiciones de operación y las distancias entre los objetivos y los sensores). Esta hipótesis solo es asumible para GNSS, donde la distancia

entre los satélites y el objetivo correspondiente y las condiciones operativas globales eran similares en toda la arquitectura.

No obstante, los LPS presentan características heterogéneas entre los distintos sensores para el posicionamiento de un objetivo en particular, lo que lleva a estimaciones muy inexactas cuando se implementaron los modelos GDOP.

La herocedasticidad en los modelos de precisión se puede introducir a través del CRLB. La CRLB se basa en la inversa de la Matriz de información de Fisher y permite obtener estimaciones insesgadas y eficientes para parámetros deterministas. Aplicado al campo de posicionamiento, basado en las distribuciones probabilísticas de incertidumbres en cada entrada de medición temporal de los sistemas de posicionamiento, la CRLB proporciona la máxima exactitud alcanzable independientemente del algoritmo de posicionamiento implementado.

La CRLB se implementa mediante la caracterización de sistemas de posicionamiento basados en el tiempo en términos de la ruta de sus señales de posicionamiento para realizar las correspondientes mediciones de tiempo y el modelado de las incertidumbres inducidas por el entorno en estas mediciones temporales.

Sección A.3

Análisis de exactitud en redes de sensores para métodos de posicionamiento asíncronos

A.3.1. Resumen

Los requisitos de exactitud para el posicionamiento de redes de sensores han crecido en los últimos años debido a la alta precisión exigida en actividades relacionadas con vehículos y robots. Estos sistemas involucran una amplia gama de especificaciones que deben cumplirse mediante dispositivos de posicionamiento basados en la medición del tiempo. Estos sistemas se han diseñado tradicionalmente con la sincronización de sus sensores para calcular la estimación de la posición. Sin embargo, esta sincronización introduce un error en la determinación del tiempo que se puede evitar mediante la centralización de las medidas en un solo reloj en un sensor de coordenadas. Esto se puede encontrar en arquitecturas típicas como los sistemas de diferencia de tiempo asincrónico de llegada (A-TDOA) y diferencia de tiempo de llegada (D-TDOA). En este artículo, se realizó por primera vez un estudio de la idoneidad de estos nuevos sistemas basado en una evaluación de la CRLB en diferentes entornos reales 3D para múltiples ubicaciones de sensores. El análisis se llevó a cabo mediante un nuevo modelo de varianza de ruido heterocedástico con un modelo de propagación de trayectoria logarítmica normal dependiente de la distancia. Los resultados mostraron que A-TDOA proporcionó menos incertidumbre en la raíz del error cuadrático medio (RMSE) en el posicionamiento, mientras que D-TDOA redujo la desviación estándar y aumentó la estabilidad en todo el dominio.

A.3.2. Modelos heterocedásticos de ruido y derivación de CRLB para arquitecturas A-TDOA

En este apartado se implementa un modelo de varianza de ruido dependiente de la distancia asociado al proceso de ubicación del sistema TDOA asíncrono.

El proceso comienza con la estimación del rango de variación de TOA debido a los entornos ruidosos. A continuación, la estimación del rango de varianza de TDOA se define en función de los supuestos de correlación de la medición del tiempo. El modelo de varianza de ruido heterocedástico se completa con la implementación del modelo de propagación de ruta-LOS que mejor se ajusta a las características de la red de sensores múltiples.

Entre las principales fuentes de errores de alcance de los sistemas de posicionamiento basados en mediciones de tiempo, la más importante para las técnicas asíncronas TDOA es la incertidumbre inducida por el ruido blanco gaussiano (WGN) en el canal de propagación. Este problema ha sido profundamente estudiado para arquitecturas TOA, cuantificándolo con el CRLB. Asumiendo señales de posicionamiento convencionales (producto tiempo-frecuencia unitario) y altos niveles de SNR en el receptor con una estimación eficiente.

Con base en la estimación de la varianza de TOA, la implementación para los sistemas TDOA se realiza bajo algunos supuestos. He y Dong propusieron que las medidas de tiempo en arquitecturas TDOA asincrónicas se consideren independientes. En consecuencia, los elementos fuera de la diagonal de la matriz de covarianza asociados con el modelado de ruido gaussiano son nulos. Según Kaune et al. , la varianza asociada con una distancia de diferencia entre dos nodos es la suma de las varianzas para cada nodo, bajo el supuesto de mediciones de tiempo no correlacionadas.

Adicionalmente, es necesario tener en cuenta que el SNR asociada con cada receptor depende principalmente de la emisión de potencia, la frecuencia de transmisión y el entorno. Este último aspecto se caracteriza por modelos de propagación para ambientes interiores y exteriores. Los modelos a gran escala predicen la intensidad media de la señal en entornos LOS basados en la distancia entre el emisor/receptor y las características de la señal. Los modelos de pequeña escala o desvanecimiento caracterizan las rápidas fluctuaciones de la señal cuando la distancia del emisor/receptor es corta, en ambas condiciones (LOS y NLOS).

Los modelos de pérdida de trayectoria a gran escala se han estudiado profundamente en las últimas décadas para modelar las comunicaciones móviles. La gran mayoría de estos métodos se construyeron bajo algunas de estas restricciones: alturas de emisor y receptor, frecuencia de transmisión y distancia emisor-receptor, entre otras. Bajo estas limitaciones, el modelado de la arquitectura TDOA asíncrona no es posible debido a las características del

emisor / receptor en múltiples redes de sensores.

Con base en los supuestos anteriores, el modelo de propagación de pérdida de trayectoria seleccionado para la simulación es el Log-normal, que elimina las restricciones sobre la geometría emisor-receptor.

La implementación final del modelo de ruido en la definición de varianza de CRLB se presenta a continuación:

$$\sigma_{ij}{}^2 = \frac{c^2}{B^2\left({}^{P_T}/_{P_n}\right)} PL(d_0)\left[\left(\frac{d_i}{d_0}\right)^n + \left(\frac{d_j}{d_0}\right)^n\right] \quad \begin{matrix} i = 1, \dots, M \\ j = 1, \dots, M \end{matrix}$$

donde d_0 es la distancia de referencia al emisor, la base a partir de la cual es válida la hipótesis del modelo log-normal, $PL(d_0)$ es la pérdida de trayectoria para esta distancia y n es el exponente de pérdida de trayectoria.

A partir de este modelado, es posible calcular las incertidumbres introducidas en cada una de las mediciones temporales de un sistema asíncronos TDOA por el ruido. Introduciendo esto en la CRLB, es posible caracterizar el grado de exactitud de este tipo de sistemas al aplicar el posicionamiento en base a M mediciones temporales. La derivación de la CRLB para arquitecturas TDOA asíncronas se detalla a continuación:

Para un sistema TDOA, las mediciones de tiempo asociadas con los receptores se modelan mediante la adición de WGN. En un entorno real, la varianza asociada a este fenómeno depende de la distancia entre emisor y receptor, induciendo herocedasticidad en la gestión de datos. En este contexto, Kaune et al. incluyen un modelo de la varianza del parámetro dependiente en el cálculo de la inversa de la matriz de información de Fisher (**J**).

$$J = \frac{1}{\sigma^2(X)}\left(\frac{\partial h(X)}{\partial X}\right)^T\left(\frac{\partial h(X)}{\partial X}\right) + \frac{1}{2}\frac{1}{\sigma^2(X)}\left(\frac{\partial \sigma(X)}{\partial X}\right)^T\left(\frac{\partial \sigma(X)}{\partial X}\right)$$

Donde la matriz de columnas **h(X)** expresa las diferencias en las distancias euclidianas entre las mediciones de TDOA de cada par de receptores, y **R(x)** es la matriz de covarianza del sistema. En ella se introducen las varianzas calculadas anteriormente para sistemas asíncronos TDOA.

La incertidumbre final se evalúa en términos de RMSE, como se muestra en la siguiente ecuación (ubicación tridimensional), donde los subíndices se refieren a los elementos

diagonales de la matriz J:

$$RMSE = \sqrt{J_{11} + J_{22} + J_{33}}$$

A.3.3. Resultados y conclusiones

En esta sección, los sistemas TDOA asíncronos se evalúan para el posicionamiento de la red de sensores. En primer lugar, se definen un conjunto de parámetros de comunicación global.

Tabla A.1. Parámetros de arquitecturas para estudio CRLB. Fueron seleccionados debido a su utilización en aplicaciones de seguimiento similares en la industria aeroespacial

Parámetro	**Magnitud**
Frecuencia de emisión	1090 MHz
Ancho de banda	100 MHz
Potencia de transmisión	400 W
Nivel medio de ruido	-94 dBm

Además de estos parámetros, la comparación entre arquitecturas se realizó en base a antenas de ganancia unitaria en todos los transceptores del sistema y en el supuesto de capacidad de comunicación full-dúplex entre elementos. Además, se consideró un supuesto de la técnica de recepción y retransmisión en las operaciones de los transceptores y un producto de frecuencia-tiempo unitario en todas las comunicaciones de las arquitecturas.

A continuación, se presenta un ejemplo de evaluación del modelo de CRLB para una arquitectura de tipo A-TDOA.

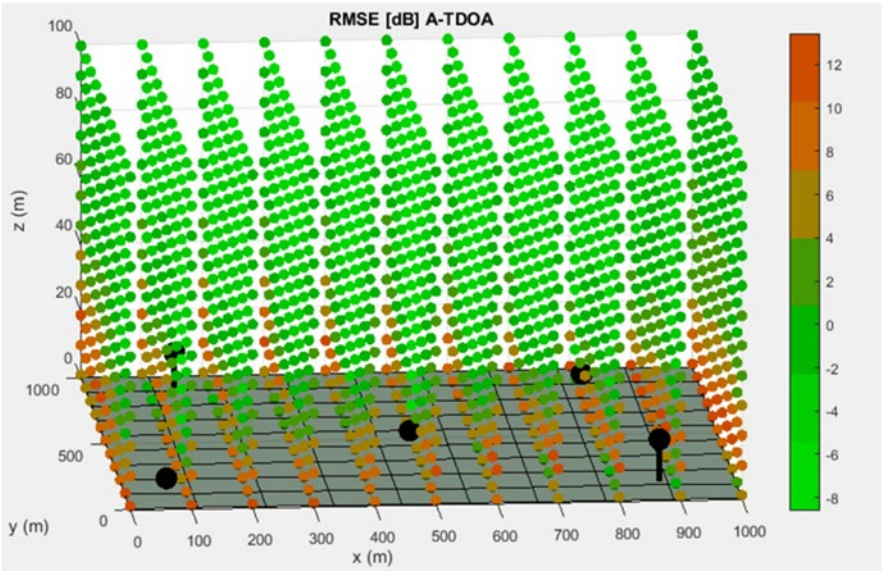

Figura A.1. Mejor distribución de los nodos de Sensor de trabajador (WS) y Sensor de coordinador (CS) para el sistema A-TDOA. La superficie base se presenta como el hiperplano gris ubicado en la parte inferior de la imagen. Los nodos están representados por esferas negras con su correspondiente titular que los une a la superficie base. La evaluación CRLB de los puntos de discretización se muestra de acuerdo con la leyenda del lado derecho.

Como conclusiones, este análisis se realizó sobre la base de una comparación CRLB donde las incertidumbres de las mediciones de tiempo originadas por el ruido dependían de la distancia. Esto resultó en herocedasticidad en la varianza asociada con la estimación del rango del sensor. Este modelo real nos permitió determinar la mejor arquitectura asíncrona TDOA con independencia del algoritmo de posicionamiento.

Sección A.4

Aproximación mediante Algoritmos Genéticos al problema de localización 3D para sistemas TDOA

A.4.1. Resumen

Las arquitecturas asincrónicas de posicionamiento basadas en mediciones de tiempo están adquiriendo una importancia creciente en los sistemas de posicionamiento local (LPS). Estas arquitecturas tienen especial relevancia en aplicaciones de precisión y navegación interior/exterior de vehículos autónomos como vehículos terrestres autónomos (AGV) y vehículos aéreos no tripulados (UAV). El error de posicionamiento de estos sistemas está condicionado por los algoritmos utilizados en el cálculo de la posición, la calidad de las medidas de tiempo y el despliegue de sensores de los receptores de señales. Una vez definidos los algoritmos y seleccionado el método para calcular las medidas de tiempo, el único criterio de diseño del LPS es la distribución de los sensores en el espacio tridimensional. Este problema ha demostrado ser NP-Hard y, por lo tanto, se recomienda una solución heurística al problema. En este trabajo se propone un algoritmo genético con la flexibilidad para adaptarse a diferentes escenarios y modelos de terreno. Este algoritmo se utiliza para determinar la mejor localización de nodos con el fin de reducir el límite inferior de CRLB con una consideración de ruido heterocedástico en cada sensor de una arquitectura de A-TDOA. La metodología propuesta permite la optimización del despliegue de sensores 3D de una arquitectura A-TDOA pasiva, incluyendo flexibilidad de modelado del suelo y consideración de ruido heterocedástico con iteraciones secuenciales, y reduciendo la discretización espacial para lograr mejores resultados. Los resultados muestran que la optimización con un 15% de elitismo y una estrategia de selección del Torneo 3 ofrece la mejor maximización para el algoritmo.

A.4.2. Algoritmo Genético con escalamiento y Función de adaptación

El GA propuesto permite la optimización 3D de la ubicación de sensores de posicionamiento en función de cualquier caracterización de la superficie base, independientemente de las fluctuaciones en la elevación del entorno de modelado. Además, esta GA admite la generación de cualquier región de optimización a nivel de superficie base (modelado AGV) o por encima de ella (modelado UAV).

La caracterización del escenario está completamente definida con dos regiones: el NLE y elTLE. NLE es el espacio donde los nodos pueden moverse libremente durante la ejecución del GA. La proyección del NLE en la superficie de la base puede tener un área igual o menor a ésta, pudiendo existir zonas de obstáculos donde no se puedan ubicar los nodos. En cuanto a la elevación del NLE, se define en base a las elevaciones máxima y mínima con respecto a la superficie de modelado.

Para resolver el problema, es necesario tener en cuenta que el espacio total de soluciones del problema de optimización depende del grado de resolución espacial requerido en la ubicación de los nodos, que a su vez estará determinado por la discretización espacial desarrollada en las regiones NLE.

La magnitud de este espacio de búsqueda impide el uso de técnicas de resolución exacta que examinen todo el espectro de soluciones para lograr la optimización del problema en cuestión. Adicionalmente, se desaconsejan las técnicas de resolución codiciosas y las basadas en una división recursiva del problema debido a la gran dependencia conjunta entre la ubicación de los diferentes nodos y la solución final.

Estos aspectos llevan a que la optimización de este problema se lleve a cabo mediante técnicas heurísticas. Entre ellos, los algoritmos genéticos presentan múltiples ventajas, entre las que se encuentran gran flexibilidad y robustez, uso de funciones de aptitud no derivables, tratamiento paralelo de soluciones y apuesta entre la diversificación y la intensificación en la búsqueda dentro del espacio de soluciones. Estas características establecen los algoritmos genéticos como la clave final para resolver el problema de localización de los nodos. Los algoritmos genéticos se basan en la hipótesis de la teoría de la evolución, donde los individuos mejor adaptados al medio sobreviven y generan descendientes, que con el paso de las generaciones adquirirán mejores características de adaptación al medio que sus predecesores [35]. De esta forma, esta metodología parte de un conjunto inicial de soluciones aleatorias cuyas aptitudes serán evaluadas mediante una función de aptitud (función de optimización

de problemas). Posteriormente, se aplicarán operadores de selección genética, cruce y mutación para generar nuevas posibles soluciones al problema a partir de las mejores de la generación anterior. Este proceso se repetirá hasta que el algoritmo converja o hasta un número predeterminado de generaciones, dando como resultado la solución final para optimizar el problema.

La parte más importante de los algoritmos genéticos es la codificación. En este sentido, la codificación permite transformar las variables del problema a un sistema en el que se pueden aplicar los operadores genéticos. La forma en que se lleve a cabo determinará en gran medida la capacidad de búsqueda en el espacio de solución y la convergencia del algoritmo.

La codificación seleccionada es de tipo binario, lo que facilita la implementación de operadores genéticos y diversifica la búsqueda de soluciones. Sin embargo, la evaluación de los individuos de la población debe realizarse en base a las coordenadas cartesianas x, y, z de cada uno de los nodos, expresándose estas en números reales.

En primer lugar, se realiza la conversión directa entre dígitos binarios y números naturales, basándose en longitudes de cadena binaria previamente definidas. Estos pueden ser invariantes para todas las coordenadas o determinarse en función de las diferencias de magnitud máxima posibles en el escenario y para cada una de las coordenadas. Esta última opción es la finalmente implementada porque permite una mayor homogeneidad en la resolución espacial de las soluciones en las tres coordenadas, y total adaptabilidad a los límites de la región NLE en todos los puntos del entorno.

En segundo lugar, cada una de las coordenadas de los nodos se transforma en números naturales a los valores en números reales en función de la geometría del entorno. Esta conversión, que se denomina escalada, se realiza mediante la siguiente relación.

$$Coor_R = \frac{Coor_N}{2^L - 1}(N_{max} - N_{min}) + N_{max}$$

donde $Coor_R$ es la coordenada cartesiana del nodo escalado en números reales, $Coor_N$ es la coordenada cartesiana del nodo expresada en números naturales, L es la longitud de la cadena binaria asociada con la coordenada en cuestión, N_{max} es el valor máximo de la coordenada en el escenario, y N_{min} es la magnitud mínima de la coordenada en el escenario.

Esta conversión real-binaria debe realizarse mediante un cálculo secuencial de las coordenadas cartesianas de cada uno de los nodos presentes en cada individuo de la población. De esta forma, en primer lugar, se escalan las coordenadas *x* de cada nodo en

función del conocimiento de las dimensiones máximas del escenario (invariantes para la coordenada *x*). A continuación, las coordenadas se escalan *y* se basan en las limitaciones espaciales para la dirección y el escenario en función de la coordenada *x* previamente escalada. Finalmente, las coordenadas *z* se escalan de acuerdo con las dimensiones máximas del entorno para la dirección *z* que depende de las coordenadas *x* e *y* previamente escaladas.

El uso de esta metodología en cualquier entorno está vinculado a la implementación de algún tipo de interpolación 1D para el escalado de las coordenadas, así como al uso de la interpolación 2D para el escalado de las coordenadas *z*.

La transformación real-binaria se rige por los mismos principios, con la condición de que la coordenada real inicial debe ser un múltiplo del paso asignado a esa escala, donde el paso se expresa mediante la siguiente ecuación:

$$Step = \frac{N_{max} - N_{min}}{2^L - 1}$$

La aplicación de la técnica de escalado, junto con una definición y análisis de los operadores genéticos y criterios de convergencia, permite adaptar la optimización a las condiciones de cada problema.

A.4.3. Resultados y conclusiones

En esta subsección se presentan algunos de los posibles resultados que se pueden alcanzar con la técnica descrita previamente. En concreto, se presenta una optimización en un entorno 3D irregular para una arquitectura A-TDOA, en base a una minimización de las incertidumbres de posicionamiento estimadas mediante los modelos de incertidumbres de ruido y derivaciones de CRLB expresadas en el Capítulo 2.

En las siguientes figuras, se muestran el nivel de error (RMSE) expresado en dBm sendas optimizaciones en escenarios irregulares con diferentes topologías.

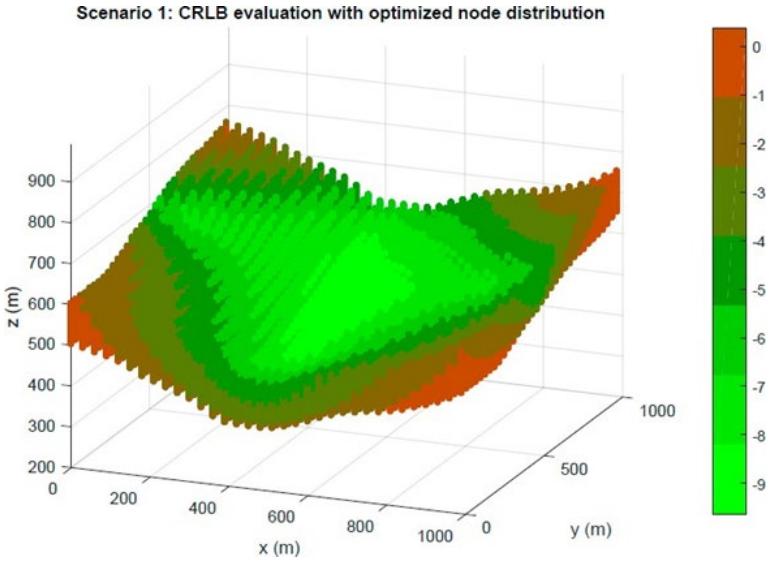

Figura A.2. Optimización en el escenario 1. Estimación de CRLB en dBm para la región TLE según la optimización de distribución de sensores A-TDOA realizada por el GA.

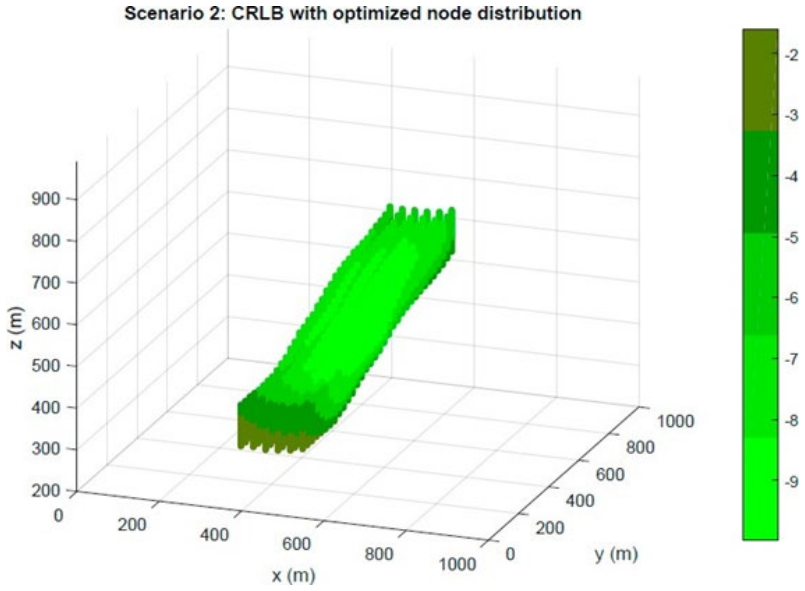

Figura A.2. Optimización en el escenario 2. Estimación de CRLB en dBm para la región TLE según la optimización de distribución de sensores A-TDOA realizada por el GA.

Finalmente se presentan resultados de exactitud para distribuciones de sensores optimizadas y aleatorias, en este caso para el escenario 1.

Tabla A.2. Resultados finales. Estadísticas de CRLB en el escenario 1 para distribuciones de nodos aleatorias y optimizadas de 5 sensores A-TDOA.

Escenario 1	**Distribution aleatoria**	**Distribution optimizada**
Media(m)	1.759	0.432
Max (m)	19.940	1.089
Min (m)	0.131	0.109
% < 0.5 m	11.44 %	65.43 %

Estos resultados muestran la posibilidad de utilizar la metodología descrita como algoritmo de colocación de sensores para aplicaciones con necesidades de altas prestaciones en el posicionamiento de objetos. Asimismo, se proporciona una técnica con un alto grado de modularidad, que se puede aplicar a cualquier arquitectura de posicionamiento basada en medidas temporales. Finalmente, la caracterización heterocedástica de la incertidumbre asociada a cada una de las medidas temporales del sistema permite un alto grado de correspondencia con la realidad, especialmente importante en los sistemas LPS.

Sección A.5

Modelo combinado de CRLB para error de ruido y relojes para la optimización de la ubicación de nodos en sistemas de posicionamiento temporales

A.5.1. Resumen

La aparición de vehículos autónomos con grandes necesidades de exactitud en la ubicación ha endurecido los requisitos de los sistemas de posicionamiento utilizados para la navegación. Los Sistemas de Posicionamiento Local (LPS) han mostrado una excelente adaptación a estas condiciones, gracias a la estabilidad y reducción de los niveles de incertidumbre de posicionamiento. La precisión alcanzada por metodologías basadas en mediciones temporales depende principalmente de las incertidumbres en las mediciones de estos sistemas. En este aspecto adquieren gran relevancia la presencia de ruido y la existencia de inestabilidades temporales en los relojes de medida, en función de la distribución de los sensores en el entorno. En este artículo, presentamos por primera un modelo de CRLB para la cuantificación de la incertidumbre global en los sistemas de posicionamiento causada tanto por el ruido como por inestabilidades temporales en los dispositivos de medición. Además, esta técnica se aplica a la optimización de distribuciones de sensores para las arquitecturas TOA, TDOA y TDOA asíncrona (A-TDOA) utilizando un algoritmo genético en un entorno 3D no uniforme. Los resultados muestran que la metodología A-TDOA supera significativamente las arquitecturas síncronas en términos de exactitud y estabilidad global cuando se consideran el ruido y los errores de reloj en las mediciones de tiempo de las aplicaciones LPS.

A.5.2. CRLB para incertidumbres combinadas de ruido y errores de relojes en los instrumentos de medida

La implementación de CRLB en el posicionamiento permite la determinación de la máxima exactitud de ubicación cuando se alteran las mediciones temporales debido a las condiciones del entorno. La idoneidad del CRLB, especialmente para LPS, se basa en la herocedasticidad de los modelos de varianza, la heterogeneidad en las circunstancias de ubicación del sensor y la flexibilidad en la caracterización de varias condiciones operativas.

De manera convencional, esta técnica se ha utilizado para caracterizar la reducción de la exactitud en la ubicación debido a errores de medición de tiempo inducidos por el ruido. La presencia de ruido en el canal de comunicación se ha modelado tradicionalmente mediante una distribución de ruido blanco gaussiano (WGN). Con base en esta suposición, Kaune et al. [29] desarrollan una forma matricial genérica del CRLB donde las incertidumbres de la medición del tiempo dependen de la distancia objetivo-sensor.

$$J_{mn} = \left(\frac{\partial h(X)}{\partial x_m}\right)^T R^{-1}(X)\left(\frac{\partial h(X)}{\partial x_n}\right) + \frac{1}{2} tr\left(R^{-1}(X)\left(\frac{\partial R(X)}{\partial x_m}\right)R^{-1}(X)\left(\frac{\partial R(X)}{\partial x_n}\right)\right)$$

En esta relación, **J** es la inversa de la matriz de información de Fisher donde *m* y *n* subíndices representan los parámetros a estimar –Coordenadas cartesianas TS–. El vector **h(TS)** indica las relaciones de distancia entre sensores y objetivos de acuerdo con el recorrido de la señal de posicionamiento en cada arquitectura. A continuación, se muestra su caracterización para las arquitecturas TOA, TDOA y A-TDOA.

$$h_{TOA_i} = \|TS - CS_i\|, \quad i = 1, \dots, N_{CS}$$

$$h_{TDOA_i} = \|TS - CS_i\| - \|TS - CS_j\|$$
$$i = 1, \dots, N_{CS} \qquad j = 1, \dots, N_{CS}$$

$$h_{A-TDOA_i} = \|TS - WS_i\| + \|TS - CS\| - \|WS_i - CS\|$$
$$i = 1, \dots, N_{WS}$$

La construcción de la matriz **R(TS)** está sujeta a diferencias significativas según las arquitecturas de posicionamiento. En el caso de TOA y A-TDOA, las mediciones de tiempo son independientes entre sí. Por el contrario, Z. Sahinoglu et al. demostró en que las

mediciones de diferencias de tiempo de TDOA están correlacionadas, lo que provoca la presencia de términos fuera de la diagonal distintos de cero en la matriz de covarianza.

Los componentes de ruido de las variaciones en la matriz **R(TS)** se construyen sobre la base de un modelo heterocedástico que se rige por un modelo de propagación de pérdida de trayectoria log-normal. Esta caracterización se ha realizado bajo el supuesto de ruido de medición no correlacionado en diferentes sensores.

Los términos de error de reloj en la matriz **R(TS)** se han definido en base a la simulación Monte-Carlo de iteraciones *l* para estimar correctamente cada variación temporal asociada con cada arquitectura de posicionamiento. Además, se introduce la resolución de tiempo para maximizar la representación de la incertidumbre del reloj. Las expresiones combinadas de varianzas para errores de reloj y ruido se presentan en las siguientes ecuaciones:

$$\sigma_{TOA_i}{}^2 = \frac{c^2}{B^2\left(P_T/P_n\right)} PL(d_0)\left[\left(\frac{d_i}{d_0}\right)^n\right] + \frac{1}{l}\sum_{k=1}^{l}\left\{CE_{TOA_i}c\right\}^2$$

$$T_{TOA_i} = T_i + U_i - U_0 + T_0(\eta_i - \eta_0) + T_i\eta_i$$

$$CE_{TOA_i} = \left|T_i - floor_{TR}\left(T_{TOA_i}\right)\right|$$

$$d_i = \|TS - CS_i\| \qquad i = 1, \dots, N_{CS}$$

$$\sigma_{TDOA_{ij}}{}^2 = \frac{c^2}{B^2\left(P_T/P_n\right)} PL(d_0)\left[\left(\frac{d_i}{d_0}\right)^n + \left(\frac{d_j}{d_0}\right)^n\right] + \frac{1}{l}\sum_{k=1}^{l}\left\{CE_{TDOA_{ij}}c^2\right\}$$

$$T_{TDOA_i} = [T_i + U_i - U_0 + T_0(\eta_i - \eta_0) + T_i\eta_i]$$

$$T_{TDOA_j} = \left[T_j + U_j - U_0 + T_0\left(\eta_j - \eta_0\right) + T_j\eta_j\right]$$

$$CE_{TDOA_{ij}} = \left|T_i - floor_{TR}\left(T_{TDOA_i}\right)\right| + \left|T_j - floor_{TR}\left(T_{TDOA_j}\right)\right|$$

$$d_i = \|TS - CS_i\|$$

$$d_j = \left\|TS - CS_j\right\|$$

$$i = 1, \dots, N_{CS} \qquad j = 1, \dots, N_{CS} \quad where\ i \neq j$$

$$\sigma_{A-TDOA_i}{}^2 = \frac{c^2}{B^2\left(P_T/P_n\right)} PL(d_0)\left[\left(\frac{d_i}{d_0}\right)^n + \left(\frac{d_{TS}}{d_0}\right)^n + \left(\frac{d_{CS}}{d_0}\right)^n\right] + \frac{1}{l}\sum_{k=1}^{l}\left\{CE_{A-TDOA_i}c\right\}^2$$

$$T_{A-TDOA_i} = \left(T_i + T_{TS} - T_{CS_i}\right)(1 + \eta_{CS})$$

$$CE_{A-TDOA_i} = \left|\left(T_i + T_{TS} - T_{CS_i}\right) - floor_{TR}\left(T_{A-TDOA_i}\right)\right|$$

$$d_i = \|TS - WS_i\|$$
$$d_{TS} = \|TS - CS\|$$
$$d_{CS_i} = \|WS_i - CS\| \quad i = 1, \dots, N_{WS}$$

donde c es la velocidad de propagación de la señal en m/s, B es el ancho de banda de la señal en Hz, P_T es la potencia de transmisión en W, Pn es el nivel de ruido medio en W que se calcula en base a la relación de Johnson-Nyquist, n es la ruta exponente de pérdida, d_0 es la distancia de referencia para el modelo logarítmico normal, $PL(d_0)$ es la pérdida de trayectoria relacionada con la distancia de referencia, U es el desfase de tiempo inicial, η es el desfase del reloj correspondiente a cada sensor, T son los tiempos ideales de trayecto de la señal y T_0 es el tiempo desde la última sincronización.

Por último, la precisión global en el posicionamiento se evalúa mediante el MSE de los elementos diagonales de la matriz $\mathbf{J}^{-1}$. Esto permite una penalización incremental cuando la precisión reduce su magnitud, lo que ayuda en el proceso de optimización.

A.5.3. Resultados y conclusiones

A continuación, se presentan los resultados de precisión tras la optimización de sensores ubicados en un entorno irregular 3D para arquitecturas TOA, TDOA y A-TDOA.

En primer lugar, se ha diseñado un escenario irregular 3D para las simulaciones. Las designaciones de áreas han seguido las consideraciones del Capítulo 4. Este entorno de simulación ha sido seleccionado con el fin de ejemplificar una posible situación de optimización en condiciones reales. De esta manera, NLE es el entorno de ubicación de nodo que indica el movimiento libre de extensión de los sensores durante la optimización, y TLE es el entorno de ubicación de destino que representa todas las ubicaciones posibles de los objetivos de posicionamiento.

Una vez seleccionado el escenario de optimización, el siguiente paso es la determinación de parámetros de configuración global que permitan la comparación entre arquitecturas de posicionamiento basadas en el tiempo.

Por último, los parámetros de configuración de GA seleccionados son Torneo 3 como procedimiento de selección, 7% de elitismo, cruce de un solo punto y probabilidad de mutación del 3%. Esta elección proporciona la mejor relación entre la maximización de la función de aptitud y la velocidad de convergencia. Cabe destacar que la optimización TDOA y A-TDOA se ha realizado con cinco sensores con el fin de desplegar el número mínimo de

ellos para lograr un posicionamiento 3D unívoco. En el caso de la arquitectura TOA, el proceso de optimización se ha realizado con cuatro y cinco sensores para facilitar la comparación y la adquisición de conclusiones.

A modo de ejemplo se presenta la optimización efectuada, con los niveles de exactitud alcanzados para las arquitecturas TOA y A-TDOA.

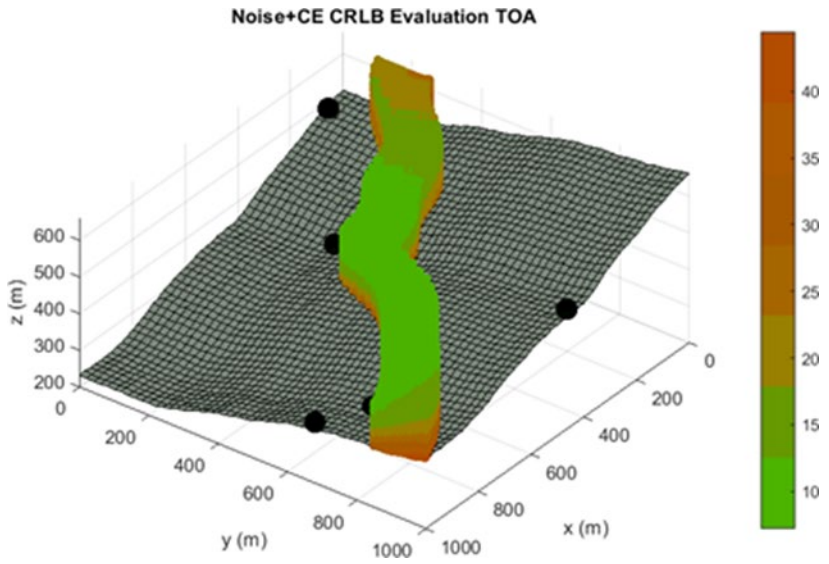

Figura A.3. Análisis RMSE en términos de ruido y errores de reloj para la arquitectura TOA con una distribución de nodo optimizada de 5 sensores.

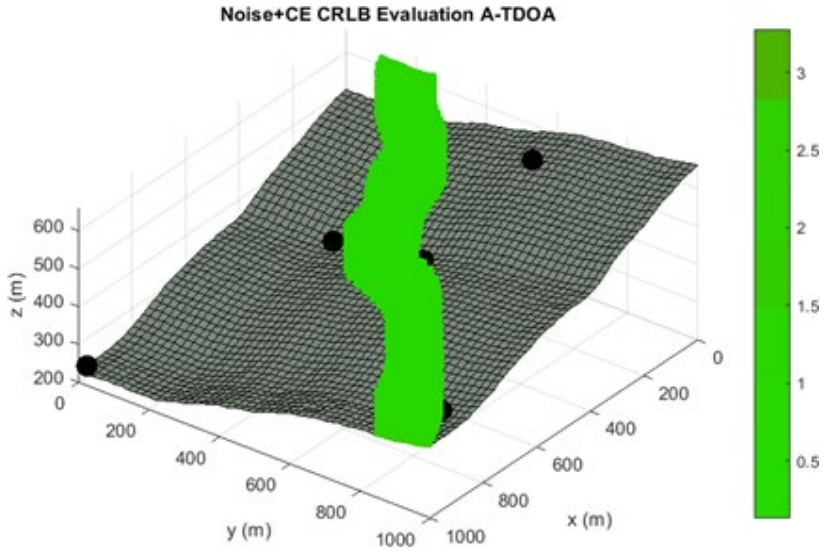

Figura A.4.Análisis RMSE en términos de ruido y errores de reloj para la arquitectura A-TDOA con una distribución de nodo optimizada de 5 sensores.

Finalmente, la comparativa de rendimiento para todas las arquitecturas temporales con el modelo de CRLB y distribuciones de sensores optimizadas mediante el GA se presenta continuación.

Tabla A.3. Análisis de precisión para las metodologías TOA, TDOA y A-TDOA después de la optimización de la ubicación de sensores cuando se consideran las incertidumbres de error de reloj y ruido. Los valores entre paréntesis indican el número de sensores en la distribución.

CRLB: Ruido y errors de reloj	**TOA (4)**	**TOA (5)**	**TDOA (5)**	**A-TDOA (5)**
Media (m)	19.993	17.962	8.152	0.704
Max (m)	77.377	44.480	24.129	3.277
Min (m)	8.761	7.177	3.124	0.130
% < 0.5 m	0	0	0	44.80
% Rejoj/Total errores	97.86	98.22	95.72	34.74

Los resultados muestran que los sistemas A-TDOA proporciona un rendimiento significativamente mejor en términos de exactitud y estabilidad que las arquitecturas TOA y TDOA. La exactitud de las arquitecturas A-TDOA es más estable debido a la eliminación de incertidumbres relacionadas con el proceso de sincronismo y la minimización combinada de la ruta de la señal de posicionamiento y las medidas de tiempo realizadas por los relojes del sensor.

Sección A.6

Optimización multiobjetivo para sistemas de posicionamiento asíncronos basada en una caracterización completa de los errores posición en entornos complejos 3D

A.6.1. Resumen

El posicionamiento de altas prestaciones es fundamental para las aplicaciones modernas de navegación autónoma de agentes. La precisión y la estabilidad de las ubicaciones previstas son factores clave para evaluar la idoneidad de las arquitecturas de posicionamiento que deben implementarse en casos del mundo real. Las metodologías A-TDOA en LPS son soluciones efectivas que satisfacen los requisitos dados y reducen las incertidumbres temporales inducidas durante el proceso de sincronización. En este artículo, proponemos una técnica para la caracterización combinada de los errores de rango - ruido y propagación sin línea de visión (NLOS) a través de la CRB. Los efectos de la propagación NLOS en la calidad de la señal se predicen con un nuevo algoritmo LOS / NLOS de trazado de rayos que proporciona distancias de viaje LOS y NLOS para enlaces de comunicación en entornos irregulares 3D. Además, proponemos un algoritmo para detectar los efectos multipath de la interferencia destructiva y la discapacidad de los caminos LOS. Las técnicas propuestas se aplican a la optimización de la colocación de sensores en escenarios reales 3D. Se utiliza un proceso de optimización multiobjetivo (MOP) basado en un algoritmo genético (GA) que proporciona los frentes de Pareto (PF) para la minimización conjunta de las incertidumbres de ubicación (CRB) y los efectos multipath para un número variable de sensores de

arquitectura A-TDOA. Los resultados muestran que el procedimiento diseñado puede determinar, antes de la implementación real, las capacidades máximas del sistema de posicionamiento en términos de precisión. Esto nos permite evaluar una compensación entre la precisión y el costo de la arquitectura o respaldar el diseño del sistema de posicionamiento bajo demandas de precisión.

A.6.2. Algoritmos de detección de distancias LOS/NLOS y detección de multipath

La presencia de objetos en la proximidad de enlaces emisor-receptor conduce a una reducción excesiva de la potencia de la señal que llega al receptor, originada por condiciones NLOS, y/o la generación de diferentes trayectos que afecten negativamente al proceso de detección y puedan generar interferencias destructivas, es decir, multipath. Estos efectos deterioran significativamente la precisión del posicionamiento y, en consecuencia, deben ser detectados y cuantificados.

En este trabajo se proponen dos algoritmos para caracterizar las propiedades de los canales de comunicación en entornos complejos 3D, donde están presentes condiciones NLOS y multipath. En primer lugar, se implementa un algoritmo de rastreo estima las distancias LOS y NLOS asociadas con un enlace de comunicación genérico entre un emisor y un receptor. Se desarrolla esta técnica bajo los requisitos de aplicaciones 3D en entornos irregulares complejos.

El algoritmo se basa en la discretización espacial del enlace emisor-receptor para cada comunicación de la arquitectura de posicionamiento, es decir, dividimos la línea entre emisor y receptor en varios puntos de evaluación. Para cada uno de estos puntos, el algoritmo compara la altura de la línea que une el emisor y el receptor con la elevación de la superficie y o obstáculos del entorno. Si la resta de las alturas del enlace y la elevación de la superficie/obstáculos es positiva, cualquier objeto interfiere con el enlace emisor-receptor en ese punto. De lo contrario, algún objeto obstruye la señal de posicionamiento. La aplicación de esta evaluación para cada punto de la discretización en cada enlace de posicionamiento permite no solo la detección de obstrucciones, sino también la cuantificación de las distancias LOS y NLOS asociadas a cada enlace.

El segundo algoritmo propuesto es una nueva técnica que permite la identificación y evaluación de todas las regiones que potencialmente podrían producir efectos multipath

adversos en los receptores. La presencia de multipath conlleva dos problemas en los receptores: la aparición de interferencias destructivas que cancelan la señal de comunicaciones y la introducción de múltiples señales que se superponen impidiendo la detección del trayecto LOS.

Las interferencias destructivas son modeladas por la zona de Fresnel, que se define en el espacio 3D como el elipsoide donde cualquier objeto ubicado total o parcialmente en su interior genera una señal reflejada que anula la transmisión original. El elipsoide se construye en función de la ubicación del emisor y del receptor, el foco del elipsoide, y el radio en cualquier punto del enlace de comunicaciones.

En entornos multipath, las señales múltiples reflejadas pueden llegar a la antena receptora con ciertos retrasos. Este fenómeno se caracteriza por la dispersión del retardo (τ_{ds}), que define el retardo mutuo máximo entre señales de diferentes caminos. La dispersión del retardo está estrechamente relacionada con la dispersión de la correlación de la señal ($\tau_c \approx 1/B$) que caracteriza la insignificancia de la semejanza en el dominio del tiempo entre dos copias desplazadas en el tiempo de la misma señal. Por tanto, si las señales consecutivas de trayectos múltiples llegan al receptor en un período de tiempo menor que la dispersión del retardo, que es igual a la dispersión de correlación en el caso más crítico, se superpondrán y las señales no podrán distinguirse. Esta característica es crítica durante la discriminación de la primera señal, ruta LOS, en sistemas de posicionamiento en los que está involucrada la ruta múltiple. Cada trayectoria reflejada con una distancia de viaje menor que la distancia de trayectoria LOS más la distancia de dispersión de correlación (τ_cc) provoca un desvanecimiento por trayectos múltiples y la imposibilidad de emplear este enlace de comunicación para el posicionamiento.

En base a estos dos factores, se propone un algoritmo para detectar la presencia de obstáculos que puedan generar interferencias destructivas y/o trayectos reflejados mínimos no discriminados. Esta técnica se basa en la evaluación de los elipsoides de trayectoria Fresnel y mínima NLOS. La Figura A.5 muestra un ejemplo de aplicación del algoritmo de detección (para más información consulte el documento original).

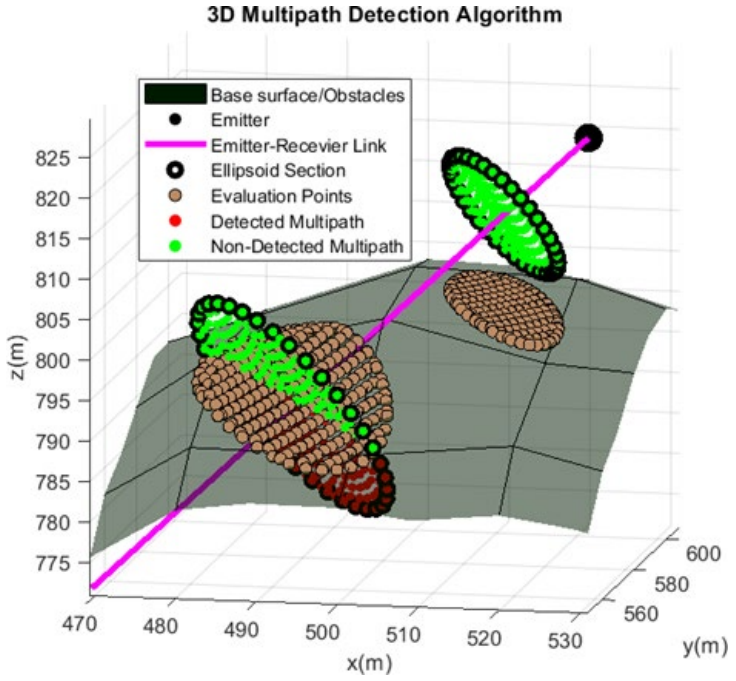

Figura A.5. Operación gráfica del algoritmo de detección 3D Multipath. Ejemplo de análisis de trayectos múltiples para dos secciones elipsoides distintas de un enlace emisor-receptor. Las zonas de obstáculos se caracterizan por tonos grises, simbolizando en este caso la superficie del suelo.

A.6.3. Derivación de CRB con condiciones NLOS para arquitecturas A-TDOA

El objetivo de esta sección es la generación de un modelo CRB genérico que estime la exactitud de la ubicación 3D cuando se consideran el ruido y la propagación NLOS. En este trabajo se aplica la derivación CRB a una arquitectura A-TDOA, como la mejor candidata en términos de precisión, estabilidad y complejidad para una aplicación LPS, debido a la eliminación de errores de reloj provocados por el sincronismo entre sensores. Sensor de target (TS) representa la posición del objeto a localizar. Sensor de coordenadas (CS) se refiere al sensor A-TDOA que es capaz de realizar mediciones de tiempo. Los sensores de trabajo (WS) abarcan todos los sensores de transpondedor de arquitecturas A-TDOA sin relojes internos para la estimación del tiempo.

Debido a la diversidad de la distancia objetivo-sensor típica de LPS, la derivación del CRB se somete a un tratamiento heterocedástico de las variaciones de estimación del proceso. En este sentido:

$$J_{mn} = \left(\frac{\partial h(X)}{\partial x_m}\right)^T R^{-1}(X)\left(\frac{\partial h(X)}{\partial x_n}\right) + \frac{1}{2} tr\left(R^{-1}(X)\left(\frac{\partial R(X)}{\partial x_m}\right)R^{-1}(X)\left(\frac{\partial R(X)}{\partial x_n}\right)\right) \quad (6.3)$$

FIM es la matriz de información de Fisher donde los subíndices *m* y *n* son los parámetros a estimar –TS coordenadas cartesianas-. Las relaciones de distancia entre sensores y objetivos se expresan mediante el vector **h(TS)**, cuya construcción depende de la arquitectura de posicionamiento implementada.

La propagación de ruido y NLOS se unen sobre la base de un modelo de propagación logarítmico normal con características diferentes para señales LOS y NLOS, basándose en el supuesto de mediciones de ruido no correlacionadas en diferentes sensores. En las siguientes ecuaciones, se calculan las expresiones de varianzas para el ruido y los efectos de propagación NLOS:

$$\sigma_{A-TDOA_i}{}^2 = \frac{c^2}{B^2\left(P_T/P_n\right)}\frac{PL(d_0)}{d_0{}^{n_{LOS}}}\left[\left(d_{i_{LOS}} + d_{i_{NLOS}}{}^x\right)^{n_{LOS}} + \left(d_{TS_{LOS}} + d_{TS_{NLOS}}{}^x\right)^{n_{LOS}} + \left(d_{CS_{LOS}} + d_{CS_{NLOS}}{}^x\right)^{n_{LOS}}\right]$$

$$d_{i_{LOS}} = \|TS - WS_i\|_{LOS}$$

$$d_{i_{NLOS}} = \|TS - WS_i\|_{NLOS}$$

$$d_{TS_{LOS}} = \|TS - \mathrm{CS}\|_{LOS}$$

$$d_{TS_{NLOS}} = \|TS - \mathrm{CS}\|_{NLOS}$$

$$d_{CS_{i\,LOS}} = \|WS_i - CS\|_{LOS}$$

$$d_{CS_{i\,NLOS}} = \|WS_i - CS\|_{NLOS}$$

$$x = n_{NLOS}/n_{LOS}$$

$$i = 1, \ldots, N_{WS}$$

donde P_T es la potencia de transmisión, P_n es el nivel de ruido medio calculado con base en la ecuación de Johnson-Nyquist, d_0 es la distancia de referencia para el modelo de pérdida de trayectoria logarítmica normal, $PL(d_0)$ es la pérdida de trayectoria referida a d_0, n_{LOS} y nN_{LOS} son los exponentes de pérdidas de propagación de trayectoria para las condiciones LOS y NLOS respectivamente, y N_{WS} es el número de A-TDOA WS. Todas las distancias d_{LOS} y d_{NLOS} se calculan mediante el algoritmo de trazado de rayos LOS/NLOS propuesto anteriormente.

Por último, la precisión global se calcula con base en el error cuadrático medio de la raíz (RMSE) de los componentes diagonales de la inversa del FIM (**J**). Esta métrica se aplica ampliamente en los sistemas de posicionamiento debido al conocimiento directo del radio de incertidumbre global en la ubicación final del objetivo inducida por cada componente cartesiano de la estimación.

A.6.4. Optimización multiobjetivo

La optimización del despliegue de nodos en arquitecturas A-TDOA con ruido, propagación NLOS e incertidumbres de trayectos múltiples debe proporcionar una conexión efectiva entre el TS y al menos cuatro WS y un CS para determinar la ubicación del objetivo. La aparición de efectos críticos de trayectos múltiples y la cancelación de trayectos LOS provoca la indisponibilidad del número necesario de sensores para determinar los puntos TLE. Por lo tanto, en estos casos se requiere la introducción de más WS y CS. El uso de una mayor cantidad de sensores aumenta los costos generales de la arquitectura al tiempo que aumenta la precisión. La obtención de una solución de compromiso a este problema se alcanza mediante una optimización multiobjetivo (MOP) de los parámetros en cuestión.

Se ha realizado una MOP basado en la caracterización del frente de Pareto (FP) para la minimización combinada de CRB y efectos multipath. Este proceso se ha realizado para un número diferente de sensores, cada uno de ellos con su propio FP. La función de adaptación del GA MOP se basa en un enfoque de maximización.

A.6.5. Resultados y conclusiones

A continuación, se presentan algunos de los resultados obtenidos tras la aplicación de todos los procedimientos presentados para condiciones NLOS con multipath. En primer lugar, se muestra un PF para exactitud y multipath, aplicado a un entorno complejo NLOS.

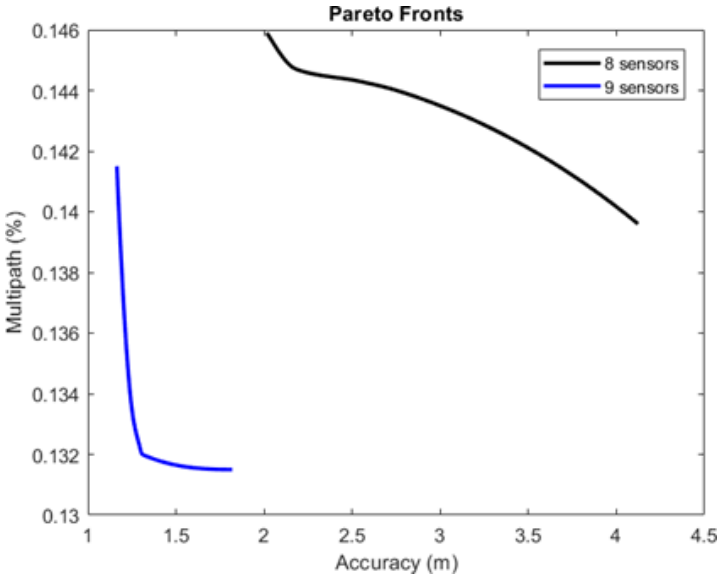

Figura A.6. Ejemplo de Frente de Pareto optimización multiobjetivo de exactitud y presencia de multipath.

Por un lado, se observa que un aumento en el número de sensores desplegados en el escenario conduce directamente a una reducción de las incertidumbres de ubicación y de los fenómenos de multipath adversos.

Seguidamente, un ejemplo de optimización y evaluación según el modelo de CRB descrito con el algoritmo LOS/NLOS de rastreo se muestra. Del mismo modo, la estimación de las condiciones de multipath se representa para la misma distribución de sensores A-TDOA.

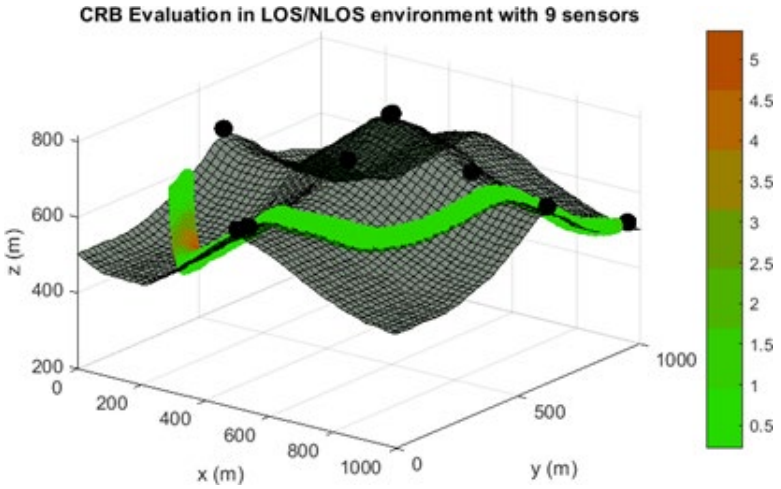

Figura A.7. Evaluación de exactitud en metros 9 sensores en MOP con igual ponderación para CRB y Multipath.

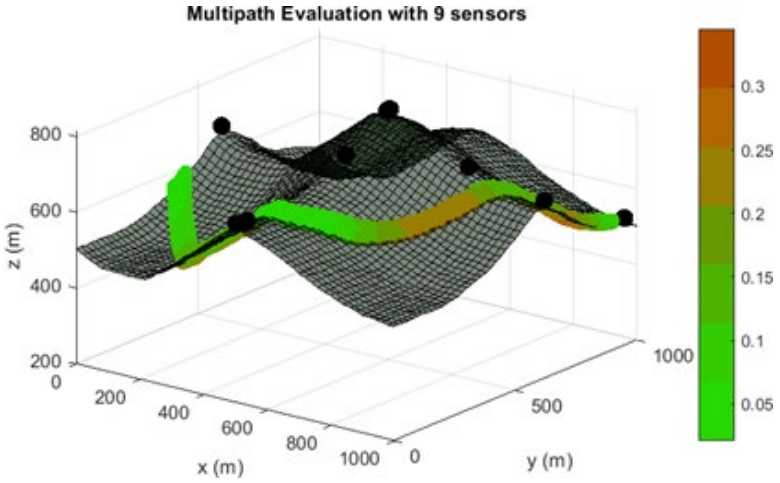

Figura A.8. Evaluación multipath para 9 sensores A-TDOA en el caso de MOP con igual ponderación para CRB y Multipath.

Los resultados muestran que la metodología diseñada proporciona un método para estimar a priori las capacidades de precisión máxima de la arquitectura A-TDOA en entornos complejos 3D. Además, el procedimiento permite determinar el número mínimo de sensores para lograr una demanda de precisión requerida, teniendo en cuenta un compromiso entre precisión, presencia de trayectos múltiples y costo del sistema.

Sección A.7

Conclusiones y líneas futuras

A.7.1. Conclusiones

Las aplicaciones modernas y futuras con altos requerimientos en los servicios de posicionamiento, como la navegación autónoma, requieren novedosos enfoques y tecnologías para proporcionar de forma satisfactoria alta exactitud bajo demanda, estabilidad y robustez durante la operación en condiciones reales, así como estimaciones realísticas del coste de implementación de estas arquitecturas. Todas estas condiciones pueden ser conseguidas mediante la optimización de la ubicación de los sensores de arquitecturas de posicionamiento en LPS, que es el principal objetivo que guía esta tesis doctoral. En este sentido, las principales conclusiones de este trabajo se presentan a continuación:

- Los GA con la nueva técnica de "scaling" para la codificación de nodos permiten la optimización de la distribución de sensores para sistemas de posicionamiento basados en mediciones temporales con total libertad en la definición de los NLE y TLE. Además, la metodología propuesta aumenta la flexibilidad en el análisis del espacio de soluciones, permite optimizaciones a demanda con resoluciones temporales variables, y posibilita las soluciones de compromiso entre representatividad de los resultados y tiempo de procesamiento del GA.
- La nueva adaptación de la CRLB para modelado de ruido demuestra que la arquitectura A-TDOA proporciona mejor rendimiento en términos de los principales estimadores estadísticos para exactitud que el sistema D-TDOA. Este comportamiento está directamente promovido por la minimización de la longitud total del camino seguido por las señales de posicionamiento para generar cada una de las mediciones temporales.
- El novedoso modelo de CRLB para incertidumbres generadas por ruido y errores de relojes en sistemas de posicionamiento basados en mediciones

temporales, en conjunción con la optimización mediante GA con "scaling", permiten el establecimiento de comparativas entre arquitecturas de posicionamiento y la obtención de múltiples conclusiones:

- La estabilidad de las incertidumbres de las mediciones temporales solo depende de la deriva del reloj del CS para las arquitecturas A-TDOA, en contraposición a los sistemas TOA y TDOA, donde la inestabilidad es favorecida por los errores de sincronismo, deriva de los relojes, y caminos de las señales de posicionamiento. Este hecho tiene una especial relevancia en LPS donde las distancias entre targets y sensores son altamente heterogéneas.
- En entornos donde las incertidumbres originadas por los errores en los relojes son prácticamente despreciables en comparación a los efectos del ruido, como en los GNSS, las técnicas TOA muestra mejor rendimiento en términos de exactitud para distribuciones de sensores optimizadas, seguidas de las arquitecturas TDOA y A-TDOA. La razón recae en la minimización de las incertidumbres inducidas por ruido en la exactitud global debida a la disminución en valor absoluto de la distancia de viaje de las señales de posicionamiento para computar cada medición temporal en esta arquitectura.
- En condiciones donde las incertidumbres generadas por los errores de relojes no pueden ser ignoradas, situación característica de LPS, las arquitecturas A-TDOA superan significativamente el resto de sistemas de posicionamiento basados en mediciones temporales debido a la reducción en la exactitud global de las incertidumbres generadas por los relojes de medición. Esto se apoya principalmente en la eliminación de los errores de sincronismo –desviación inicial de sincronización y lapso temporal desde la última sincronización– mientras que se mantienen minimizados las incertidumbres inducidas por el ruido. Adicionalmente, este comportamiento favorece la estabilidad y robustez de los sistemas A-TDOA, convirtiéndose en potenciales candidatos para aplicaciones de altos requerimientos en LPS.

❖ Los nuevos algoritmos de "LOS/NLOS ray-tracing" y "detección de

multipath", en combinación con la optimización mediante GA con "scaling" en la codificación y los modelos de CRB para caracterizar las condiciones NLOS en sistemas de posicionamiento basados en mediciones temporales, proporcionan un nuevo método para estimar a priori el máximo rendimiento de arquitecturas de posicionamiento antes de la implementación real para entornos complejos tridimensionales. Además, se posibilitan las optimizaciones multiobjetivo para obtener Frentes de Pareto (PF) entre exactitud, multipath, número de sensores desplegados, y coste del sistema gracias a los modelos y algoritmos presentados.

A.7.2. Líneas futuras

El advenimiento de los vehículos autónomos, en sus variantes terrestre y aérea, en combinación con las existentes y futuras aplicaciones con grandes demandas en la exactitud en la localización, requieren de nuevos enfoques en los sistemas de posicionamiento donde el servicio de localización sea no solo altamente preciso, sino que sea elevadamente robusto y estable en todas las zonas de funcionamiento del sistema. El entendimiento de esta necesidad es esencial para la implementación segura de las nuevas aplicaciones. En este sentido, el trabajo presentado en esta tesis doctoral es solamente el principio de la futura investigación en este ámbito de estudio, siendo las líneas de investigación más representativas las que se presentan a continuación.

La experimentación en condiciones outdoor e indoor debe ser llevada a cabo para validar y mejorar la calidad de los modelos de incertidumbre de ruido, errores de relojes y condiciones NLOS para diferentes tecnologías de posicionamiento. Concretamente, las comunicaciones de banda ultra-ancha (UWB) son una técnica muy prometedora para aplicaciones de alta-exactitud en entornos indoor. Para escenarios outdoor, una plétora de posibles tecnologías basadas en señales de tipo "*pulse compression*" con técnicas NOMA de multiplexación puede ser analizadas para aplicaciones de altos requerimientos. Adicionalmente, la colección de datos experimentales posibilita la adopción de técnicas de Inteligencia Artificial (IA) supervisadas para construir modelos de incertidumbre más complejos con mayor representatividad para reducir la distancia entre simulaciones y realidad.

Los GA son una técnica perfectamente adaptada para resolver el NLP. Sin embargo,

al igual que el resto de metodologías heurísticas, está expuesta a optimizaciones locales, problemas de convergencia y transiciones complicadas entre las etapas de diversificación e intensificación. En este sentido, se pueden alcanzar mejoras potenciales incrementando la robustez del método durante la optimización de entornos discretos sujetos a discontinuidades NLOS. Se pueden alcanzar otras mejoras en términos de rendimiento con la adopción de nuevos procedimientos de optimización que permitan una reducción de los periodos de estancamiento, gracias a la combinación de diferentes operadores genéticos o la asociación con otros procedimientos de optimización heurísticos/exactos. Finalmente, estudios acerca de las características de las funciones objetivo pueden permitir futuras transformaciones a funciones de adaptación más resolubles con menor susceptibilidad a caer en optimizaciones locales.

Por último, se debe realizar más investigación acerca de las arquitecturas A-TDOA, como los sistemas más prometedores en términos de exactitud, estabilidad y robustez para aplicaciones modernas de altas prestaciones como la navegación autónoma. Particularmente, las arquitecturas A-TDOA presentan distintos tipos de sensores, donde los CS juegan un papel crucial durante el posicionamiento. En este sentido, análisis de accesibilidad y optimizaciones para condiciones de operación normales y en situaciones de fallo de sensores deben ser realizas para futuras implementaciones de estos sistemas. Además, las estrategias de "recepción y retransmisión" características de estas arquitecturas deben ser modeladas en los ámbitos de exactitud y accesibilidad, como el principal punto de diferencia con los sistemas basados en mediciones temporales tradicionales.